INFORMATION TO USERS

This manuscript has been reproduced from the microfilm master. UMI films the text directly from the original or copy submitted. Thus, some thesis and dissertation copies are in typewriter face, while others may be from any type of computer printer.

The quality of this reproduction is dependent upon the quality of the copy submitted. Broken or indistinct print, colored or poor quality illustrations and photographs, print bleedthrough, substandard margins, and improper alignment can adversely affect reproduction.

In the unlikely event that the author did not send UMI a complete manuscript and there are missing pages, these will be noted. Also, if unauthorized copyright material had to be removed, a note will indicate the deletion.

Oversize materials (e.g., maps, drawings, charts) are reproduced by sectioning the original, beginning at the upper left-hand corner and continuing from left to right in equal sections with small overlaps.

Photographs included in the original manuscript have been reproduced xerographically in this copy. Higher quality 6" x 9" black and white photographic prints are available for any photographs or illustrations appearing in this copy for an additional charge. Contact UMI directly to order.

Bell & Howell Information and Learning
300 North Zeeb Road, Ann Arbor, MI 48106-1346 USA
800-521-0600

UMI®

11

AN ISOTOPE SUBSTITUTION-NMR STUDY OF TRIOXANE/DIOXOLANE COPOLYMERIZATION

by

Patrick Dunn

A dissertation submitted to the Graduate Faculty in Chemistry in partial fulfillment of the requirements for the degree of Doctor of Philosophy, The City University of New York

1998

This manuscript has been read and accepted for the Graduate Faculty in Chemistry in satisfaction of the dissertation requirement for the degree of Doctor of Philosophy.

9/15/98
Date

Chair of Examining Committee

9/15/98
Date

Executive Officer

Supervisory Committee

The City University of New York

Abstract

An Isotope Substitution-NMR Study of Trioxane/Dioxolane Copolymerization

by

Patrick Dunn

On the subject of the trioxane (**TOX**)/dioxolane (**DOL**) copolymerization, the present work represents the first attempt to apply extensively the method of isotope substitution in conjunction with state of the art **NMR** spectroscopy to gather hitherto unattainable detailed mechanistic information. A systematic compilation of data from *in-situ* ^{13}C, ^{1}H, and **DEPT NMR** spectra of cationic initiated **TOX/DOL** copolymerization with isotope labeling of three *co*reactants was accomplished. Replacing **TOX** with **TOX-d_6** as *co*monomer resulted in a much enhanced dynamic range for resonance detection and remarkably improved overall resolutions of ^{1}H **NMR** spectra, *including direct pentad detection for the first time*. Three distinct stages of reaction marked by the changes in formation rates of copolymer sequences can be distinguished. In the first stage, activated **DOL** preferentially reacts with CD_2O to produce deuterium labeled trioxepane (**TOP-2,2-d_2**). Concurrently, **TOP-(2,2-d_2)** generates all the observed sequences and additional *co*monomers simultaneously. In the second stage, the **TOP-(2,2-d_2)/DOL** copolymerization results in the increased formation of pentads with two ethylene oxides, "**E**", units. In the third stage, transacetalization involving pentad

sequences with two and three "E" plays a major role. Replacing **DOL** with **DOL-(2,2-d_2)** as *co*monomer resulted in significantly improved resolution in the methylene oxide, "M", region of ^{1}H NMR spectra due to the elimination of the intense **DOL** acetal proton peak. Kinetic curves approach those with natural isotopic abundance since only 10% of the "M" units are deuterium substituted. Four distinct stages of copolymerization marked by increased generation of specific sequences and information in addition to the **TOX-d_6** system was observed. The first stage also includes the copolymerization of excess formaldehyde with **TOP** resulting in the overall increase in the generation of "M-centered" sequences. Before the second stage, **TOX/TOP-(2,2-d_2)** copolymerization was observed resulting in the increased generation of "one E-pentads" and **DOL**. In the second stage, **DOL/TOP-(2,2-d_2)** copolymerization results in the increased generation of "two E-pentads" as noted in the **TOX-d_6** system, while transacetalization accounts for the increase rate of generation of "one E-pentads". Stage three marks the dominance of **TOX-d_6** and **CD_2O** in generating "five-M pentads" and "one E-pentads" via transacetalization and polymerization reactions. In the polymerization systems with **$C^{13}H_3OCH_2OC^{13}H_3$** as chain transfer agent, the early initiation of **TOP** was verified.

ACKNOWLEDGEMENT

The author expresses his thanks to Professor Nan Loh Yang for his expert supervision and assistance during all phase of this project and to Doctor Hsin Wang for his assistance in NMR. He wishes to thank the Thesis Committee Members: Dr. G. Collins, Dr. D. Locke and Dr. C. Steiner for their guidance. The support of the Magnet Fellowship, the Chemistry Department at the College of Staten Island, the Graduate School and University Center, CUNY, and Hoechst/Celanese Inc. is gratefully acknowledge.

Table of Content

List of Figures

I. Introduction

A. Background

The processes involved in the copolymerization of trioxane, **TOX**, with dioxolane, **DOL**, have been documented since early 1920 by Staudinger[1]. Based on chemical evidence, various mechanisms for chain transfer and end-group formation were proposed.[2] This thesis represents the first investigation on this subject using modern high field **C-13** and proton **NMR** in conjunction with isotope labeling syntheses.

i. Fundamentals[2]

Jaacks laid a sound foundation for this copolymerization system through considering various possibilities relating to the mechanistic and kinetic processes based on chemical evidence. The need to account for the polymerization and depolymerization of formaldehyde and cyclic formals was recognized. This copolymerization is further complicated by hydride transfer and transacetalization involving the liquid and crystalline phases. The *co*monomer **DOL** is considered to be preferentially incorporated in the growing polymer chains in solution but becomes randomized in transacetalization processes involving dissolved chains and crystalline interfaces as well as depolymerizations. Transacetalization as a process of randomizing ethylene-oxide units from **DOL** was supported by Weissermel, Fischer, Gutweiler and Hermann.[3]

The depolymerization of **TOX/DOL** copolymer chains is terminated by ethylene oxide units (**Reaction I.A.i. 1**). The products of this depolymerization are hydroxy ethyl capped chains and formaldehyde.

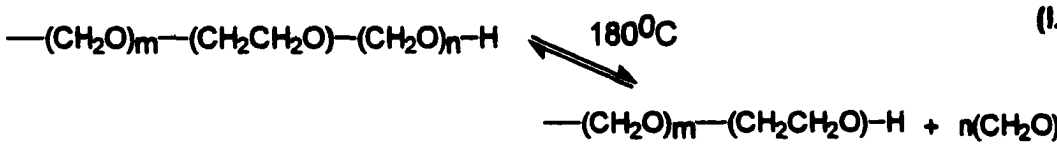

(I.A.i. 1)

Reaction (I.A.i. 2) represents the formation of cyclic oligiomers via fast backbiting reactions. This reaction implies backbiting as a mechanism for synthesizing **TOX**, **DOL**, trioxepane, **TOP**, tetroxane, **TET**, and other cyclic acetals.

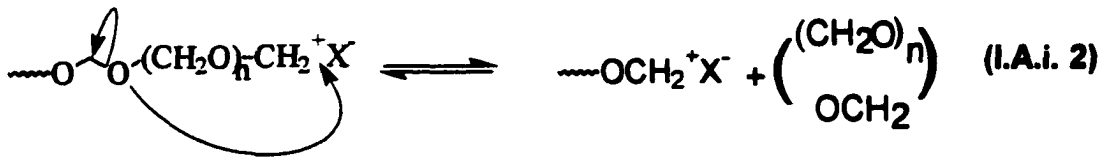

(I.A.i. 2)

Reaction (I.A.i 3) illustrates transacetalization involving dissolved chains and crystalline interfaces. Although the ethylene-oxide unit is larger (by one more CH_2 unit) than the methylene-oxide unit, it is possible for ethylene-oxide units to become incorporated in the crystalline structure.

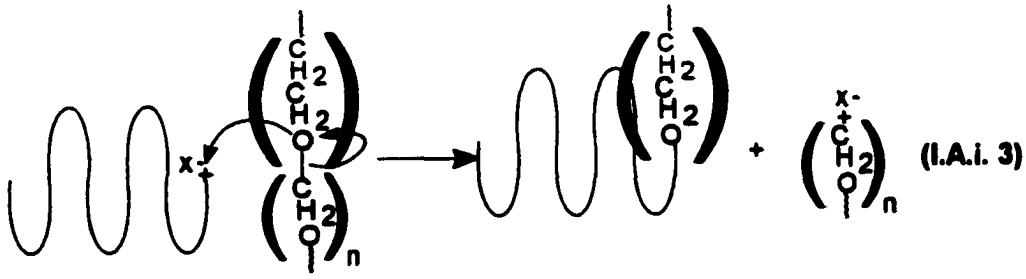

(I.A.i. 3)

Reaction (I.A.i. 4) depicts propagation via *tert*-oxonium ions with the free electron pairs of **TOX** oxygens acting as nucleophile.

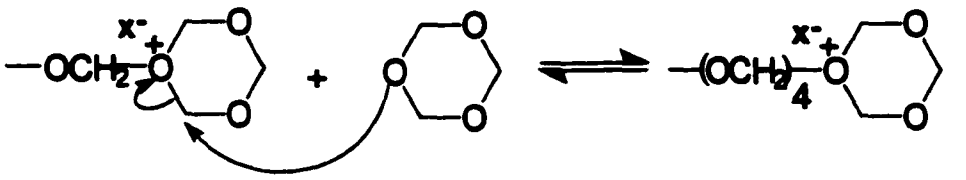

(I.A.i. 4)

Reaction (I.A.i 5) shows propagation via resonance stabilized carbenium ion.

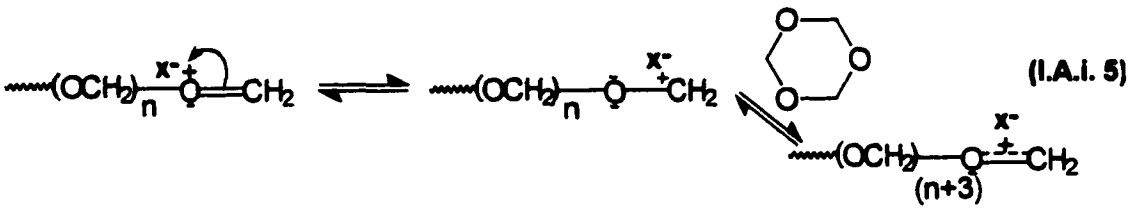

(I.A.i. 5)

Many of the active components, e.g. formaldehyde and cyclic acetals were directly observed using **NMR** (see Sections **ii** and **iii**).

I.A.ii. Proton NMR[4]

Further details for the mechanism of **TOX/DOL** copolymerization were recently obtained from ***in-situ*** **^{1}H NMR (200 MHz)** monitoring of the cationic initiated comonomer melt. Kinetic insertion of formaldehyde into **TOX** and **DOL** occurred in the early stages of copolymerization, resulting in the formation of **TET** and **TOP** respectively.[3,5] Because the growth of **TET** and **TOP** peaks occurred before triad sequence peaks as seen in these **^{1}H** spectra, backbiting as a route of generating **TET** and **TOP** became open to question. Although previous claims of backbiting for **TET** and **TOP** generation was thus somewhat refuted, the possibility of backbiting can exist in later stages of the copolymerization. The kinetic profiles of various reactive species

obtained in the *in-situ* ^{1}H NMR analysis of the comonomer melt support the sequence of reactions described below.

The reaction of the initiator boron trifluoride etherate (BF_3OEt_2) with water produce diethylether and initiator, *co*initiator complex ($[BF_3OH^-]H^+$), as shown in **Reaction (I.A.ii. 1)**.

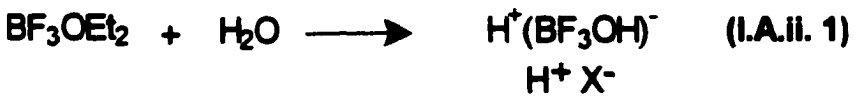

(I.A.ii. 1)

Reaction (I.A.ii. 2) depicts **TOX** initiation. In the comonomer melt, **DOL** is preferentially initiated because of its greater basicity and reactivity in comparison to **TOX**.

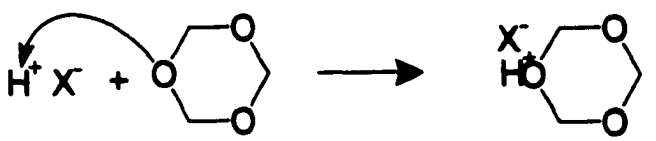

(I.Aii. 2)

Reaction (I.A.ii. 3) shows the equilibrium existing between the oxonium ion and carbenium ion. As shown by Jaacks[2], the carbenium ion is also resonance stabilized by sharing the free electron pair of the adjacent oxygen atom. The stabilization of the carbenium ion also exists for initiated **DOL**.

(I.Aii. 3)

The equilibrium between polymerization and depolymerization was considered to be important (**Reaction I.A.ii. 4**):

(I.Aii. 4)

Reaction (I.A.ii. 5) shows the initiation of **TOX** by the resonance stabilized carbenium generated from the dissociation of **TOX**. This reaction along with **reaction (I.A.i 5)** indicates that propagation can result from both oxonium and carbenium ions. The concentrations of these propagating ions are assumed to reach steady state.

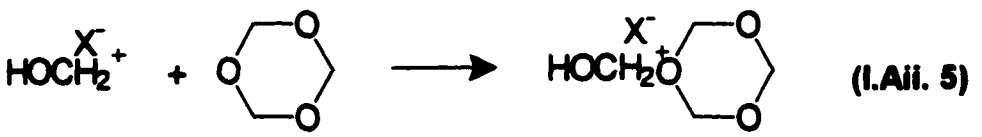

(I.Aii. 5)

Based on the observation that **TOP** appeared before copolymer sequences, it was deduced that formaldehyde was kinetically inserted into protonated **DOL** to give protonated **TOP (Reaction I.A.ii.6)**:

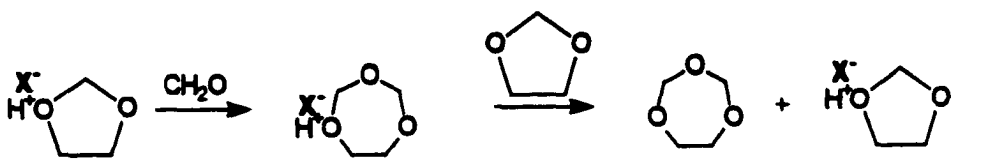

(I.Aii. 6)

Proton transfer from protonated **TOP** to a more reactive base such as formaldehyde or **DOL** generates **TOP**.

Reaction (I.A.ii. 7) shows the possibility of ring opening instead of formaldehyde insertion. As discussed earlier, ring opening also depends on the steady state concentrations existing between oxonium and carbenium ions.

(I.Aii. 7)

iii. C-13 NMR and isotope labeling[6]

NMR (300 and 500 **MHz**) experiments with **DOL-(2-^{13}C)** as *co*monomer were conducted to observe ***in situ*** the copolymerization of **TOX/DOL**. The application of **NMR** with higher field strengths and much improved stability resulted, even without shift-agent, in resolution of the pentad peaks and revealing heptad peaks. This study support previous copolymerization scheme based on proton **NMR** work.[4]

In the present work, the labeled compounds used in the further investigation of **TOX/DOL** copolymerization include perdeuterated **TOX, (TOX-d_6)**, **TOX**, deuterated

DOL, (DOL-2,2-d_2), DOL and ^{13}C labeled dimethoxymethane ($C^{13}H_3OCH_2OC^{13}H_3$). The bulk TOX/DOL copolymerization of labeled monomer, with unlabeled comonomer was followed *in-situ* by ^1H, DEPT and ^{13}C NMR experiments of the pre-cloud period.

I.B. Thesis Statement and Outline

Recent proton[4] and C-13[6] NMR studies have made significant contributions to the subject, including assignment of NMR resonance peaks for important species involved in TOX/DOL copolymerization. Unlike methods requiring "quenching followed by analysis", the *in-situ* NMR studies collected kinetic information without disturbing the multi-equilibria involved in the copolymerization processes. These investigations firmly establish that *in-situ* NMR characterization of polyacetal copolymerization systems offers great advantages in furthering the research in this field. However, previous proton experiment with low field strength (200 MHz) yielded overlapping triad sequences.[4] The C-13 experiment failed to give quantitative kinetic data.[6] The present study applies state of the art NMR instrumentation in conjunction with the approach of isotope substitution to investigate the copolymerization. *The isotope substitution work involved the first syntheses of perdeuterated TOX, (TOX-d_6), deuterated DOL, (DOL-2,2-d_2), and ^{13}C labeled dimethoxymethane ($C^{13}H_3OCH_2OC^{13}H_3$).* The copolymerization of labeled TOX and DOL with unlabeled *co*monomers were followed *in-situ* using ^1H, DEPT and ^{13}C NMR experiments during the pre-cloud period. The combination of isotope labeling and the state of the art instrumentation resulted in significant advancement in understanding the mechanistic and kinetic details of the copolymerization systems.

The synthesis and application of TOX-d_6 as *co*monomers for the polymerization

systems opens the door to detailed analysis of microsequences. Sections (IIIA.i.-iv.) describe the ^{13}C, DEPT and ^{1}H NMR spectra obtained in conjunction with this labeled comonomer. Section (IIIA.iv) describes a detailed mechanistic scheme as revealed by monitoring kinetic profiles of active species using ^{13}C, DEPT and ^{1}H NMR. In the ^{1}H NMR spectra, pentad resolution was achieved directly for the first time. The correlation of rate data from the "E" and "M" regions of the spectra showed conclusively the monomer responsible for generating specified microsequences at different periods of the copolymerization reaction. The ^{13}C and DEPT spectra resolved hydrogenated components from delta-deuterated labeled components, offering a more in-depth understanding of the ^{1}H NMR spectra. The spectra obtained in these experiments can serve as the basis for detailed end-groups characterization.

Section (III.B. i.-iv.) describes the monitoring of the copolymerization of DOL-(2,2-d_2) with TOX using ^{13}C, DEPT and ^{1}H NMR. A detailed mechanistic scheme was developed based on peaks assigned in ^{13}C, DEPT and ^{1}H NMR spectra and kinetic curves of all components resolved in the ^{1}H NMR spectra. The analysis of the copolymerization mechanism in this section, complementing results described in section (IIIA.), brings the understanding of the copolymerization processes closer to the systems with natural isotopic abundance.

The reactions of the ^{13}C labeled chain transfer agent dimethoxymethane ($C^{13}H_3OCH_2OC^{13}H_3$) in TOX/DOL copolymerization systems were monitored using *in-situ* ^{13}C NMR (Sections III.C) as a means of following the initial and final steps of the copolymerization processes. Because the ^{13}C spectra of these experiments were, at this

time, not quantitative, the assigned peaks were used only qualitatively. The assignment of resonance peaks and qualitative observation of species support the mechanistic schemes derived in the previous sections.

Reference

1 Staudinger, H. *Die Hochmolecularen Organischen Verbindungen*, Springer: Berlin, (1932)

2 Jaacks, Volker. Adv. Chem. Ser. **91**, 371 (1969).

3 Weisermel, K., Fisher, E., Gutweiler, K., Hermann, H. D., Cherdron, H., Angew. Chem. Int. Ed. **6**, 526 (1967).

4 Lu, N., Collins, G. L., Yang, N. L. *Makromolek. Chem., Macromolec. Symp.*, **42/43**, 425 (1991)

5 Collins, G.L., Greene, R.K., Benardinelli, F. M., Ray, W.H. J. Polym. Sci. Polym. Chem. Ed. **19**, 1597 (1971).

6 Werner, M. **CUNY** Ph.D. Thesis, 1996.

II. Experimental

A. Isotope substitution syntheses

The isotope substitution preparation of deuterated dioxolane (DOL-2,2-d_2), perdeuterated TOX (TOX-d_6) and ^{13}C labeled dimethoxymethane ($C^{13}H_3OCH_2OC^{13}H_3$) are all the first syntheses. The three labeled compounds allow us to track different aspects of the copolymerization processes.

i. Sources of Chemicals

The natural abundance reactants used were obtained from Aldrich and Fisher Scientific, while isotope labeled reactants were obtained from Cambridge Isotope. All reactants purchased were of the highest purity available and were used without further purification unless described otherwise.

ii. Deuterated Dioxolane (DOL-2,2-d_2)

The reaction set-up included a single neck 100 mL round bottom flask fitted with a condenser adapter, thermometer, an air inlet for dry argon, a 50 mL collection flask and magnetic stirring system. To the 100 mL flask were added under stirring 5.0 g of deuterated paraformaldehyde, 10.35 g ethylene glycol, 0.5 g p-toluenesulfonic acid monohydrate, and 50 mL dibutylphthalate as solvent. The reaction mixture was maintained at boiling temperature (72-75°C) under dry argon with the reaction flask kept in an oil bath at 100°C. The reaction product dioxolane refluxed and gradually distilled out along with trace amounts of water. The temperature of the oil bath was continually increased to provide a distillation rate of ca. one drop of product per second. As further

increase in bath temperature did not yield distillate, a vacuum pump was attached in place of air inlet, allowing additional collection of the **DOL-(2,2-d_2)** with the collection flask now submerged in an ethanol, dry ice bath. This **DOL-(2,2-d_2)** distillate was then dried over **$CaCl_2$** first and later distilled from **CaH_2** and stored under refrigeration in a dessicator. Yields, after purification and drying, of up to 60% can be expected from this synthesis. The purity of the **DOL-(2,2-d_2)** product was established using proton NMR (Figure **II.A.ii-1**) and C-13 NMR (**Figure III.B.i-1**).

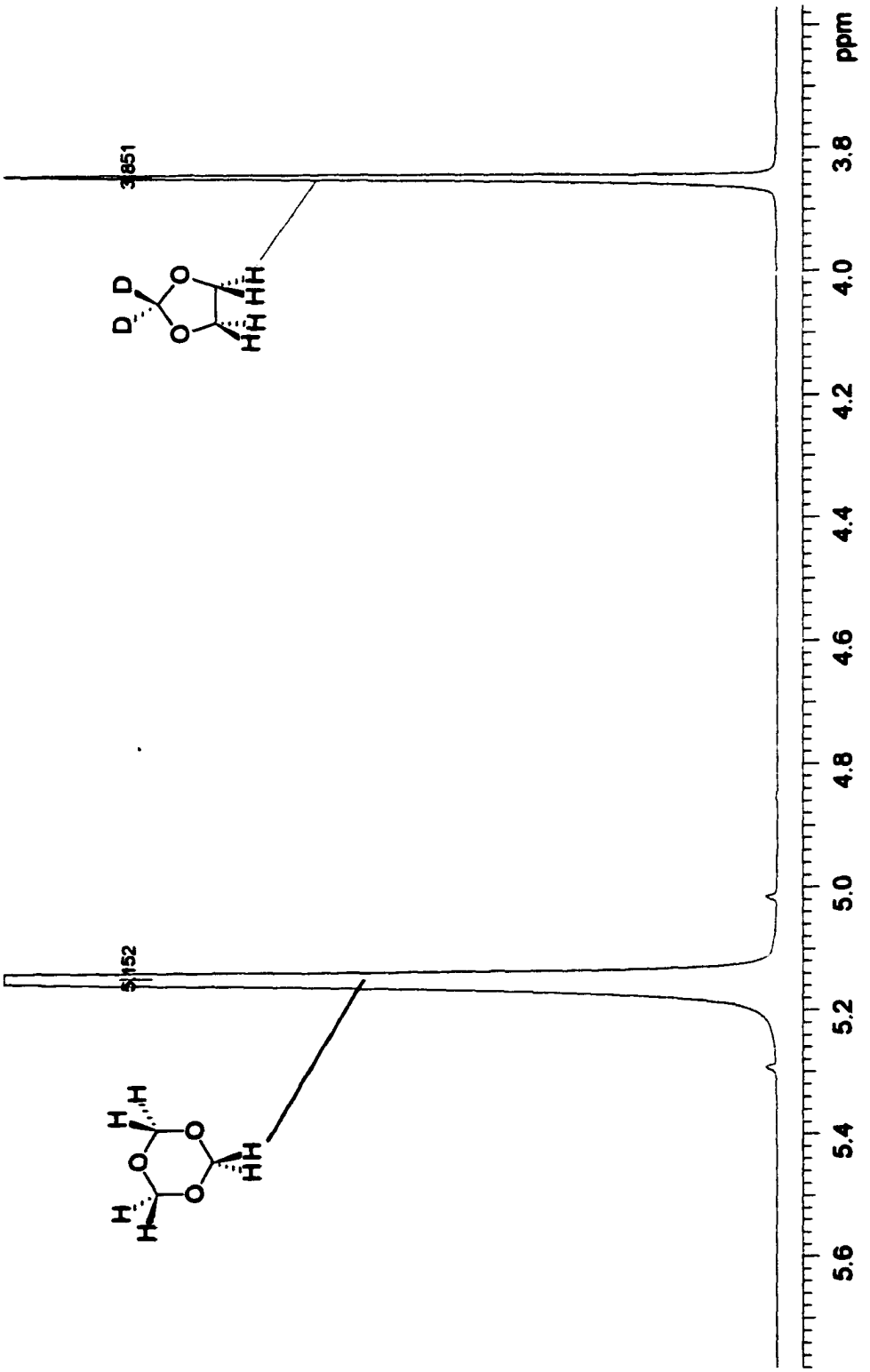

Figure (II.A.ii 1) ^{1}H spectrum before initiation of **TOX/DOL-(2,2-d$_2$)**-"Spectrum of **DOL(E)** from **DOL-(2,2-d$_2$)** Monomer". Monomers' mole ratio: (3,1), spectrometer: 600 MHz Probe: **ID600-s**.

iii. Trioxane

Trioxane was synthesized as a pre-run to perdeuterated TOX synthesis. The set-up for this synthesis included a 50 mL round bottom flask, equipped with a fractionating column and distillation head fitted with a thermometer, collection flask, a magnetic stirring system and gas inlet for dry argon atmosphere. The collection flask was submerged in an ice water bath. The entire arm of the fractionating column and the initial portion of the distillation head adapter was externally heated to maintain a temperature of 70°C for the duration of the reaction. To the 50 mL round bottom reaction flask 5.0 g paraformaldehyde, 0.75 g Dowex 50 (cation exchange resin) and 2.91 g water were added and stirred continuously. Dowex 50 obtained from Aldrich is a strong cation exchange resin. This reaction mixture was maintained at 100°C until a uniform suspension was obtained. Then the bath temperature was increased to 115°C to maintain distillation rate of one drop trioxane in water per second between the temperature range of 90-95°C. The crude trioxane was recrystallized from triethylamine and washed with hexane. The yield from this synthesis was in the low twenty percent range. Based on observations on this synthesis, the following modified procedure was used.

iii.a. Perdeuterated TOX (TOX-d_6)

In contrast with the synthesis described in (Section iii), in the improved procedure a layer of dibutylphthalate was placed over the reactants to prevent splattering and over heating as well as to facilitate stirring. Perdeuterated trioxane (TOX-d_6) synthesis was

conducted using an assembly of a 100 mL round bottom flask fitted with a condenser adapter with a gas inlet adapter, a collection flask and a magnetic stirring system. To the 100 mL flask were added 10 g deuterated paraformaldehyde, 1.5 g of water, 2.0 g Dowex 50 in 45 mL dibutylphthalate. A drying tube was attached to the air inlet adapter. The reaction mixture was heated to 100°C in a temperature bath under stirring. This temperature was maintained until droplets of moisture were visible in the condenser adapter (twenty-four hours). At this point, the bath temperature was increased to 120°C. The **TOX-d_6** crystals gradually deposit along the inner bore of the condenser adapter, over a period of one week. Yield before purification of 69% can be expected from this synthesis. A totally jacketed continuous reflux Fuchs modeled after one used previously[1] with the following modifications was designed and employed in the purification and drying efforts of **TOX-d_6**. The storage head of the Fuchs continuous reflux apparatus was reduced from 1000 mL to 50 mL to accommodate the refluxing of a small volume of **TOX-d_6**. The syringe port was designed so that the syringe needle entered a one mL trough located above the storage head stopper to facilitate the complete removal of the labeled monomer. All ports in this continuous Fuchs style reflux apparatus were jacketed or brought close to the oil jacket to prevent crystallization which invariable leads to polymerization and obstruction of continuous reflux. The purity of the final product was established using **C-13 NMR (Figure III.A.i 1)**.

iv. ^{13}C Labeled Dimethoxymethane ($C^{13}H_3OCH_2OC^{13}H_3$)

To a 50 mL round bottom reaction flask were added 5.0 g ^{13}C labeled methanol, 2.34 g paraformaldehyde, and 0.2 g p-toluenesulfonic acid. The round bottom reaction flask was equipped with an oil temperature bath, a magnetic stirring device, a distillation head containing a thermometer inlet, air inlet and a collection flask. The bath temperature was maintained at 65°C (20°C above the boiling point of $C^{13}H_3OCH_2OC^{13}H_3$) under stirring. The white suspension of paraformaldehyde in methanol gradually became transparent as the catalyzed breakdown of the chains progressed. After the formation of a clear solution, $C^{13}H_3OCH_2OC^{13}H_3$ began to distill. The reaction was forced to generate $C^{13}H_3OCH_2OC^{13}H_3$ continuously by increasing the temperature as the volume of the reactant diminished. Distillation rate was temperature controlled to approximately one drop per second. The purpose for the precise temperature control was to ensure that higher boiling homologues of $C^{13}H_3OCH_2OC^{13}H_3$ did not distill. Although the yield before purification was high, the addition of four sodium beads with stirring for twenty-four hours resulted in the partial breakdown of the product as indicated by the crystalline deposits on the side of the round bottom flask and on the sodium beads. As a result, the yield after purification was only 29.8%. The longer chain homologues of $C^{13}H_3OCH_2OC^{13}H_3$ that remained in the reaction flask and the purified $C^{13}H_3OCH_2OC^{13}H_3$ collected were stored in separate collection bottles, sealed, and refrigerated in a dessicator. The purity of the product was established using C-13 NMR: (Figure III.C-1).

II.A.v. Final Monomer Purification[1]

Unlabeled trioxane was purified for the NMR experiments by refluxing at bath temperature (135°C) continuously over sodium in a Fuchs style apparatus, under a dry argon atmosphere for at least forty eight hours. The distillation head and condenser were oil heated to maintain a temperature of 65°C. Before use, the trioxane was collected in the distillation head where it was removed by hot syringe immediately before use.

As with the unlabeled trioxane, the unlabeled dioxolane was stirred continuously over sodium beads in a dry argon atmosphere within a standard continuous Fuchs distillation apparatus. Dioxolane was refluxed for a minimum of two hours before being collected in the storage head where it was removed by hot syringe.

II.B. Copolymerization

II.B.i. Copolymerization Monitored Using 300 MHz NMR Spectrometer

The assembly for NMR samples required meticulous drying: 10 mm NMR tubes, vortex plugs, septa, and magnetic stirrer were dried for two hours in a vacuum oven at 70°C. Dry trioxane maintained at 85°C in the distillation head was injected in hot tared NMR tubes. Immediately after weighing TOX, the tube was placed in a 65°C oil bath. The desired feed of deuterated or unlabeled dioxolane was transferred using hot syringe to the NMR tube through the septa from the storage vials (DOL-(2,2-d_2) or distillation head (DOL).

The 10 mm NMR tube was charged with an approximate 3:1 TOX, DOL-(2,2-d_2)

feed ratio and 20 ppm boron trifluoride etherate as initiator. The carrier solvent for the initiator (2,4 dioxane) was referenced at 66.66 ppm and 3.66 ppm in ^{13}C/DEPT and ^{1}H NMR experiments respectively unless otherwise noted for spectra presented before initiation. The ^{13}C and DEPT NMR experiments allow the observation of ^{13}C nuclei associated with methylene-oxide, M, ethylene-oxide, E, and deuterated methylene-oxide, M', units, A charge of 3/1 for TOX/ DOL-(2,2-d_2) will lead to a molar ratio of 9:1:1 for M: E, and M'. A Varian ten millimeter Broad Band Probe with range (^{31}P-^{15}N) was used in the DEPT and ^{13}C kinetic experiments. The temperature range for this probe is -150 to +150°C. The pulse angle used in these experiments was 45° with relaxation time of 2 to 4 seconds and number of transients 128 unless otherwise stated.

II.B.ii. Copolymerization Monitored Using 600 MHz NMR Spectrometer

NMR tubes (5 mm) and external lock insert were dried for two hours in a vacuum oven at 76°C. Dry perdeuterated trioxane maintained at 85°C in the distillation head was transferred by injection into an NMR tube maintained at 100°C. Immediately after weighing TOX, the tube was placed in a 65°C oil bath. The desired feed of dioxolane obtained from the DOL reflux apparatus was added using a hot syringe through the septum cap of the NMR tube. After charging the NMR tube with the monomers, an external lock tube (Wilmad, CAT NO. WGS-5BL coaxial insert) was inserted. Dimethylsulfoxide (DMSO) was placed in the coaxial insert as a lock solvent (Z_0= 9000). This Z_0 value was initially determined by locking on the deuterated DMSO within the insert while leaving the external volume empty. The determination of the lock position for deuterated DMSO was important to prevent locking on deuterated TOX

during the copolymerization experiment. Locking on **TOX-d_6** results in fluctuations of the lock level followed by unlocking, as **TOX-d_6** separates into different components and sequences in the reaction medium and copolymer. The following changes were introduced in the **NMR** experiment to optimize the resulting spectra. The receiver gain was maximized to detect weaker peaks at fewer scans. The spectral width was optimized to prevent baseline convolution. The sample spinning was turned off to eliminate spinning side bands that were out of phase. These spinning side bands would have totally obscure developing peaks, because of their contributions to baseline distortions. Because the spectrometer was shimmed to high resolutions, the loss in resolution due to non-spinning was acceptable. As with the use of the 300 MHz instrument, the carrier solvent for the initiator (2,4 dioxane) was referenced at 66.66 ppm and 3.66 ppm in ^{13}C and ^{1}H **NMR** experiments respectively unless otherwise noted for spectra presented before initiation.

The 5 mm **NMR** tube was again charged with approximately 3:1 ratio **TOX-d_6/DOL** or **TOX/DOL-(2,2-d_2)** mixture and 20 ppm boron trifluoride etherate as initiator. With **TOX/DOL/$C^{13}H_3OCH_2OC^{13}H_3$** as reactants, 20 ppm initiator **(BF_3OEt_2)** was also added. A 5 millimeter Indirect Detection Broad Band probe **(ID600-s)** from Nalorac with temperature range +150 to -150° was used in these kinetic experiments. The pulse angle used in these experiments was 30° with relaxation time of seven seconds (this covers more than five time the longest delay time of five seconds in the ^{1}H **NMR**) for collection of 128 transients in general.

References

[1] Werner, M. CUNY Ph.D. Thesis, 1996.

III. Results and discussion

A detailed mechanism of **TOX/DOL** copolymerization was developed based on **NMR** observations followed by analysis in mechanistic terms for copolymerization systems with different isotope substitutions. Because methylene oxide units in these experiments can be deuterium labeled **-CD_2O-, (M')**, or unlabeled ,**-CH_2O-, (M)**, notation for assigned peaks include the possibility of isotope labeling within observed sequences. For example, the notation "**(M/M')E(M/M')E(M/M')**" refers to a pentad with **-CD_2O- (M')** or unlabeled **-CH_2O- (M)** as the center with '**M**' underlined to indicate the unit being observed. The notation "**M/M**" indicates the unit can either contain hydrogen or deuterium. In Section (**IIIA.i**, ^{13}C spectra), the resolution of hydrogenated components from γ-deuterium labeled components in conjunction with **TOX-d_6** as labeled comonomer adds to information obtained from ^1H **NMR** spectra where these two species cannot be resolved. Similarly, **DEPT** (Section **IIIA.ii**) spectra in conjunction with **TOX-d_6** as labeled comonomer corroborate assignment from ^{13}C spectra and support the detailed mechanistic analysis of ^1H **NMR** spectra. It should be noted that **DEPT** inverse detection pulse sequence[1] results in the elimination of resonance intensities from alpha deuterium labeled **C-13** nuclei. In the ^1H **NMR** spectra, *pentad resolution was achieved directly for the first time*. Section (**III.A.iii**) describes in mechanistic detail the copolymerization of **TOX-d_6/DOL**, while Section (**III.A.iv**) illustrates the derived mechanistic scheme. Section (**III.B.i-iv**) is arranged similar to sections (**III.A.i-iv**). Sections (**III.C.i-iv**) describes ^{13}C **NMR** spectra of homopolymerizations and copolymerizations of **TOX**, **DOL** and **TOX/DOL** in conjunction with **$C^{13}H_3OCH_2OC^{13}H_3$** as ^{13}C labeled chain transfer agent. This section gives insight into

all aspects of **TOX/DOL** homopolymerization and copolymerization reactions. **Figure (III 1)** shows structures and their representative mnemonics used in this document.

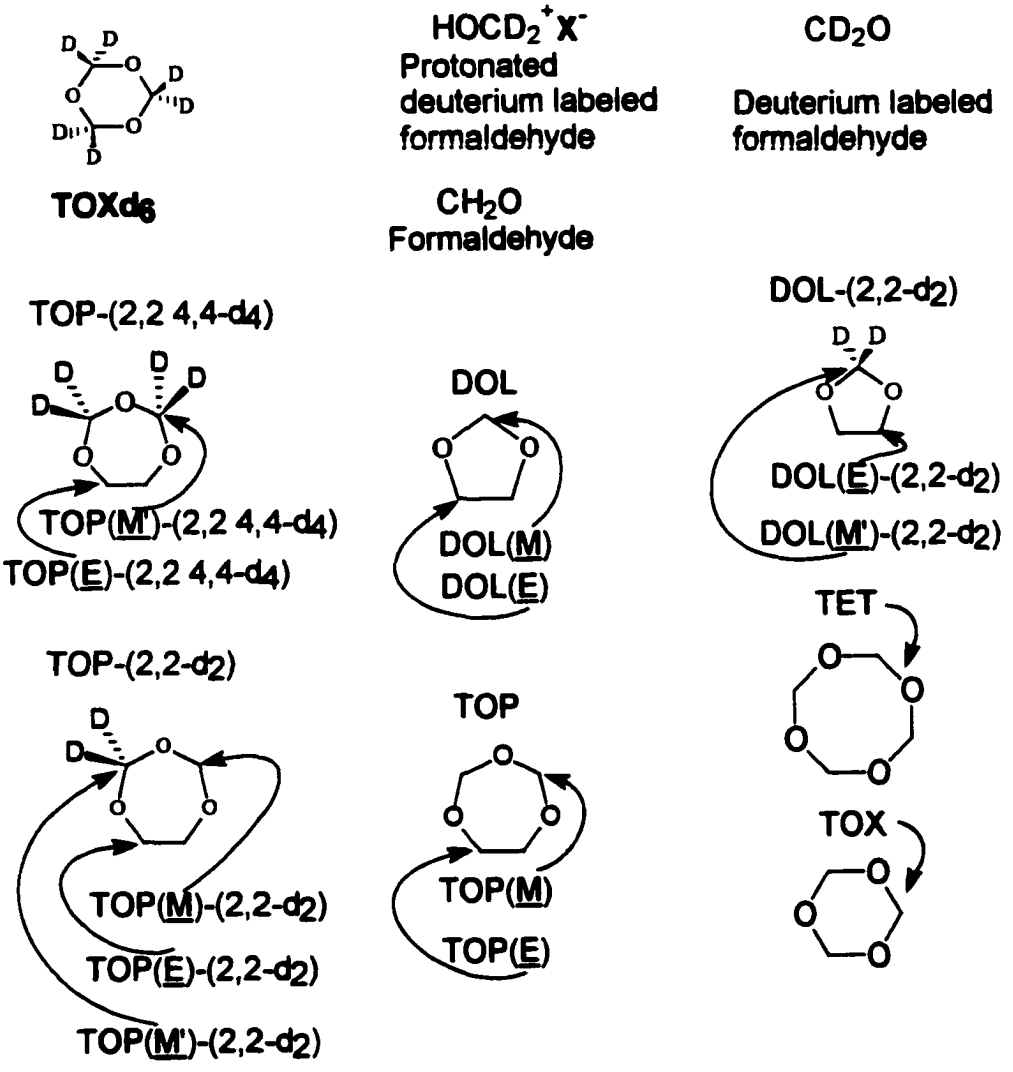

Figure (III 1)

III.A. TOX-d_6/DOL Copolymerization

The *in-situ* C-13 and DEPT NMR experiments of this copolymerization system resulted in the detection of enhanced shielding for α, and γ-deuterium substituted C-13 nuclei, giving insight into mechanistic routes responsible for their generation. The relative rates for generating different species were established based on the consideration of C-13 resonance peaks assigned for isotope labeled species in conjunction with kinetic curve of active species obtained from *in-situ* ^{1}H NMR. The proton and C-13 studies complement each other. The former provides a means of monitoring quantitatively with high sensitivity developing species in the initial stage of the copolymerization. The latter offers much enhanced resolution due to broader spectral width.

i. *In-Situ* ^{13}C NMR Analysis

The initial spectrum (Figure III.A.i. 1) in the *in-situ* ^{13}C NMR analysis of TOX-d_6/DOL copolymerization shows an up-field shift, due to hyperconjugation[2], of approximately 0.65 ppm for TOX-d_6 in comparison to the chemical shift of 93.23 ppm for carbons attached to protons only. The chemical shift and $J_{^{13}C\text{-}^2H}$ for TOX-d_6 is 92.58 ppm and 25 Hz respectively. Thus, the deuterium enhanced shielding of carbons in TOX-d_6 is similar to that of acetal carbons in DOL-(2,2-d_2) (0.64 ppm), giving additional supporting structural evidence for TOX-d_6. The DOL(M) peak is also seen at 94.43 ppm in this figure.

As copolymerization proceeds, the resonance of TOP(M) emerges within the quintet splitting of TOX-d_6 (Figure III.A.i. 2). The TOP(M)-(2,2-d_2) acetal peak is shifted up-field to 92.79 ppm, overlapping with one of the quintet splitting of TOX-d_6.

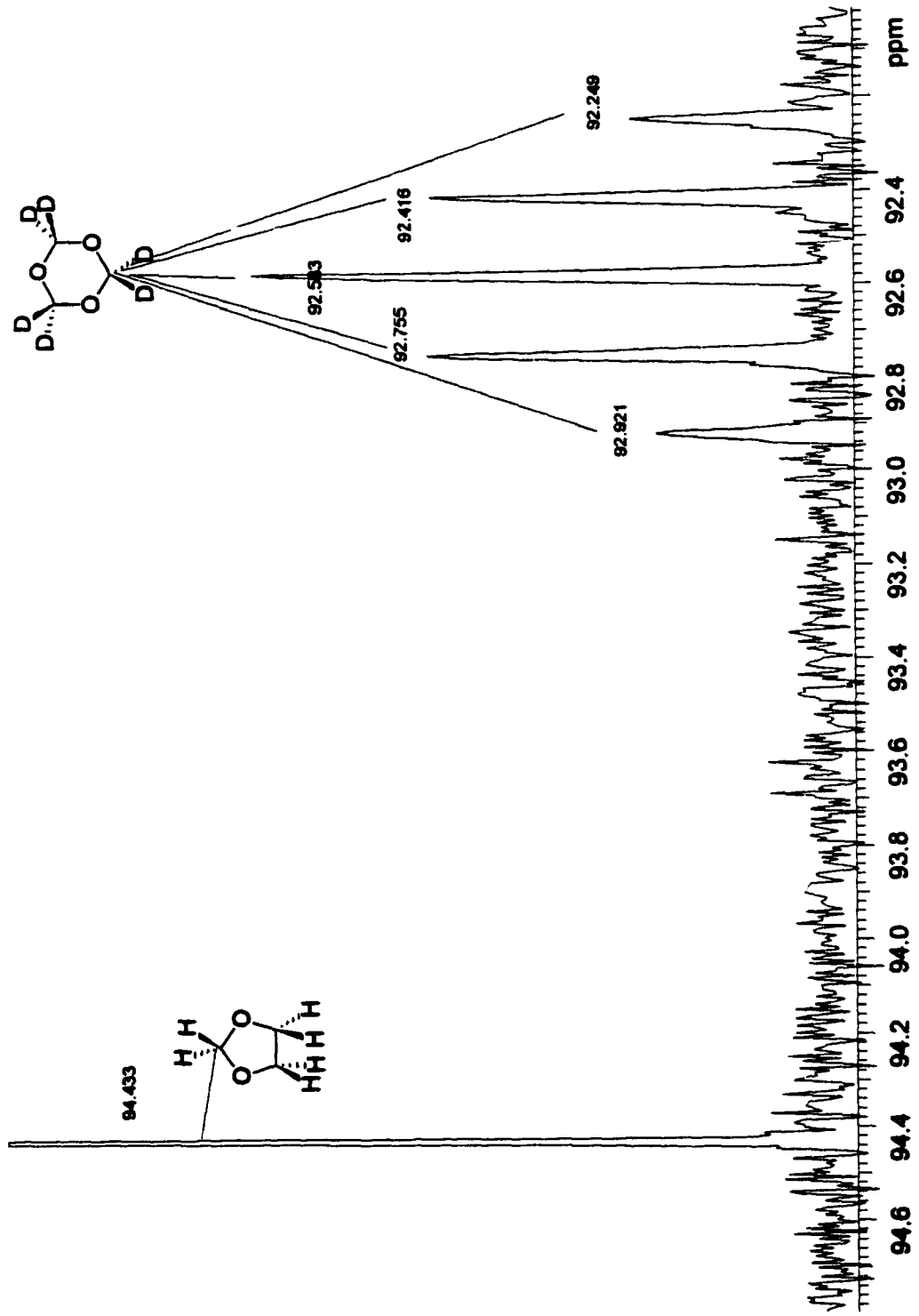

Figure (III.A.1.1) ^{13}C spectrum of **TOX-d_4/DOL** copolymerization before initiation
Monomers' mole ratio: (3,1), spectrometer: operating at 150 **MHz**, probe: **ID600-s**.

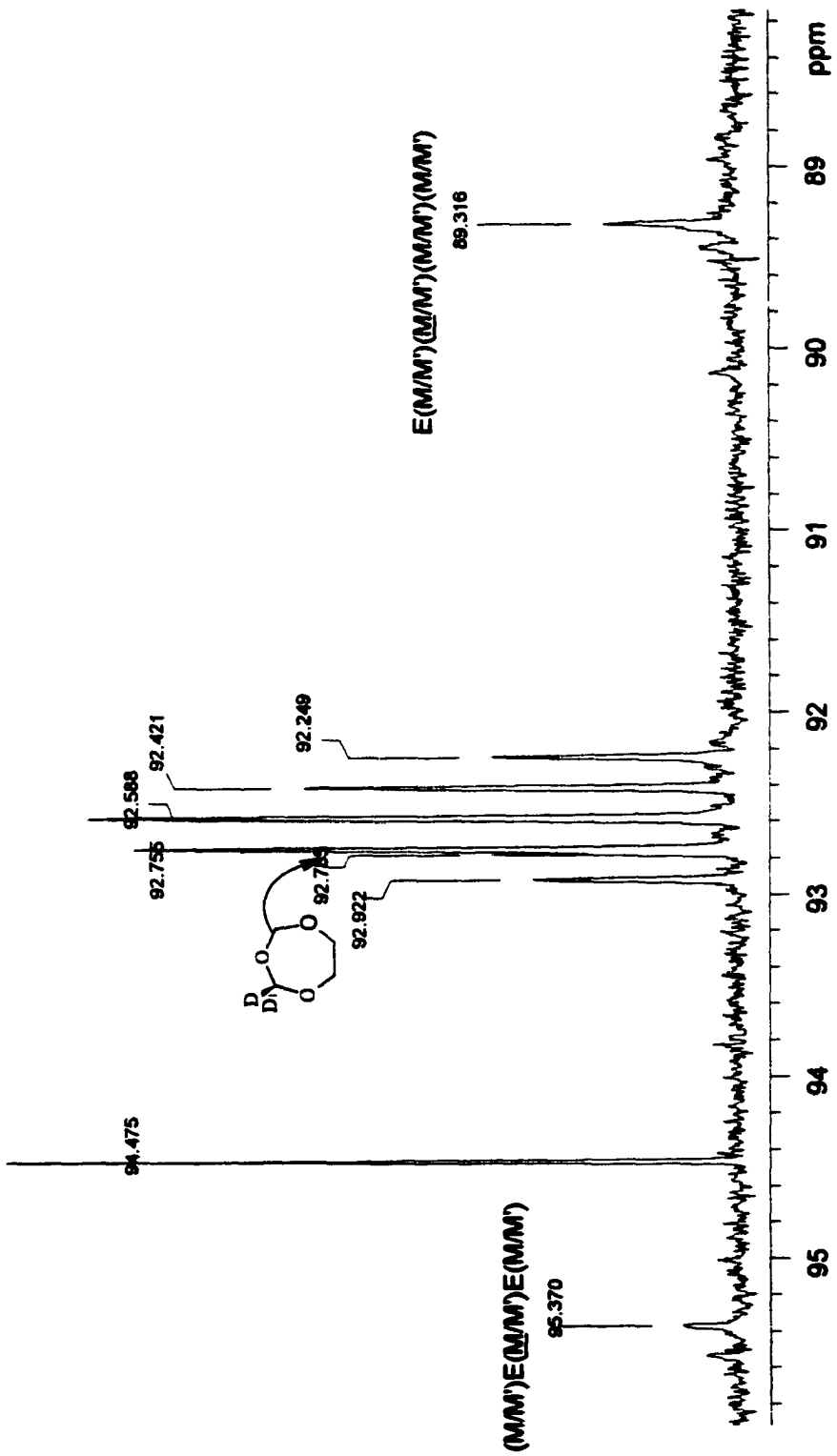

Figure (III.A.i. 2) ^{13}C spectrum of **TOX-d_4/DOL** copolymerization-"Emergence of Pentad Sequences and **TOP**". Monomers' mole ratio: (3,1), spectrometer: 600 MHz, probe: Nalorac, **DOL** conversion: 37% **DOL(E)**.

The **TOP(M)-(2,2-d_2)** peak was clearly seen in **DEPT** experiment **(Section ii)**. The peaks for **TOP(M')-(2,2 4,4-d_4)** were not observed due to its low concentration and the spreading of absorption intensity over quintet splitting.

The assignment of sequence peak **(M/M')E(M'/M)E(M/M')** at 95.37 ppm agrees with previous natural abundance experiment[3]. This sequence resonance occurs as a singlet confirming that the observed undeuterated methylene oxide units are surrounded by ethylene oxide units. The **E(M/M')(M'/M)(M/M')(M/M')** peak at 89.32 ppm was also assigned previously from natural abundance experiments.[3]

In the "E" region **(Figures III.A.i. 1-3)**, the **TOP(E)** peak at 69.54 ppm, **TOP(E)-(2,2-d_2)** at 69.48 ppm and **TOP(E)-(2,2 4,4-d_4)** at 69.56 ppm are also resolved and assigned based on their relative intensities in two isotope substitution copolymerization systems, i.e. **TOX-d_6/DOL** and **TOX/DOL-(2,2-d_2)** (see Section **III.B**). A qualitative analysis of the **TOP(E)** peaks reveals that the **TOP(E)-(2,2-d_2)** is consistently larger in comparison to **TOP(E)** and **TOP(E)-(2,2 4,4-d_4)** peaks as expected. This is explained by the high initial concentration of **TOX-d_6** and the single mechanistic route required for **TOP-(2,2-d_2)** synthesis. The **TOP-(2,2 4,4-d_4)** dominates over **TOP(E)**, reflecting the higher concentration of **CD_2O** to **CH_2O** (9/1).

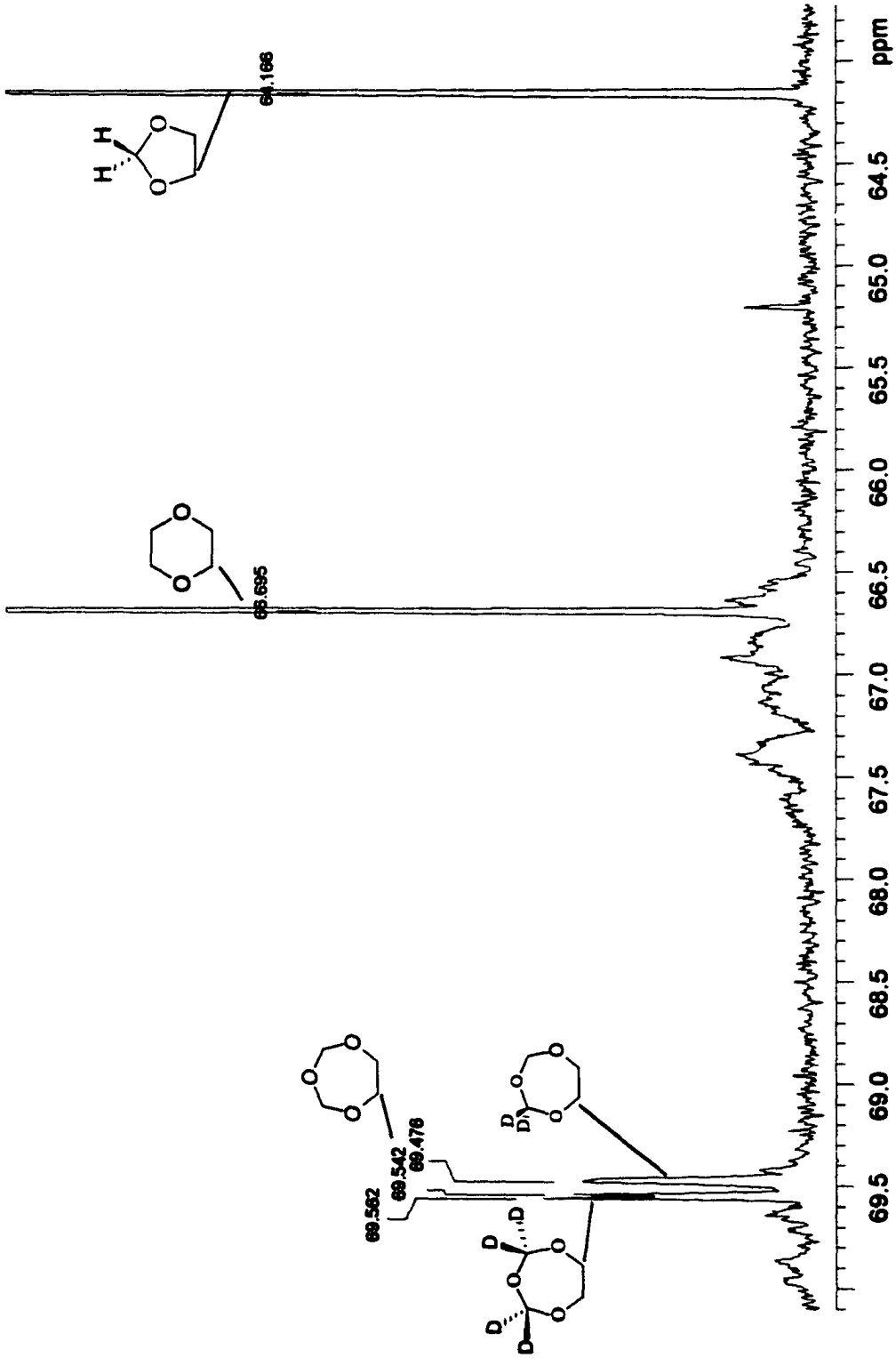

Figure (II.A.i.3) ^{13}C spectrum of **TOX-d_4/DOL** copolymerization-"Resolution of **TOP(E)** peaks". Monomers' mole ratio: (3,1), spectrometer: 600 **MHz**, probe: **ID600-s**, **DOL(E)** conversion: 37% .

III.A.ii. DEPT NMR Analysis

DEPT NMR experiment allows us to focus on only hydrogenated carbon atoms in the present system involving isotope substitution. The ***in-situ*** **DEPT NMR** analysis of the **TOX-d_6/DOL** copolymerization was conducted using a Varian Unity Plus Spectrometer fitted with an indirect detection probe operating at 150 **MHz** for carbon. This experiment tracks the components originating from **DOL** reactions. The spectrum **(Figure III.A.ii. 1)** immediately after initiation shows peaks including: **DOL(M)** at 94.51 ppm, **TOP(M)** at 92.75 ppm and **TOP(M)-(2,2-d_2)** at 92.72 ppm. The observation of **TOP(M)** and **TOP(M)-(2,2-d_2)** peaks adds to the understanding of the **^{1}H NMR** analysis of the comonomer melt. In the **^{1}H NMR** analysis **(Section III)** one peak at 4.89 ppm was assigned to **TOP(M)**. This shows that the chemical shift effect on hydrogen due to δ-deuterium substitution in proton **NMR** is not observable.

In the **'E'** region of the **DEPT** spectrum **(Figure III.A.ii. 1)**, the **TOP(E)-(2,2 4,4-d_4)**, **TOP(E)**, and **TOP(E)-(2,2-d_2)** representative peaks are located at 69.54, 69.53 and 69.46 ppm respectively. The singlet peak at 66.66 ppm represents 2,4-dioxane used as carrier solvent for initiator and as reference. In proton spectra, this peak was referenced at 3.66 ppm. The peak furthest up-field in the spectrum (64.12 ppm) represents **DOL(E)**. Up to 50% **DOL(E)** conversion in the pre-cloud period, **TOP(E)-(2,2-d_2)** maintained a greater concentration in comparison to **TOP(E)-(2,2 4,4-d_4)** and **TOP(E)** **(Figures III.A.ii. 1-2)**. The concentration of **TOP(E)-(2,2 4,4-d_4)** was also greater than **TOP(E)**, as was expected for a reaction system with (9/1) **CD_2O** to **CH_2O**.

Later on, the development of the sequence peaks **(M/M')E(M'/M)E(M/M')** 95.38

ppm, (M/M')E(M'/M)(M/M')(M/M') 92.56 ppm, E(M/M')(M'/M)(M/M')(M/M') 89.67 ppm, and E(M/M')(M'/M)(M/M')E 89.15 ppm are observed **(Figure III.A.ii 3)**. Peaks assigned to **TOX** (93.23 ppm), **TOX-d_2** (93.14 ppm) and **TOX-d_4** (93.10 ppm) begins to emerge. **TOX** reacts quickly while **TOX-(2,2-d_2)** and **TOX-(2,2 4,4-d_4)** persist in the copolymer melt. The spectra obtained from **DEPT NMR** analysis of this copolymer show that the "**M**-unit" of **DOL** separates efficiently into different sequences.

The "**E**-region", **(Figure III.A.ii 3)** shows the resolution of **DOL(E)** at 64.12 ppm and **DOL(E)-(2,2-d_2)** at 64.11 ppm, giving a 0.012 ppm as the γ-deuterium isotope effect on **DOL(E)**. A deuterium shielding of 0.06 ppm for **TOP(E)** with respect to **TOP(E)-(2,2-d_2)** was observed. The observation of **DOL(E)-(2,2-d_2)** also confirms its synthesis in this copolymerization system.

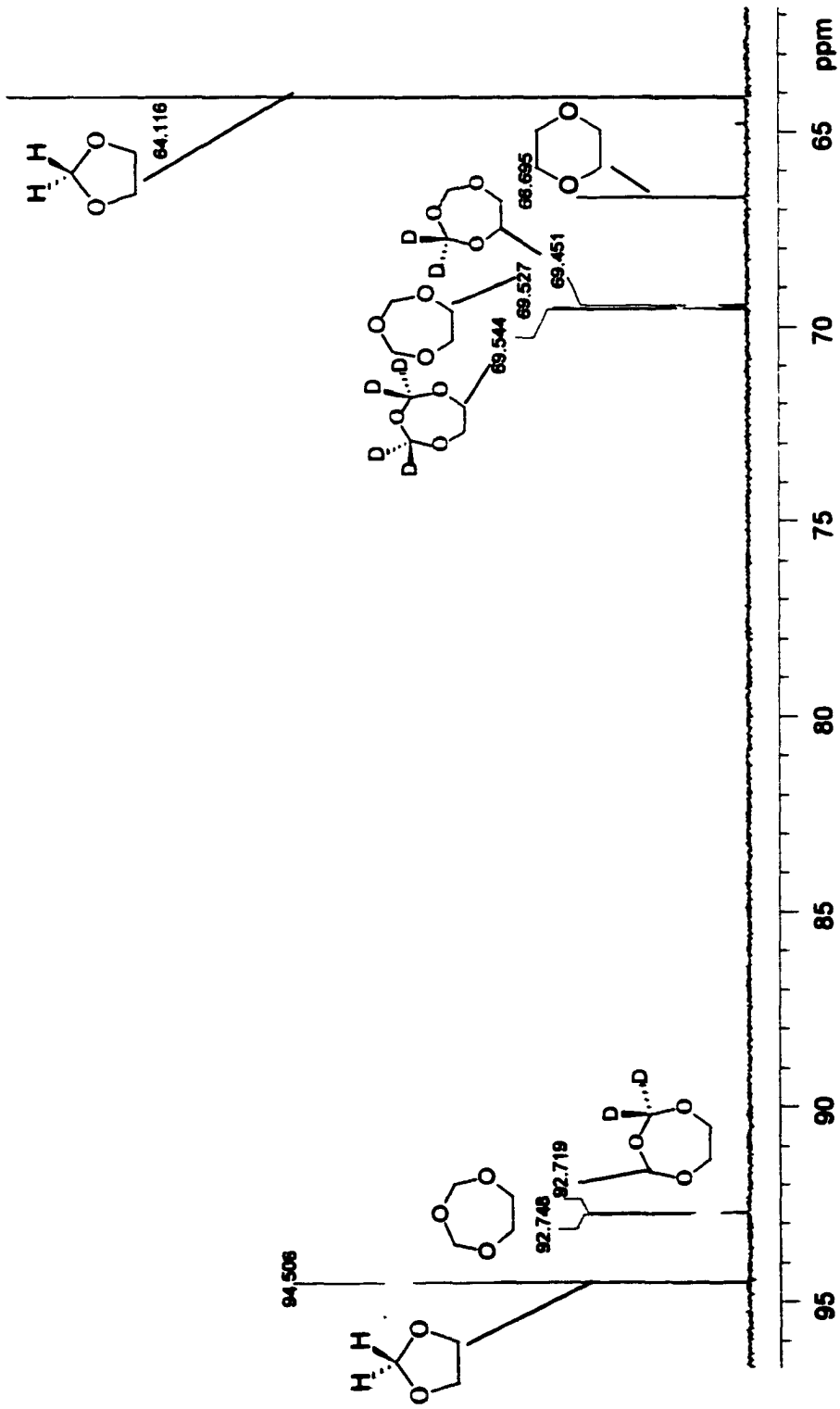

Figure (III.A.ii. 1) **DEPT** spectrum of **TOX-d_4/DOL** copolymerization-"Elimination of **TOXd_4** peaks". Monomers' mole ratio: (3,1), spectrometer: 600 **MHz** probe: **ID600-4**, **DOL(E)** conversion: 16% .

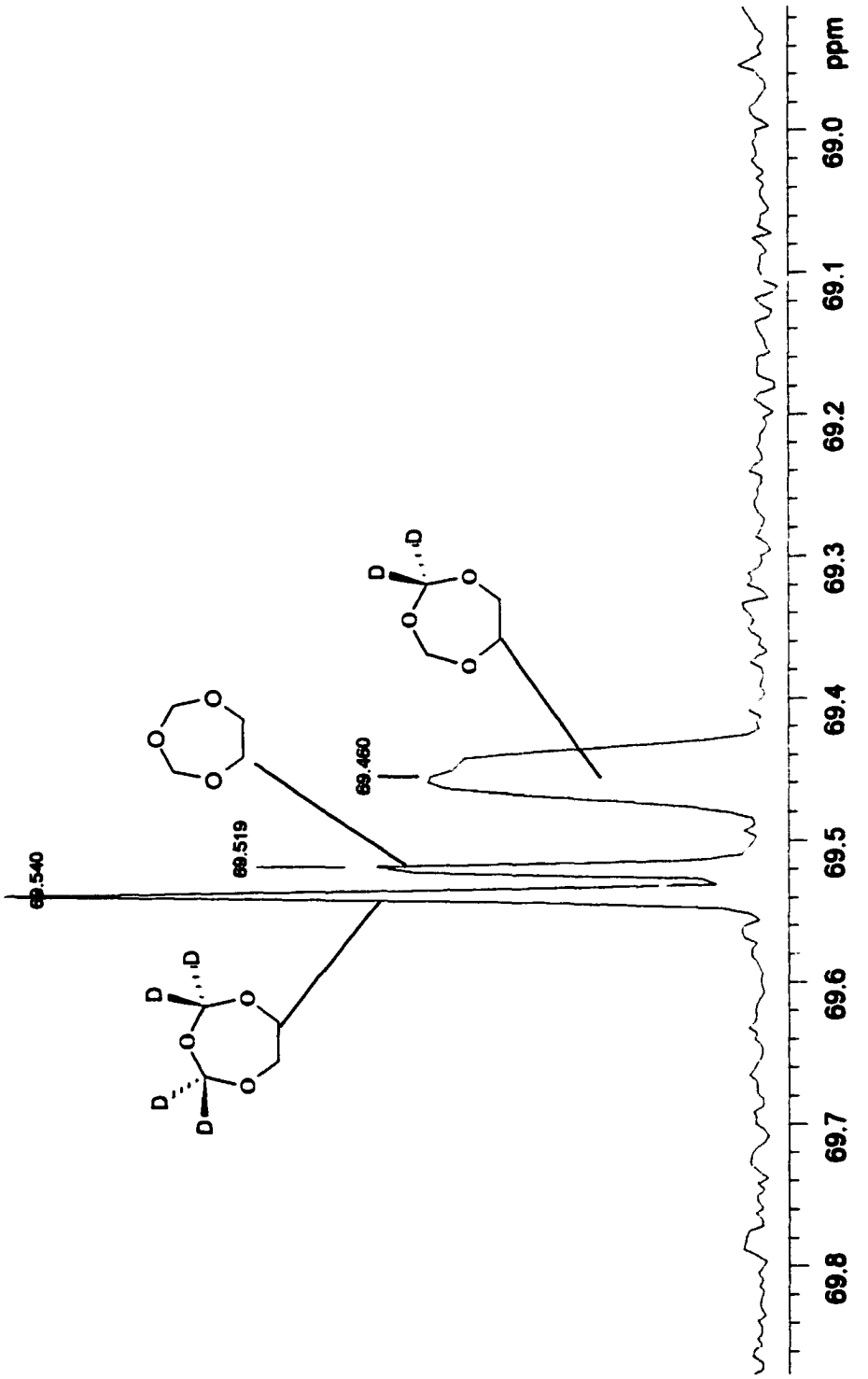

Figure (III.A.ii. 2) **DEPT** spectrum of **TOX-d_4/DOL** copolymerization-"**TOP(E)** assignment". Monomers' mole ratio: (3,1), spectrometer: 600 **MHz**, probe: **ID600-s**, **DOL(E)** conversion: 54% .

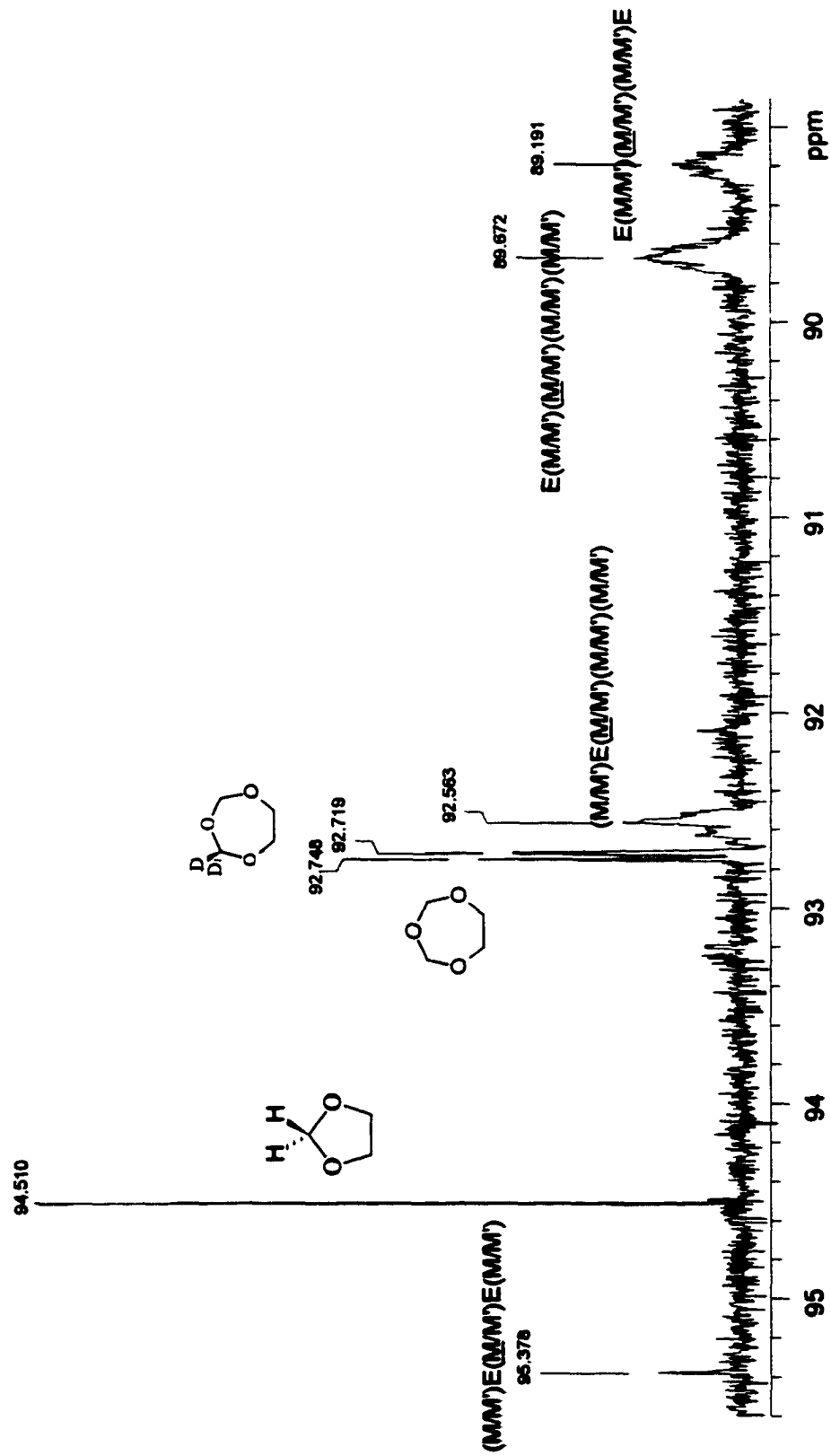

Figure (III.A.ii.3) **DEPT** spectrum of **TOX-d$_4$/DOL** copolymerization-"M-region". Monomers' mole ratio: (3,1), spectrometer: 600 MHz *probe*: **ID600-4**, **DOL(E)** conversion: 81%.

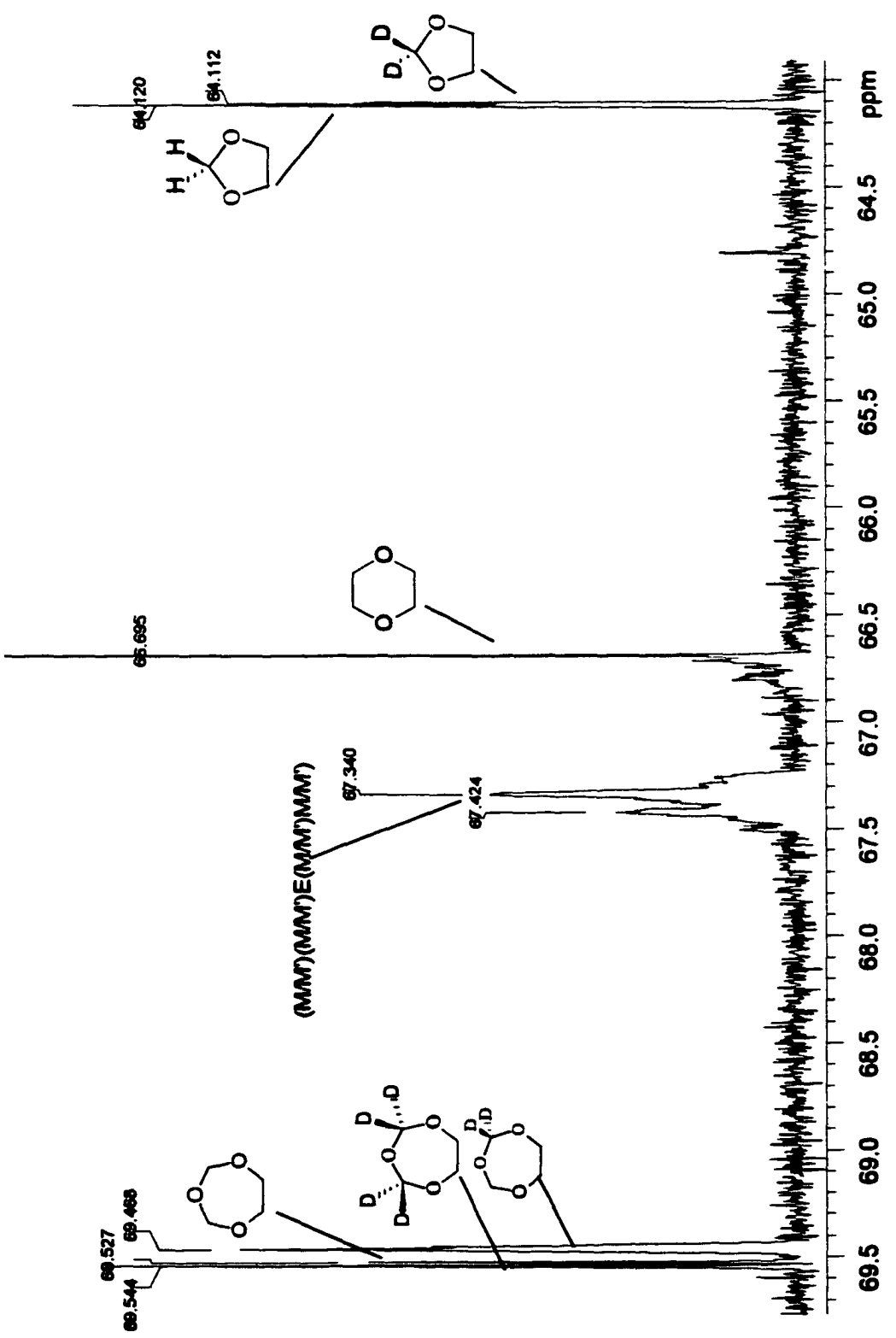

Figure (III.A.ii. 4) **DEPT** spectrum of **TOX-d$_4$/DOL** copolymerization-"**E**-region". Monomers' mole ratio: (3,1), spectrometer: 600 **MHz**, probe: **ID600-s**, **DOL** conversion: 81%

III.A.iii. ^{1}H NMR Analysis

The processes involved in the cationic copolymerization of perdeuterated trioxane/dioxolane (**TOX-d_6/DOL**) were investigated using *in-situ* ^{1}H NMR. Replacing **TOX** with **TOX-d_6** as monomer eliminates the ^{1}H peaks originating from **TOX**, hence improving signal dynamic range as well as overall resolutions of the spectra. This resolution persists until solidification of the copolymerization system at 90 to 95% **DOL** conversion. This deuterium labeled system allows us to focus on the kinetics involving all species derived from **DOL**. Species from the ethyleneoxide unit "**E**" of **DOL** will manifest themselves as in the case of natural isotopic abundance. Evidence from these experiments show three distinct stages marked by net increases in the rates of sequences formation. In the first stage, activated **DOL** preferentially reacts with formaldehyde to produce deuterium labeled trioxepane (**TOP-2,2-d_2**). Concurrently, **TOP-(2,2-d_2)** generate all the observed sequences and additional comonomers simultaneously. In the second stage, the effect of **TOP-(2,2-d_2)/DOL** copolymerization results in the increased formation of several sequences. In the third stage, transacetalization involving pentad sequences with two and three "**E**" and the propagating chain end results in the separation of **E** units in the copolymer chains.

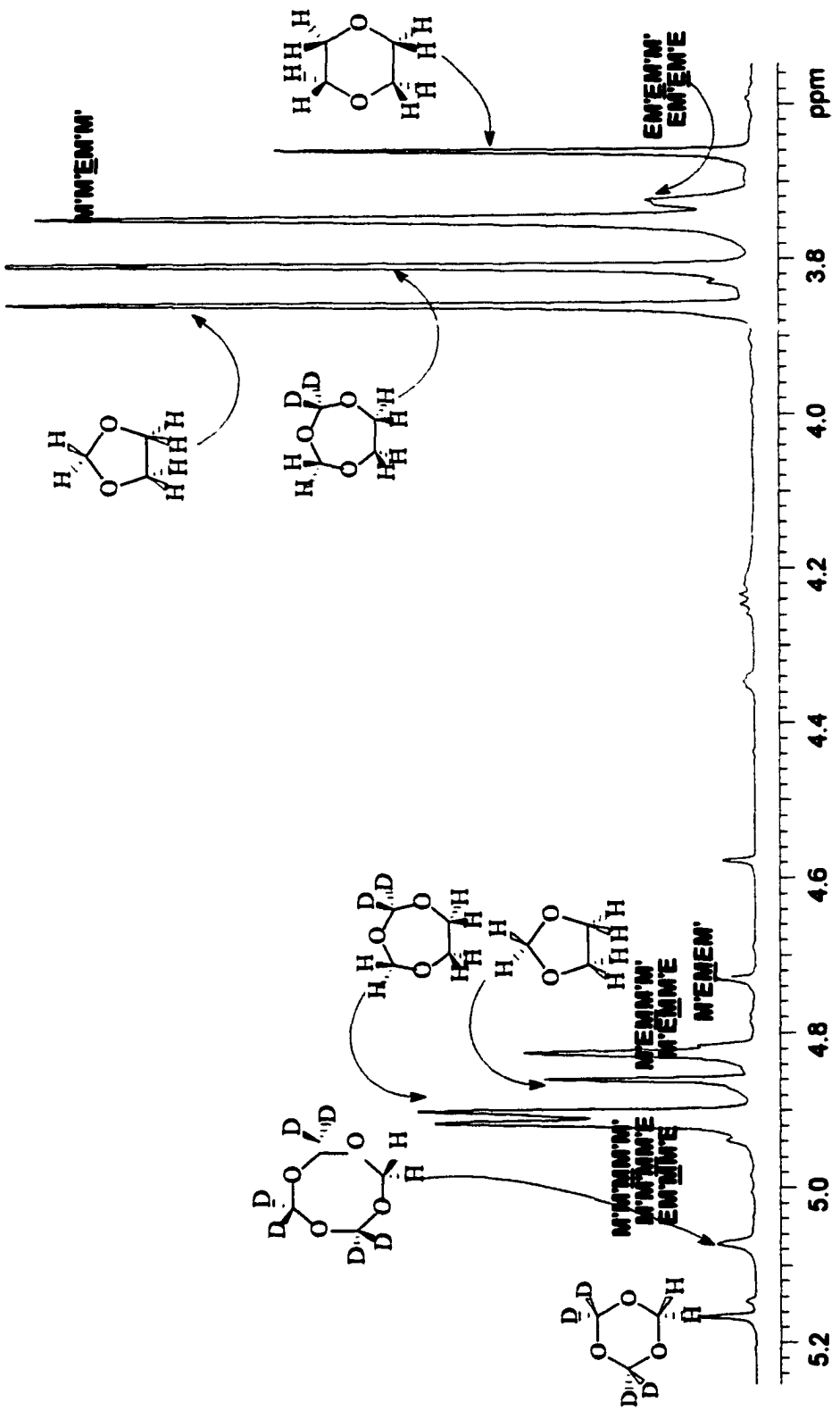

Figure (III.A.iii 1) **^{1}H** spectrum of **TOX-d_4/DOL** copolymerization-"Peak Assignment for: (**M** and **E** regions)" Monomers' mole ratio: (3,1), [**BF_3OEt_2**]: 20 ppm, spectrometer: 600 **MHz**, probe: ID600-s, **DOL(E)** conversion: 70%.

Assignments and Observations

In-situ **^{1}H NMR (600 MHz)** observation of the copolymerization of perdeuterated trioxane, **TOX-d_6**, with 1,3-dioxolane, **DOL**, led to a wealth of information not available from systems with natural isotopic abundance. Pentad resolution was achieved with a significant improvement in overall dynamic range. Pentad resolution was confirmed from the assignment of nine sequence peaks. The spectrum (**Figure III.A.iii 1**) before introduction of initiator displayed an essentially two to one peak ratio for the oxyethylene, **E**, (3.86, $^1J_{^1H-^{13}C}$ 73) and oxymethylene, **M**, (4.86, $^1J_{^1H-^{13}C}$ 84) groups of **DOL**. $^3J_{^1H-^1H}$ coupling (7 Hz) forming three peaks were also observed for the ethylene protons of **DOL**, i.e. three bond correlation between ethylene hydrogens attached to ^{13}C nuclei and those attached to ^{12}C nuclei splits the **DOL(E)** satellites into two triplets. Compared with the **M** of **DOL**, **DOL(M)**, the **DOL(E)** is consumed at a slower rate. Up to 40% **DOL(E)** conversion, the peak intensity ratio for **DOL(E)/DOL(M)** was clearly greater than two, suggesting the production of **DOL-(2,2-d_2)**. Concurrently, the development of a hydrogenated formaldehyde peak at 9.68 ppm was observed.

Because methylene oxide units in this experiment can be deuterium labeled -CD_2O- (**M**) or unlabeled -CH_2O- (**M**), the peak assigned as **MEMEM** (4.74 ppm) observed first at approximately 2% **DOL(E)** conversion is more accurately represented as **(M/M)E(M /M)E(M/M)**. Three pentads sequences with **E**-center **(M/M)(M/M)E(M/M)(M/M)** (3.75 ppm), **E(M /M)E(/M/M)(M /M)** (3.73 ppm), **E(M /M)E(/M/M)E** (3.726 ppm), were later observed at approximately 3% **DOL(E)** conversion. The delayed observation of the **E**-center pentads resulted from their overlapping with the ^{13}C satellite peaks of **DOL(E)**. Partial resolution was also observed

for (M/M)E(M/M)(M/M)(M/M) (4.83 ppm) from (M/M)E(M/M)(M/M)E (4.82 ppm) and E(M/M)E(M/M)(M/M) from E(M/M)E(M/M)E peaks. As a result, the relation between the sequences E(M/M)E(M/M)E and (M/M)E(M /M)E(M/M) could not be observed.

The presence of the pentad sequences (M/M)(M/M)(M /M)(M/M)(M/M), E(M/M)(M /M)(M/M)(M/M), and E(M/M)(M /M)(M/M)E were not ascertained until 12% DOL(E) conversion due to the overlap with TOP(M), while the sequences (M/M)E(M /M)(M/M)(M/M) and (M/M)E(M /M)(M/M)E were not observed until 14% DOL(E) conversion due to overlap with DOL(M). The peak areas for the sequences (M/M)(M/M)(M /M)(M/M)(M/M), E(M/M)(M /M)(M/M)(M/M), and E(M/M)(M /M)(M/M)E were calculated by subtracting one half of TOP(E)'s peak area from the region containing these peaks. These peaks were resolved in separate experiments involving TOX and DOL-(2,2-d_2) as comonomers (Section III.B). Subtracting one half of TOP(E) peak area to eliminate TOP(M) is only approximate, because of the presence of TOP with varying numbers of deuterium labels at the acetal carbons; thus the (M/M)(M/M)(M /M)(M/M)(M/M), E(M/M)(M /M)(M/M)(M/M), and E(M/M)(M /M)(M/M)E peak areas are under-represented. This also prevents the quantification of TOP(E) to TOP(M) peak ratio with different numbers of deuterium. During the course of polymerization, "M" from DOL(M) and E from DOL(E) were distributed over a number of species with the conservation of total units. Thus, the total integrated intensity of DOL(M), TOP(M), TOX, tetraoxane, TET, formaldehyde, E(M /M)(M /M), E(M /M)E and (M/M)(M /M)(M/M) remains unchanged over the period of observation. The same behaviors was observed for the intensities of resonances derived form DOL(E).

Mechanism

The kinetic profiles for the species involved in the copolymerization are represented by curves in **Figure (III.A.iii 1)**. From these kinetic curves, the average growth and consumption rates for each component at different stages were determined.

The rates of active components versus spectrum number (time) are depicted in **Figure (III.A.iii. 2)**.

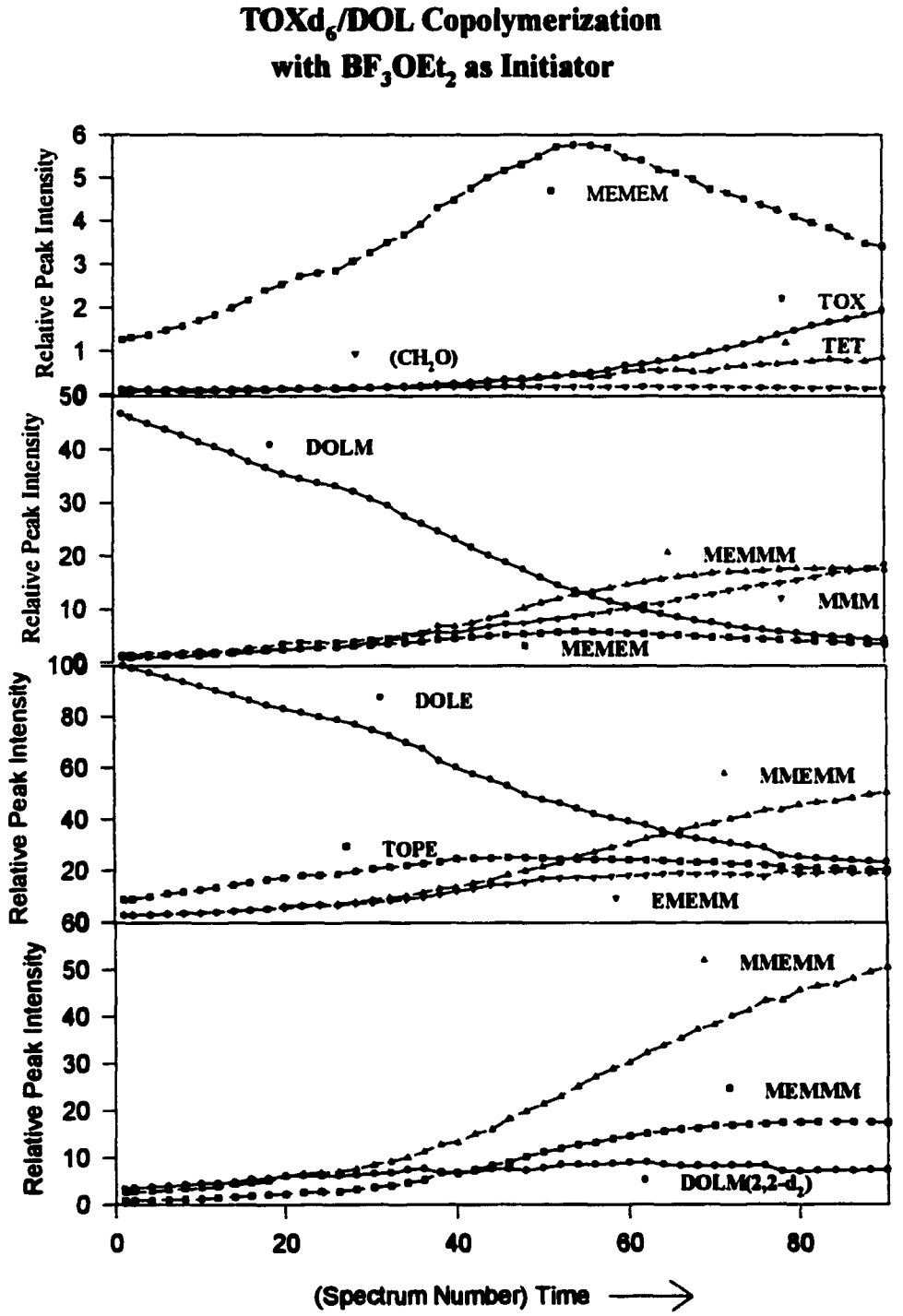

Figure (III.A.iii 1) Kinetic Curves of active component in TOX-d_6/DOL Copolymerization with BF_3OEt as Initiator. Relative integral obtained from ^1H NMR spectra.

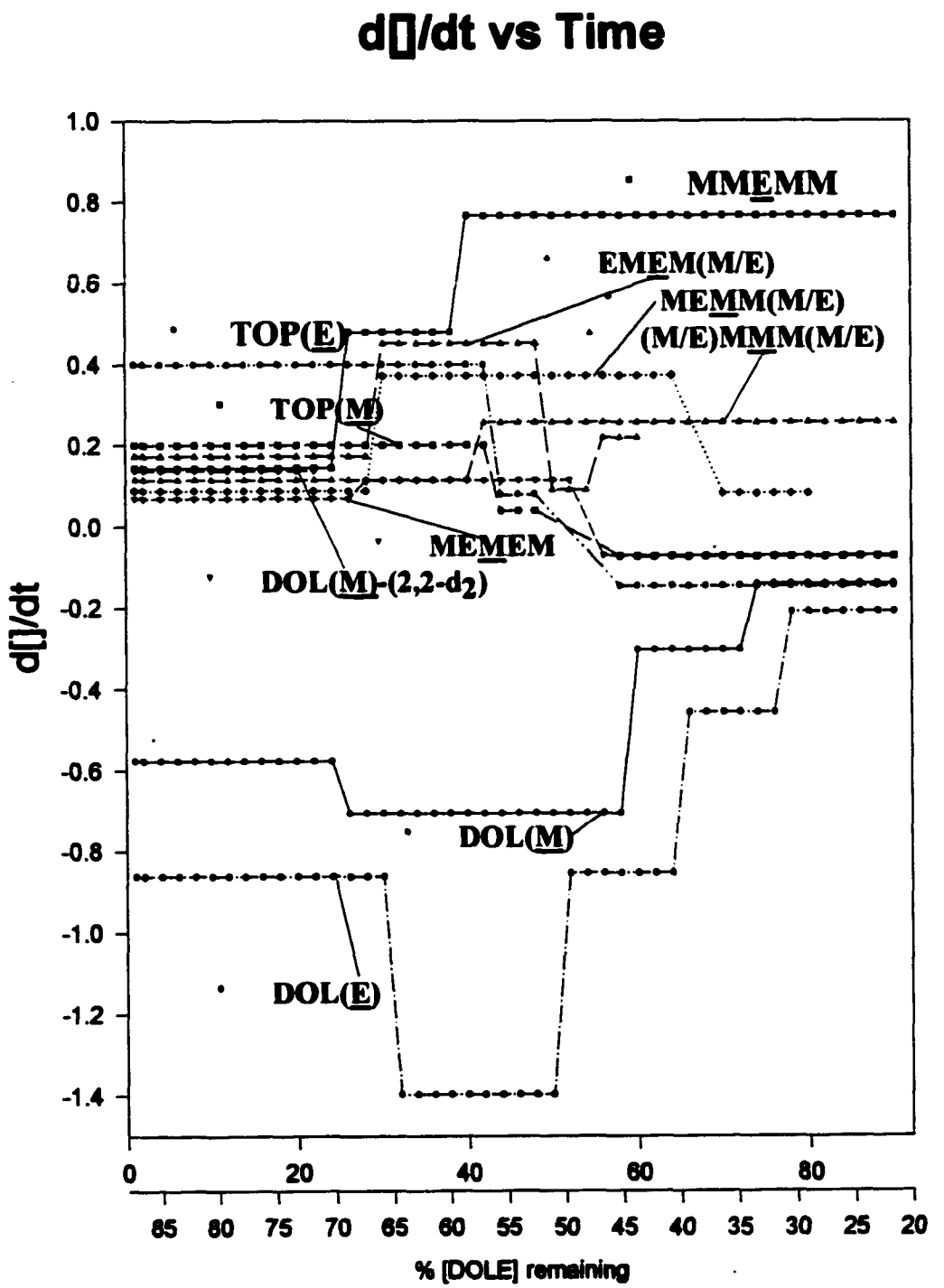

Figure (III.A.iii. 2) Rate Curves of active components in TOX-d_2/DOL Copolymerization.

The symbol '[]' in Figure (III.A.iii 2) represents concentration of various active components.

Stage 1

Initial processes

After initiation, **TOX-d_6 (1)** dissociates to yield deuterated formaldehyde **(3)** and protonated deuterium labeled formaldehyde (**$HOCD_2^+X^-$**), **(3a)** as seen in **reaction (i)**.

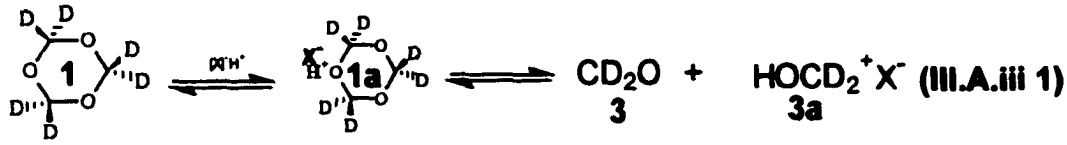

(III.A.iii 1)

After initiation in the presence of high concentrations of **TOX-d_6**, the generation of deuterium labeled formaldehyde is favored[4,5], after initiation. This process provides a means for the continued production of **CD_2O (3)**. Thus, **(3a)**, in turn, reacts with **(1)** to continue the catalytic dissociation of **TOX-d_6**. In fact, without the continued presence of **(3a)** throughout the initial processes, the dissociation of **(1)** would halt, resulting in premature termination. This is usually encountered in cases with low initiator concentrations.

The protonation of **DOL (2)** forming protonated **DOL (2a)** occurs simultaneously with the protonation and dissociation of **TOX-d_6**. The protonation of **DOL** to form **(2a)** is shown in **reaction (III.A.iii 2)**.

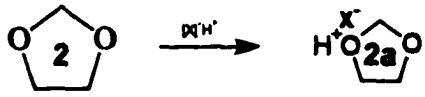

(III.A.iii 2)

The protonated **DOL** produced then reacts with deuterium labeled formaldehyde. forming protonated **TOP-(2,2-d_2) (4a)**, **(Reaction III.Aiii 3)**. It should be noted that **TOP-(2,2-d_2)** has three different reactive sites labeled 4_a, 4_b and 4_c. The subscripts are used to distinguishing reactive sites on **TOP-(2,2-d_2)** from activated structures at these sites (**4a**, **4b**, **4c**).

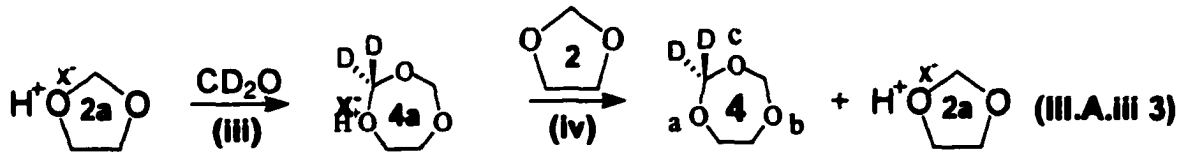

(III.A.iii 3)

The insertion of CD_2O[4] **(3)** into **(2a)** to form **(4a)** is followed by rapid proton exchange to **(2)** forming **(2a)** and **(4)**. The higher basicity and concentration of **(2)** in comparison to **(4)** ensures an efficient proton transfer. This cycle continues to produce **(4)** depending on the availability of **(3)**. The rapid build up of **TOP-(2,2-d_2)** shows the high efficiency of this process. This cycle results in the conversion of a large portion of the initiating protons to **(2a)**. The reactions of **DOL** with **(3a)** or **(2a)** with **(3)** to produce **TOP-(2,2-d_2)** dominate the initial processes. The generation of **TOP-(2,2-d_2)** is coupled with its polymerization. The net rate of production of **TOP-(2,2-d_2)** is approximately twice its consumption in polymerization reactions (*vide infra*). The reactions of **(3a)**, $HOCD_2^+$,

obtained from the dissociation of **(1a)** with **DOL** can preferentially form sequences.

The structure **(2a)** initiates copolymerization by reacting with 4_a, 4_b and 4_c. The activated structures formed from these unions are different from the activated structures formed by way of protonation. Because **(2a)** has resonance structures, carbenium ↔ oxonium, it is a softer acid than the initiator. The reaction of **(2a)** with **TOP-(2,2-d_2)** at 4_a, 4_b and 4_c forms the structures indicated in **Reaction (III.Aiii 4)**.

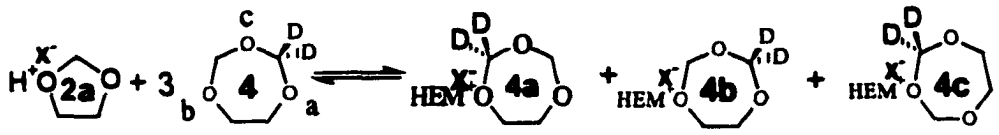

(III.A.iii 4)

The stability of **(4a)** and **(4b)** are similar while the stability of **(4c)** is definitely lower. The resonance carbenium structures of **(4a)**, **(4b)** and **(4c)** allow their involvement in comonomer syntheses. Upon ring opening, the structure **(4b)** was considered likely to dissociate[6], giving hydrogenated formaldehyde **(7)** and the cyclic oxonium ion of **DOL-(2,2-d_2) (5a)**.

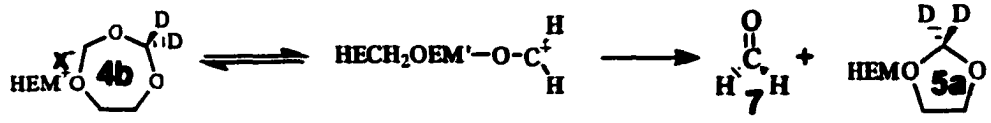

(III.A.iii 5)

Equilibrium charge transfer of **(5a)** to **(2)** then results in the formation of **DOL-(2,2-d_2) (5)**.

Alternately, the initiation at site 4_c followed by intra molecular charge transfers to the more basic site 4_b results in the formation of **(5a)**. This then results in the generation of **(5)** by way of equilibrium charge transfer to **(2)**.

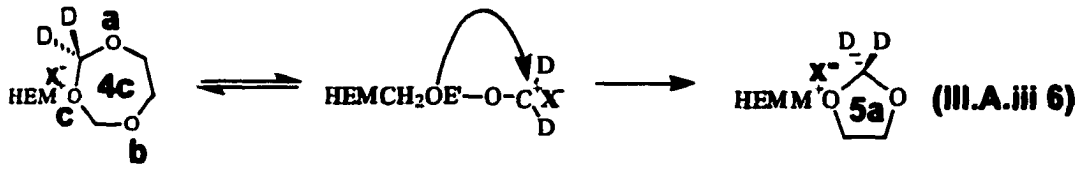

(III.A.iii 6)

This route has the advantage of circumventing the elimination of CH_2O from activated **TOP-(2,2-d_2)** to yield **DOL-(2,2-d_2)** observed. This followed by equilibrium charge transfer to **2a** results in the formation of **5**. The elimination of CH_2O or CD_2O from activated **TOP-(2,2-d_2)** to form **DOL** is unlikely because **TOP-(2,2-d_2)** is being generated rapidly throughout the copolymerization reaction. As a result, an independent route for the synthesis of CH_2O **(Reaction III.A.iii 6)** was developed. This route can also generate **(2a)** as seen in separate copolymerization systems of **TOX/DOL-(2,2-d_2)**. The polymerization reactions of **TOP** occur simultaneously with these syntheses. These polymerization reactions of **TOP** provides the routes for the initial generation of the observed sequences.

The structure **(4c)** can also incorporate CD_2O **(3)** by insertion without changing its oxonium ion **(Reaction III.A.iii 7)**.

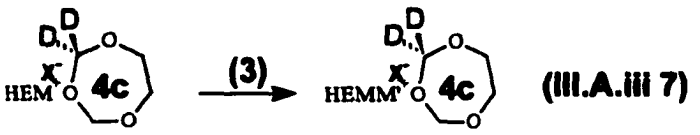

(III.A.iii 7)

This allows the system to incorporate excess deuterium labeled formaldehyde to generate sequences. In natural abundance experiments, this would result in a higher net rate of formation of all M-centered pentads.

Comonomers syntheses

Generation of CH_2O

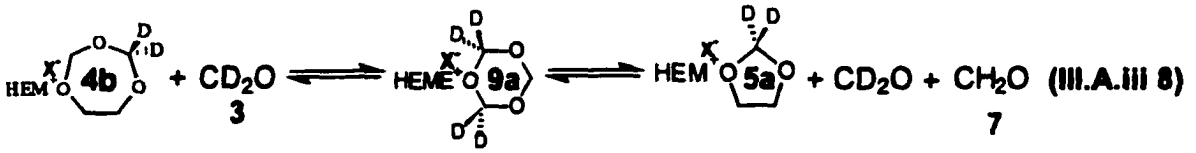

(III.A.iii 8)

The insertion of (3)[5] into structures (4b) results in the formation of (9a). The formation of (9a) early in the copolymerization reaction is followed by rapid dissociation to give CD_2O, CH_2O, and (5a) or (2a). This route for the generation of CH_2O is independent of the generation of (5) and as such explains the difference in formation rate of these species. The generation of (5) is approximately 100 time faster than the generation of unlabeled formaldehyde (7). This observation along with the negligible consumption of CH_2O in the presence of a large concentration of CD_2O suggests a route for the simultaneous generation

of (7) and (5) independent of the dissociation of initiated **TOP-(2,2-d_2)**. Later in the copolymerization, the structure labeled **(9a)** in **Reaction (III.A.iii 8)** persists long enough to synthesize **TOX-(d_4)**, **TET-(d_6)** and to form the major proportion of propagating chain ends. The generation of structure **(10a)** requires the insertion of formaldehyde[5] in **(9a)** as seen in **Reaction (III.A.iii 9)**.

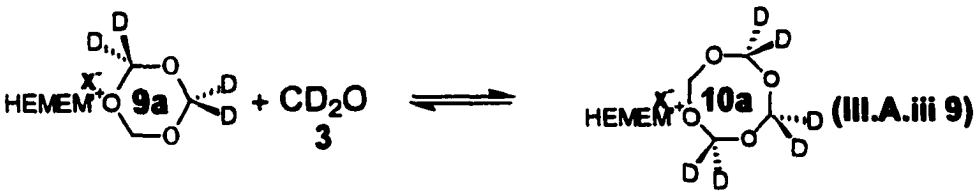

These activated structures can then produce sequences or generate the cyclic monomers observed including: **TOX-d_4**, **(9)**, or **TET-d_6**, **(10)**, along with other such monomers with different numbers of deuterium atoms. The observed generation of these structures confirms the occurrence of formaldehyde insertion[5] as depicted in Reaction **(III.A.iii 9)**.

TOP

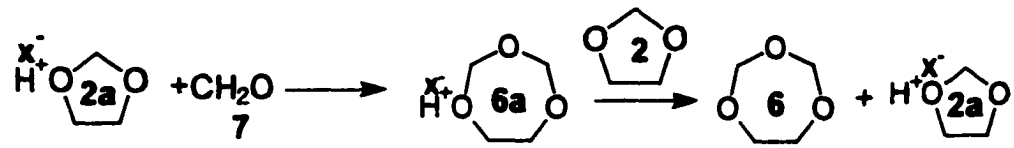

(III.A.iii 10)

The insertion[7,8] of CH_2O in (2a) results in the formation of (6a), followed by charge transfer to (2) gives (6) (**Reaction III.A.iii 10**). Because the rate of (7) production in this system and the concentration of (2a) are low, the rate of (6) production also has to be low.

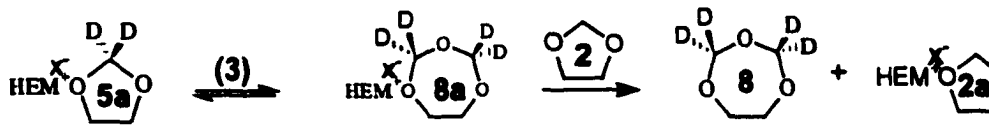

(III.A.iii 11)

The possibility of CD_2O reacting with the structure (5a), (**Reaction (III.A.iii 11)**, is high, because of the rapid generation of CD_2O (3) obtained from the dissociation of **TOX-D_6**. This reaction followed by charge transfer to (2) results in the formation of **TOP-(2,2 4,4-d_4)**, (8), and (2a). The possibility exists in this case for an intra-molecular charge transfer resulting in the generation of protonated **DOL** and (8). This route for the generation of **TOP-(2,2 4,4-d_4)** shows that **TOP**'s production is not limited to protonated **TOP-(2,2-d_2)**. For the instances where intra molecular reaction can produce activated **DOL**, the question arises whether intra or inter molecular reaction is required with (2a).

TOP Homopolymerization (Scheme I)

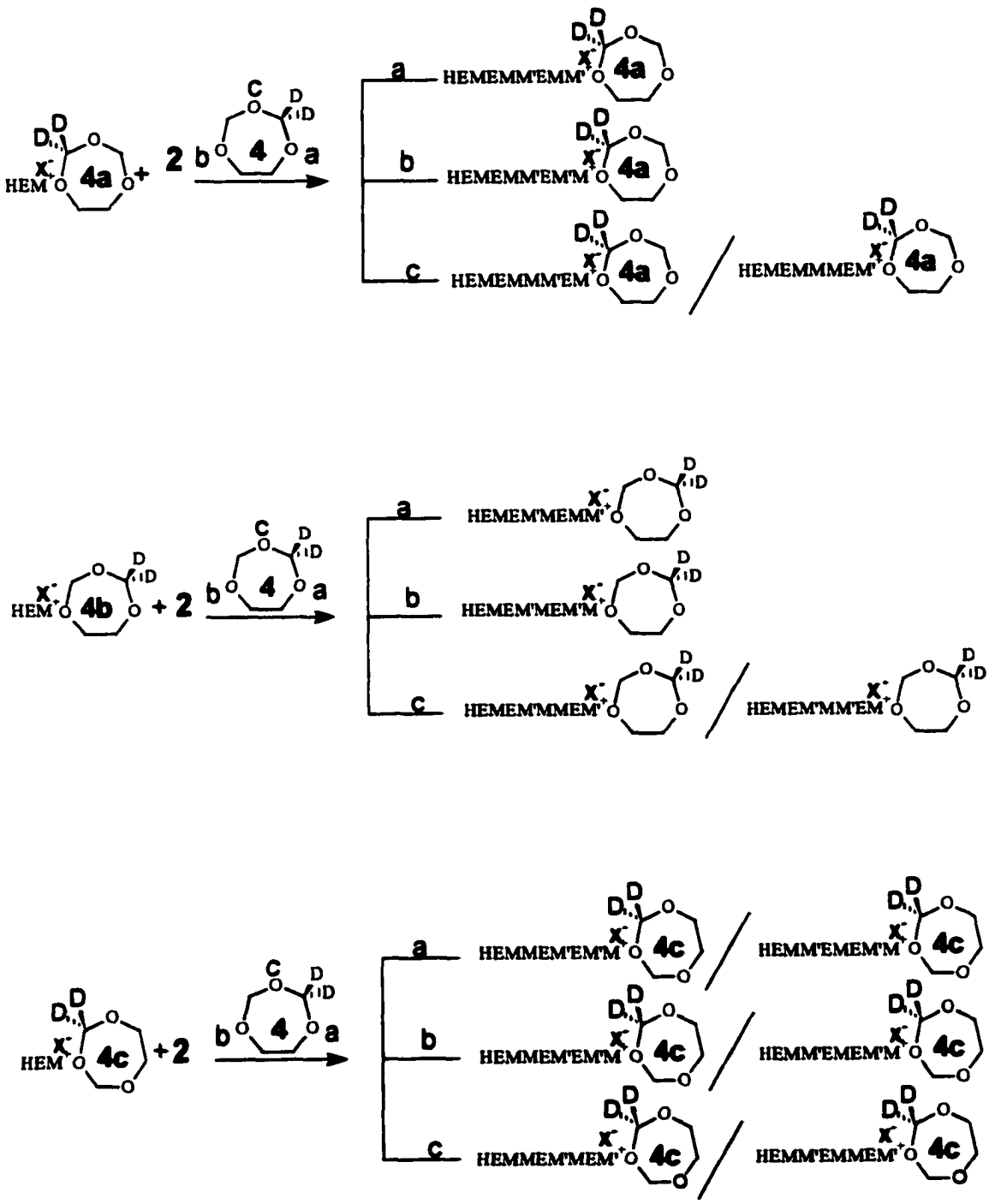

Scheme I

Scheme (I) shows all the possible microstructures produced in the homopolymerization of **TOP-(2,2-d_2)**. These microstructures in terms of pentad sequences include: **(M/M)E(M /M)E(M/M), E(M /M)E(/M/M)(M /M), E(M /M)E(/M/M)E, (M/M)(M/M)E(M/M)(M/M), E(M/M)(M /M)(M/M)E, (M /M)E(M/M)(M /M)E** plus **(M /M)E(M/M)(M /M)(M/M)**. The two pentad sequences excluded from the above list are **EMMMM** and **MMMMM**, where except the observed **M**, the methyleneoxide unit can be either hydrogenated or deuterium labeled. These two sequences are generated at later stages by transacetalization. The homopolymerizations of **(4_a), (4_b)** and **(4_c)** produce the sequences, **(M/M)(M/M)E(M/M)(M/M), (M /M)E(MM)(M/M)E** plus **(M /M)E(M/M)(M /M)(M/M)**. The cross polymerization of **(4b,4_c)** and **(4a,4_c)** produce the sequences **(M/M)E(M /M)E(M/M), E(M/M)(M /M)(M/M)E, E(M /M)E(/M/M)(M /M)** plus **E(M /M)E(/M/M)E**. The rate ratio of building up **TOP-(2,2-d_2)** to the **E(M/M)M(M/M)E** sequence is two to one early in the copolymerization and only the cross polymerization reactions of **TOP-(2,2-d_2)** can produce this sequence at a high net rate. The copolymerization equation[9] governing the reaction of **TOP-(2,2-d_2)** can be given as follows.

$$\frac{d[4_a]}{d[4_b]} = \frac{[4_a](r_1[4_a]+[4_b])}{[4_b]([4_a]+r_2[4_b])}$$

Substituting $d[4_a]/dt=d[4_c]/dt$ and $[4_a]=2[4_c]$ in equation (1) gives the following relation.

$$1 = \frac{2[4_b]^2(2r_1 + 1)}{[4_b]^2(2 + r_2)} \text{ or } (4r_1 = r_2)$$

The reactivity ratios r_1 and r_2 are defined as k_{4a4a}/k_{4a4c} and k_{4c4c}/k_{4c4a} respectively. The sequences generated by propagations associated with by r_1 and r_2 are **EM(M)(E)MM/EM(M)(M)EM** and **ME(M)MEM/ME(M)(E)MM** respectively without stipulation of **M** and **M**. These sequences in some cases relate two observed pentad sequences. For example, the polymerization of **TOP**, generating the **[EMM][EMM]** sequence, represents two pentads: **EMMEM** and **MMEMM**. In cases such as this, the average rates of the two pentad sequences are taken to represent the **4a/4a** propagation. This gives experimental values for k_{11}/k_{12} and k_{22}/k_{21} equal to (0.040)/(0.051) and (0.044)/(0.045) respectively. From these values of k_{11}/k_{12} and k_{22}/k_{21}, the values of r_1 and r_2 were found to be equal to (0.40) and (1.96). The value of r_1/r_2 (0.21) satisfies the copolymerization relation for **TOP**, r_1/r_2=1/4 within experimental error. The net rates of formation for the related sequences **MEMMM** plus **MEMME** show **MMEMM** to be slightly lower. This could result from the contribution of **EMEMM** to the **MEMME** and **MEMMM** sequences respectively. Of course, these contributions depend on the placement of the **M** units within the pentad sequences under discussion. The net rate of generation of these sequences (6×10^{-4} M/min) was maintained until 25% **DOL(E)** conversion. Similar rates were previously obtained.[10]

Stage II

At approximately 26% **DOL(E)** conversion, the rate of **DOL** consumption increases and the net rate of **TOP-(2,2-d_2)** production decreases. This results in the increased rate of formation of the following sequences: **(M/M)(M/M)E(M/M)(M/M)** ($1.75E^{-3}$ M/min), **(M /M)E(M/M)(M/M)(M/M)** plus **(M /M)E(M/M)(M/M)E** ($3.16E^{-3}$ M/min), **E(M /M)E(M/M)(M/M)** plus **E(M /M)E(M/M)E** ($1.57E^{-3}$ M/min) and **(M /M)E(M/M)E(M/M)** ($7.98E^{-4}$ M/min).

These rate data reveal a disproportionately high rate of formation for the **(M /M)E(M/M)(M/M)(M/M)** plus **(M /M)E(M/M)(M/M)E** pentad sequences, indicating that the rate of copolymerization of **TOP** with **DOL** has significantly increased. This copolymerization of **TOP/DOL** results in the increased generation of the **(M /M)E(M/M)(M/M)(M/M)** plus **(M /M)E(M/M)(M/M)E**, **(M /M)E(M/M)E(M/M)** and **E(M /M)E(M/M)(M/M)** plus **E(M /M)E(M/M)E** sequences. The sequences **E(M /M)E(M/M)(M/M)** plus **E(M /M)E(M/M)E** also includes the sequences **(M /M)E(M/M)(M/M)(M/M)** plus **(M /M)E(M/M)(M/M)E** in **TOP/DOL** copolymerization. The copolymerization reactions of **TOP/DOL** are more likely to give two-**E**'s sequences instead of one-**E** sequences. The disproportionately low net rate of increase for the two-**E** sequences **(M /M)E(M/M)E(M/M)** shows that transacetalization involving these sequences occur throughout the three stages of the copolymerization reactions. The high basicity of the oxygen of the $(ME)_n$ chains lead to a high rate of charge transfer to these sites, resulting in the separation of the **E** units in the $(ME)_n$ sequence. The increased formation of **(M/M)(M/M)E(M/M)(M/M)** reflects the reactions of **TOX-d_6** as a

monomeric unit with **TOP-(2,2-d_2)**.

Stage III

At around 41% **DOL(E)** conversion, the rate of formation of the **MMEMM** pentad sequence makes its final significant increase. This reflects transacetalization[6,7] involving **$(ME)_m$** and **$(MME)_n$** sequences with carbenium endgroups associated with **$(MMM)_o$** sequences.

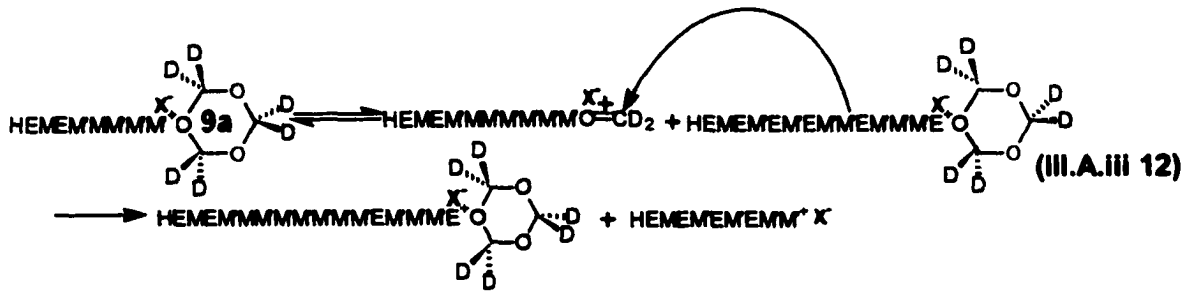

(III.A.iii 12)

At approximately 66% **DOL(E)** conversion, the rate of formation of **(M /M)E(M/M)(M/M)(M/M)** plus **(M /M)E(M/M)(M/M)E** sequences started to decrease. The kinetic curve for **E(M /M)E(M/M)(M/M)** plus **E(M /M)E(M/M)E** levels off earlier than that of **(M /M)E(M/M)(M/M)(M/M)** plus **(M /M)E(M/M)(M/M)E** sequences. These randomization by way of transacetalization are confirmed by the observation of an initial growth followed by a decline in peak areas of **(M /M)E(M/M)E(M/M)**, and **(M /M)E(M/M)(M/M)E** resonances. The **(M /M)E(M/M)E(M/M)** peak started its decline first and was later followed by the decline

of the (M /M)E(M/M)(M/M)E peak, indicating that (M /M)E(M/M)E(M/M) is more susceptible to transacetalization than (M /M)E(M/M)(M/M)E.

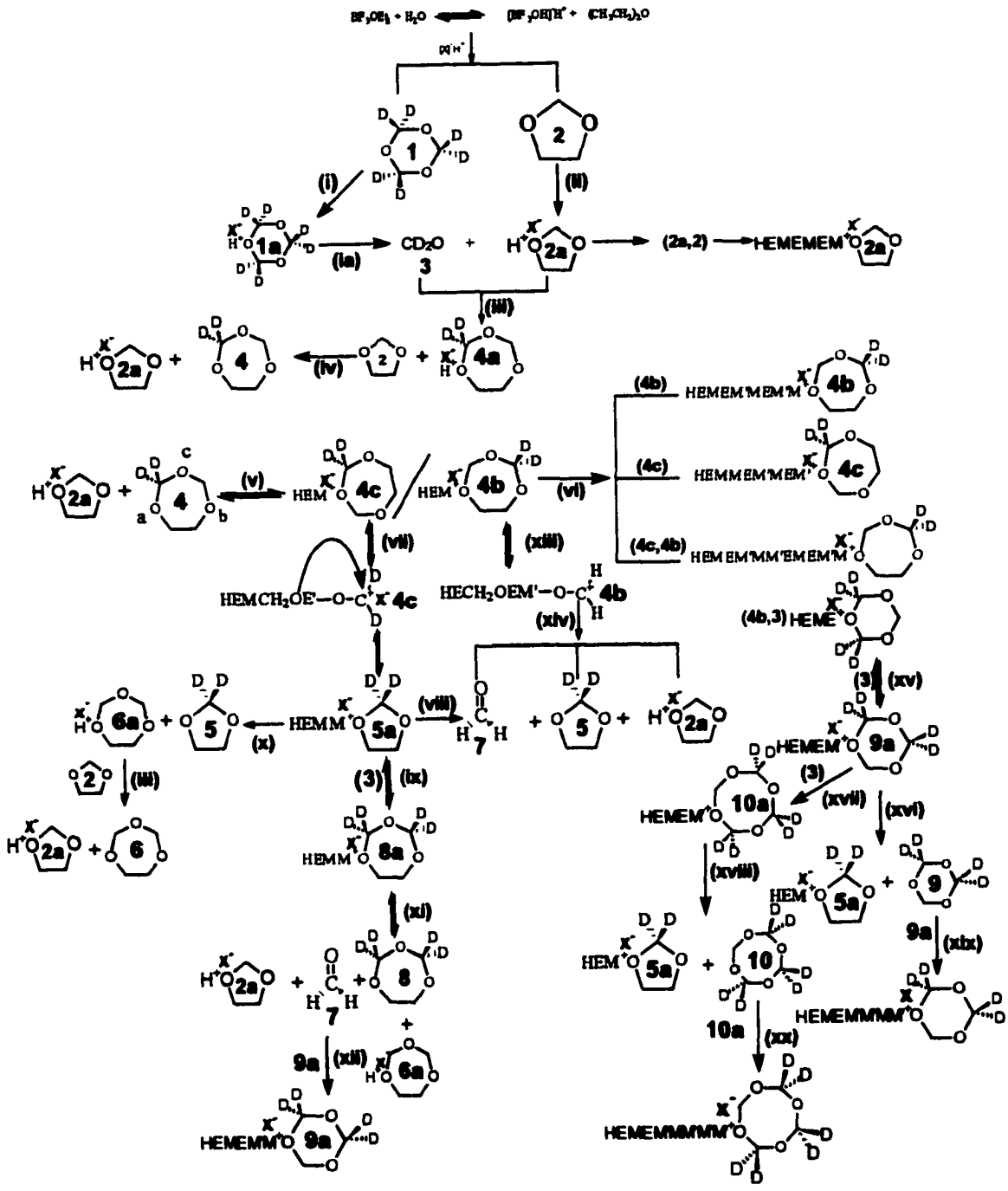

Scheme 2

III.B. TOX/DOL-(2,2-d_2) Copolymerization

As in the **TOXd_6/DOL** copolymerization system, the ***in-situ*** **C-13** and **DEPT NMR** experiments of **TOX/DOL-(2,2-d_2)** copolymerization system resulted in the detection of enhanced shielding for alpha and gamma deuterated components. The relative growths of components as reflected by this system with lower concentration of isotope substitution corroborate the **TOXd_6/DOL** experiments and give further insight into all proposed mechanistic routes. Increased resolution observed in the **M**-region of **DEPT** spectra resulted in the *first detection of sequences due to heptads and gamma deuteration.*

i. In-Situ ^{13}C NMR analysis

The spectrum before initiation **(Figure III.B.i. 1)** in the ***in-situ*** ^{13}**C NMR** analysis of the **TOX/DOL-(2,2-d_2)** copolymerization shows **DOL(M)-(2,2-d_2)** at a chemical shift of 93.86 ppm, along with 2n+1 $J_{^{13}C\text{-}^{2}H}$ coupling (25.3 **Hz**). This represents an up-field shift, due to α-deuteration, of approximately 0.64 ppm for **DOL(M)-(2,2-d_2)** in comparison to a chemical shift of 94.49 ppm for the natural abundance **DOL(M)**. As polymerization progresses, the unlabeled **DOL** acetal peak at 94.50 ppm develops further **(Figure III.B.i. 2)**. The two **TOP** acetal peaks at 92.75 and 92.64 ppm give insight into the presence of **TOP** and **TOP-(2,2-d_2)**, with the latter shifted up-field 0.11 ppm due to γ-deuteration. The **TOP(M)-(2,2 4,4-d_4)** peak is undetected due to multiple splitting and low concentration. Three **TOP(E)** peaks with different levels of deuteration are observed **(Figure III.B.i. 3)**.

The peaks in the "**E**-region" includes **TOP(E)-(2,2-d_2)** at 69.47 ppm, **TOP(E)** at 69.53 ppm, and **TOP(E)-(2,2 4,4-d_4)** at 69.55 ppm. These three species evolve differently.

Initially the **TOP(E)-(2,2 4,4-d_4)** signal was similar in intensity to the **TOP(E)** signal, while the **TOP(E) -(2,2-d_2)** peak was larger than the other two **TOP(E)** signals **(Figures III.B.i. 3)**. This greater concentration of **TOP-(2,2-d_2)** was still evident towards the end of the pre-cloud period. The concentration of **TOP** also dominates that of **TOP-(2,2 4,4-d_4)** towards the end of the precloud period, as expected **(Figure III.B.i. 4)**. This results from the low concentration of **DOL-(2,2-d_2)** in this reaction system.

The increased concentration of **TOP(E)** results from the higher initial concentration of formaldehyde compared with deuterium labeled formaldehyde (10:1) and thus confirms its assignment. The quintet splitting in **^{13}C NMR** analysis make it virtually impossible to detect **TOP(M')-(2,2 4,4-d_4)** acetal peaks. The presence of **TOP-(2,2 4,4-d_4)** was deduced from **TOP(E)-(2,2 4,4-d_4)** at chemical shift 69.55 ppm.

^{13}C NMR detection of **TOP(M)-(2,2-d_2)** shows a down field shift of approximately 0.02 ppm in relation to natural abundance **TOP** in this reaction system. Shift due to γ-deuteration allows the identification of the various deuterium labeled species generated during the copolymerization. For the copolymer sequences, in some cases heptad resolution along with the effect of γ- deuteration is possible **(Figure III.B.i. 5)**. The resolution is much improved in **DEPT** spectra (Section **III.B.ii**). The assignment of the sequence peaks in **(Figure III.B.i. 5)** is consistent with shifts related to γ-deuteration within detected sequences and heptad resolution. The assignment of **MEMMM** to chemical shift 92.65 ppm with an overlapping up-field peak reflects the possibility of deuteration effect, i.e. **(M'/M)E(M/M')(M'/M)(M/M')** or heptad sequences, i.e. **(M/M'/E)(M'/M)E(M/M')(M'/M)(M/M') (M/M'/E)**. Similar considerations can be applied

to the peaks at 92.20 ppm and the slightly up-field peak. However, in the non-labeled system, only one peak was observed (Figure III.C.iii-3). Therefore these two peaks can be assigned to (M'/M)E(M)ME and (M'/M)E(M)(M')E. The weaker up-field peak is assigned to (M'/M)E(M)(M')E pentad, reflecting the low percentage of deuterium labeled monomer used in this experiment. ^{13}C nuclei with α-deuteration will not be detected readily due to multiple deuterium splitting and low concentration. The overlapping peaks in the "M pentad" region around 89.77 ppm show signs for the effects of gamma deuteration and heptad resolution. These sequence peaks dominate toward the end of the pre-cloud period as is expected for all "M-pentad" sequences. Similar explanations can be applied to the sequences E(M/M')(M'/M)(M/M')(M/M') at 89.30 ppm appearing as multiple peaks. This again results from gamma deuteration and heptads. The multiple peaks around 88.71 ppm can be firmly assigned to γ-deuteration effect in the pentads E(M/M')(M'/M)(M/M')E based on the singlet observed at this position for EMMME for natural abundance system[3] (Figure III.C.iii-3).

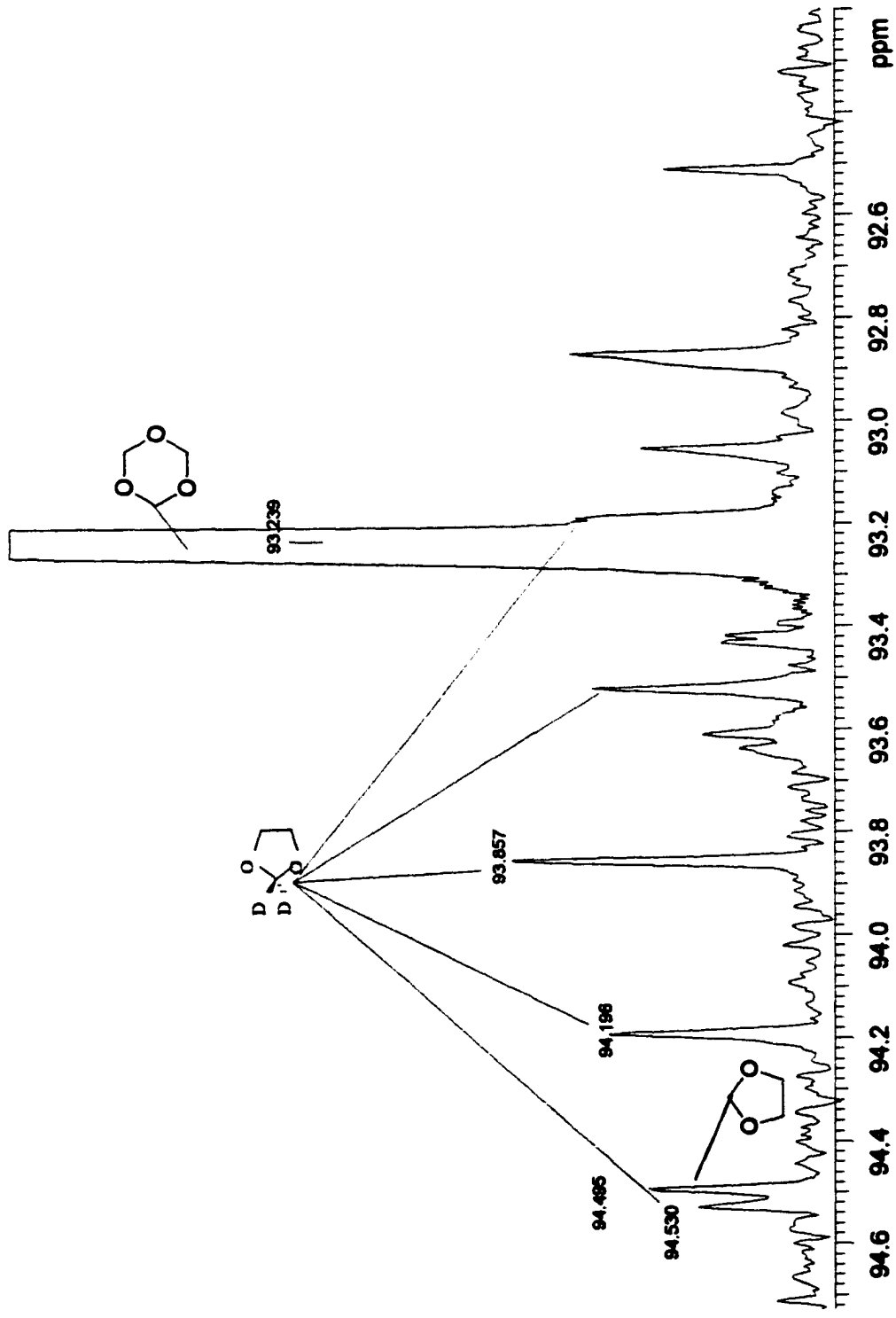

Figure III.B.1.1 ^{13}C spectrum before initiation of **TOX/DOL-(2,2-d_2)** copolymerization-"Quintet splittings and up-field shift for **DOL(M)-(2,2-d_2)** due to α-deuterium effect". Monomers' mole ratio: (3,1), spectrometer: 150 **MHz** probe: **ID600-s**.

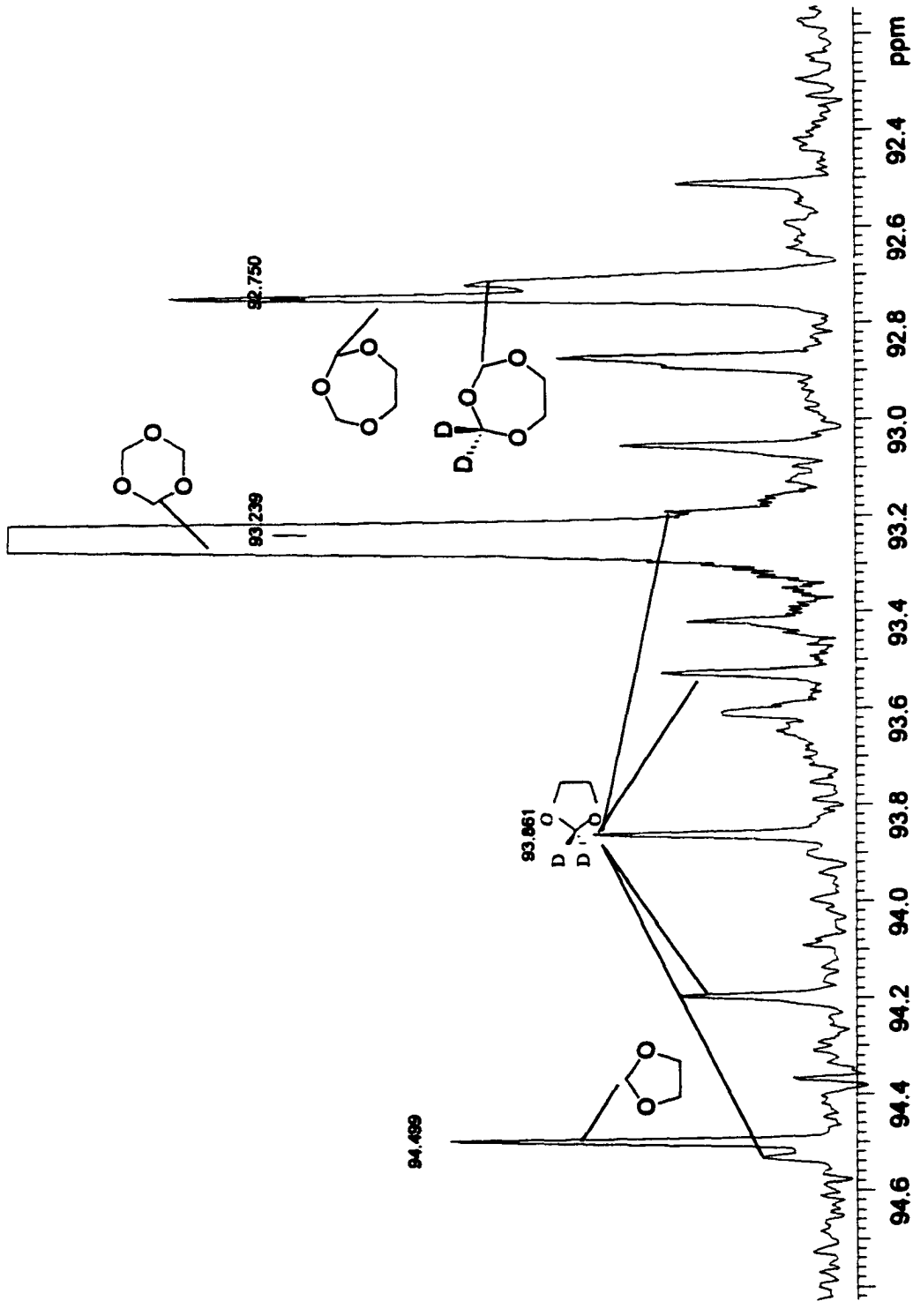

Figure (III.B.i. 2) ^{13}C spectrum of **TOX/DOL-(2,2-d_2)** copolymerization-"Evidence for **TOP** and **DOL** Syntheses". Monomers' mole ratio: (3,1), spectrometer: 600 **MHz**, probe: **ID600-s**, **DOL(E)** conversion: 18%.

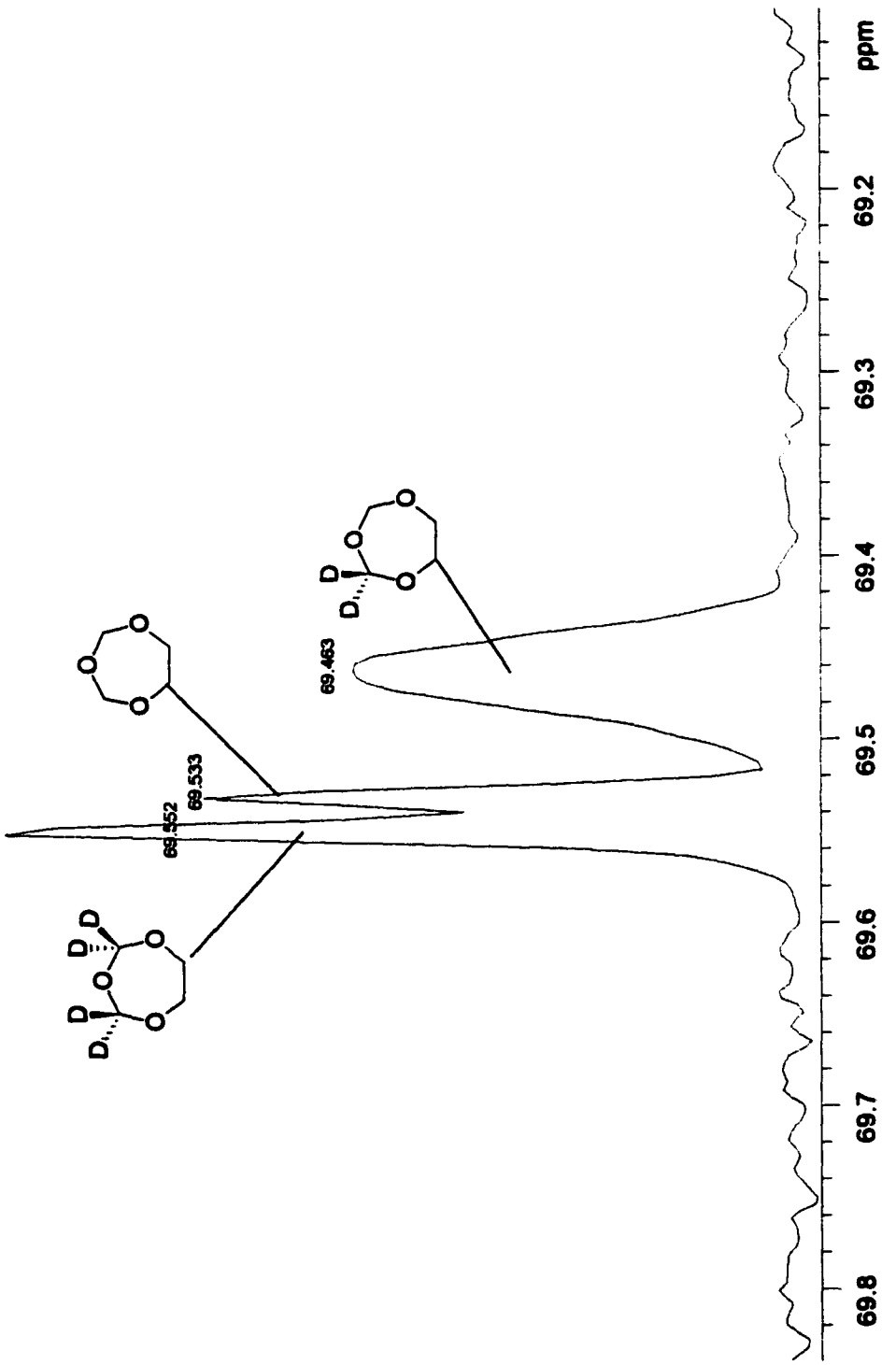

Figure (III.B.1.3) ^{13}C spectrum of **TOX/DOL-(2,2-d_2)** copolymerization-"E-Region". Monomers' mole ratio: (3,1), spectrometer: 600 **MHz**, probe: **ID600-a**, **DOL(E)** conversion: 18%.

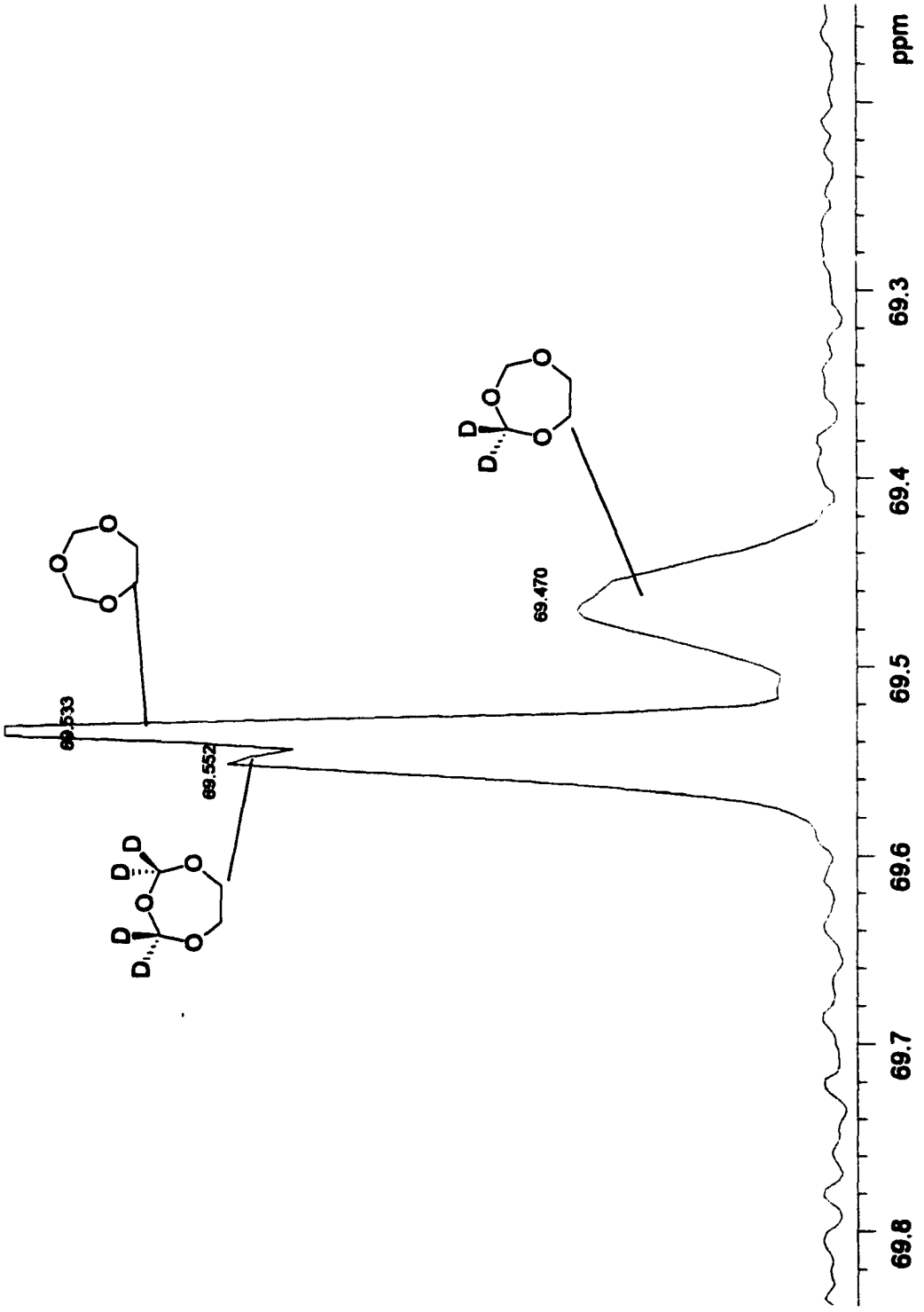

Figure (III.B.1. 4) ^{13}C spectrum of **TOX/DOL-($2,2\text{-}d_2$)** copolymerization-"**E-Region**". Monomers' mole ratio: (3,1), spectrometer: 600 **MHz**, probe: **ID600-s**, **DOL(E)** conversion: 76%.

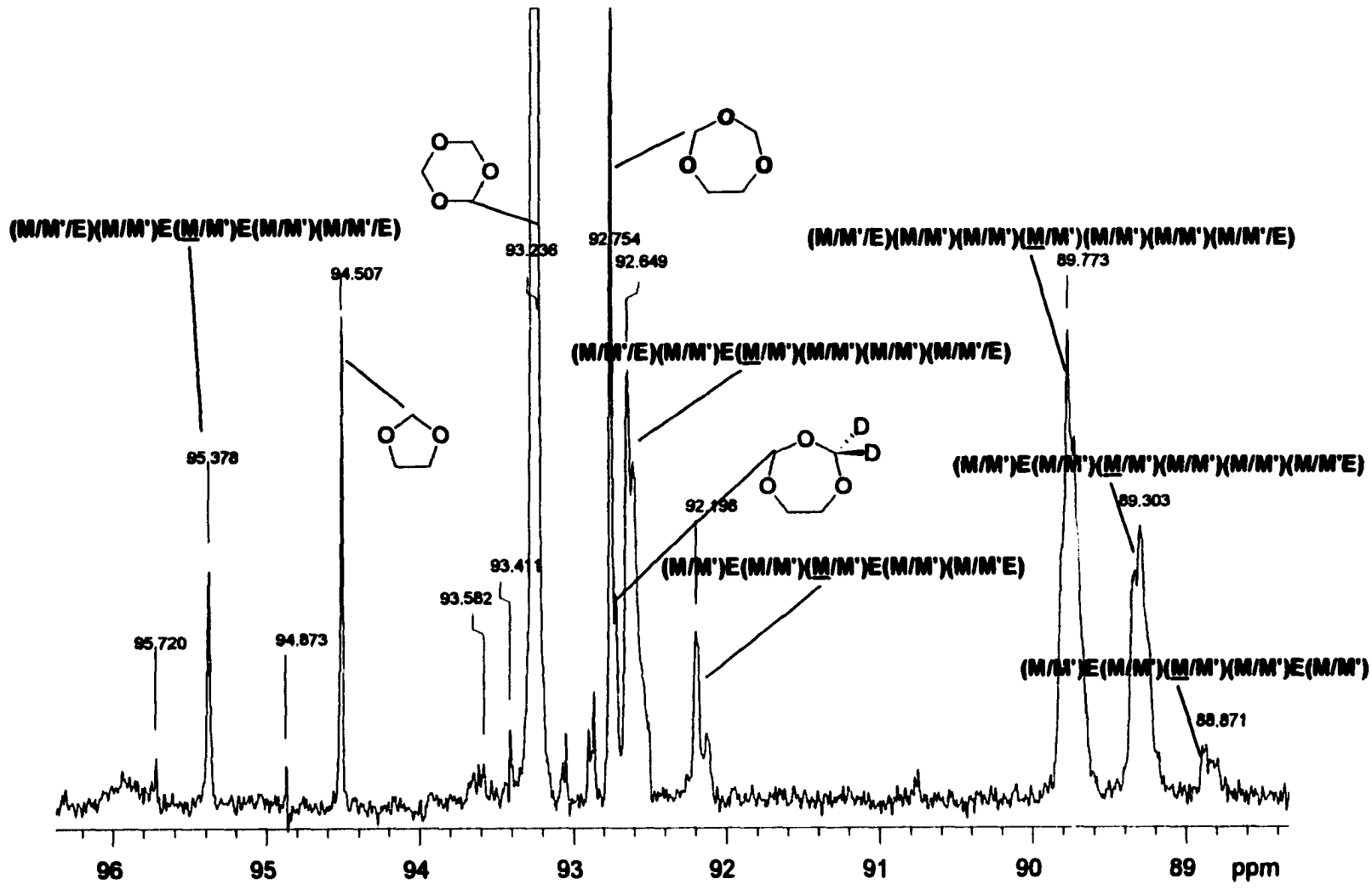

Figure (III.B.i. 5) ^{13}C spectrum of **TOX/DOL-(2,2-d_2)** copolymerization-"Evidence Supporting Heptad Resolution and α-deuterium effect". Monomers' mole ratio: (3,1), spectrometer: 600 **MHz**, probe: **ID600-s**, **DOL(E)** conversion: 76%.

ii. *In-Situ* DEPT analysis

In comparison to **Figure (III.A.i. 1)**, the **DEPT NMR** spectrum shown in **Figure (III.B.ii. 1)** reveals the elimination of the **DOL(M)-(2,2-d_2)** peak. The gradual growth of the **DOL(M)** peak at 94.5 ppm confirms its synthesis. Two peaks for **TOP(M)** at 92.75 ppm and **TOP(M)-(2,2-d_2)** at 92.71 ppm are identified.

In the "E-region", the **TOP(E)**, **TOP(E)-(2,2-d_2)** and **TOP(E)-(2,2 4,4d_4)** peaks **(Figure III.B.ii. 2)** confirm that the detected ^{13}C nuclei are not deuterated as expected. In the region for **E(M'/M)E(M/M')(M/M')** pentad (66.88 – 66.80 ppm), two peaks are observed, corresponding to two heptads: **(M/M')E(M'/M)E(M/M')(M/M')(E)** and **(M/M')E(M'/M)E(M/M')(M/M')(M/M'/E)**. In the region for **E(M'/M)E(M/M')(E')** pentad (66.60 ppm), only one peak is observed as expected, since only one heptad **(M'/E)(M'/M)E(M/M')(E/M)** is possible. In the region for **(M'/M)(M/M')(E(M/M')(M/M')**, three peaks are observed at 67.50, 67.43 and 67.35 ppm, corresponding to the three possible heptads: **(M'/M)(M'/M)(M/M')E(M/M')(M/M')(M'/M)**, **(M'/M)(M'/M)(M/M')E(M/M')(M/M')E** and **E(M'/M)(M/M')E(M/M')(M/M')E**. Assignment for each individual peak cannot be made at this time. **DEPT** spectrum in "M-region" **(Figure III.B.ii. 3)** confirms the assignment in Figure **(III.B.i-iv)**.

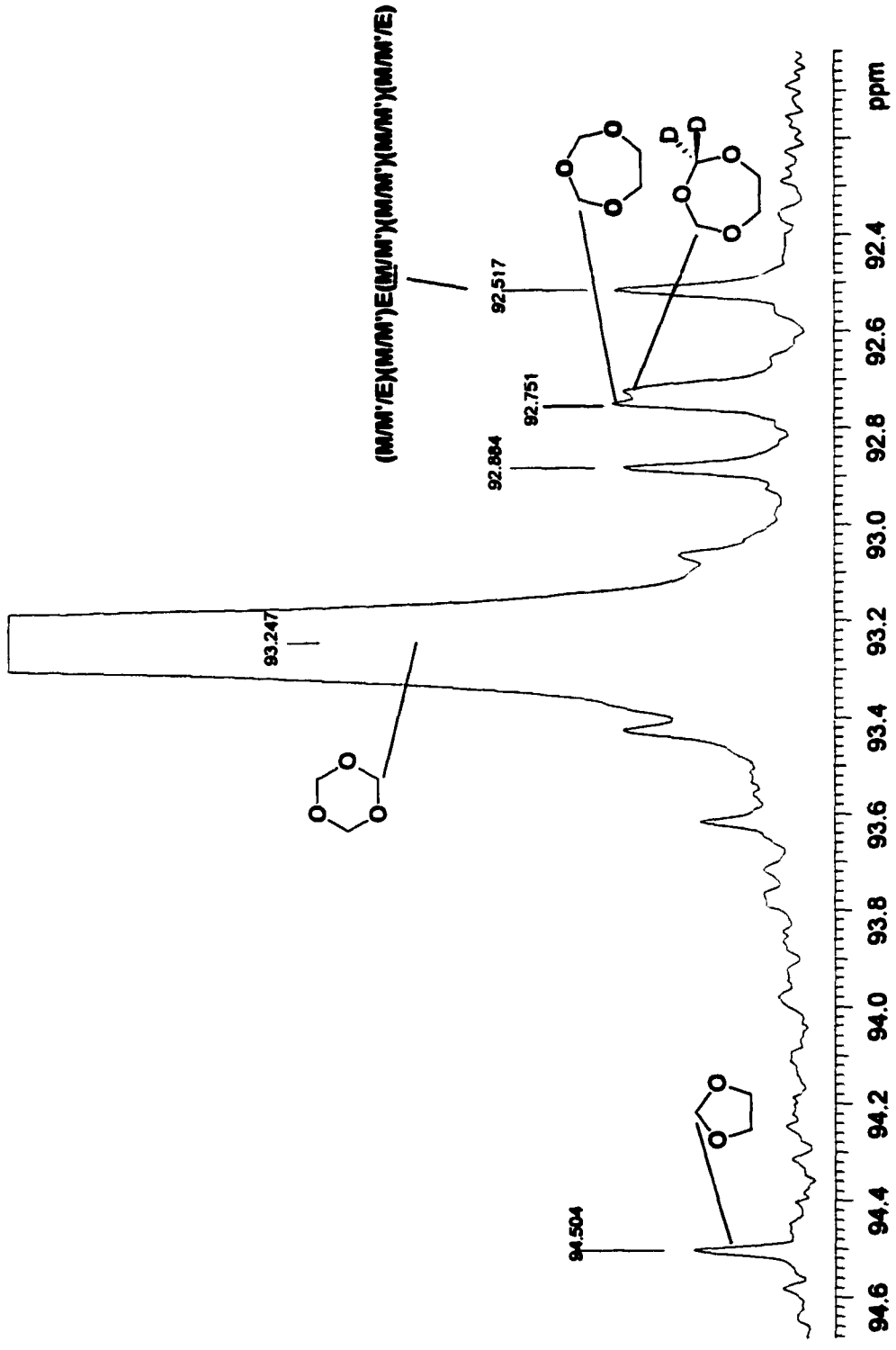

Figure (III.B.iii. 1) **DEPT** spectrum of **TOX/DOL-(2,2-d_2)** copolymerization. "Showing the Elimination of **DOL(M)-(2,2-d_2)** Peaks". Monomer mole ratio: (3,1), spectrometer: 600 **MHz**, probe: **ID-600-s**, **DOL(E)** conversion: 15 %.

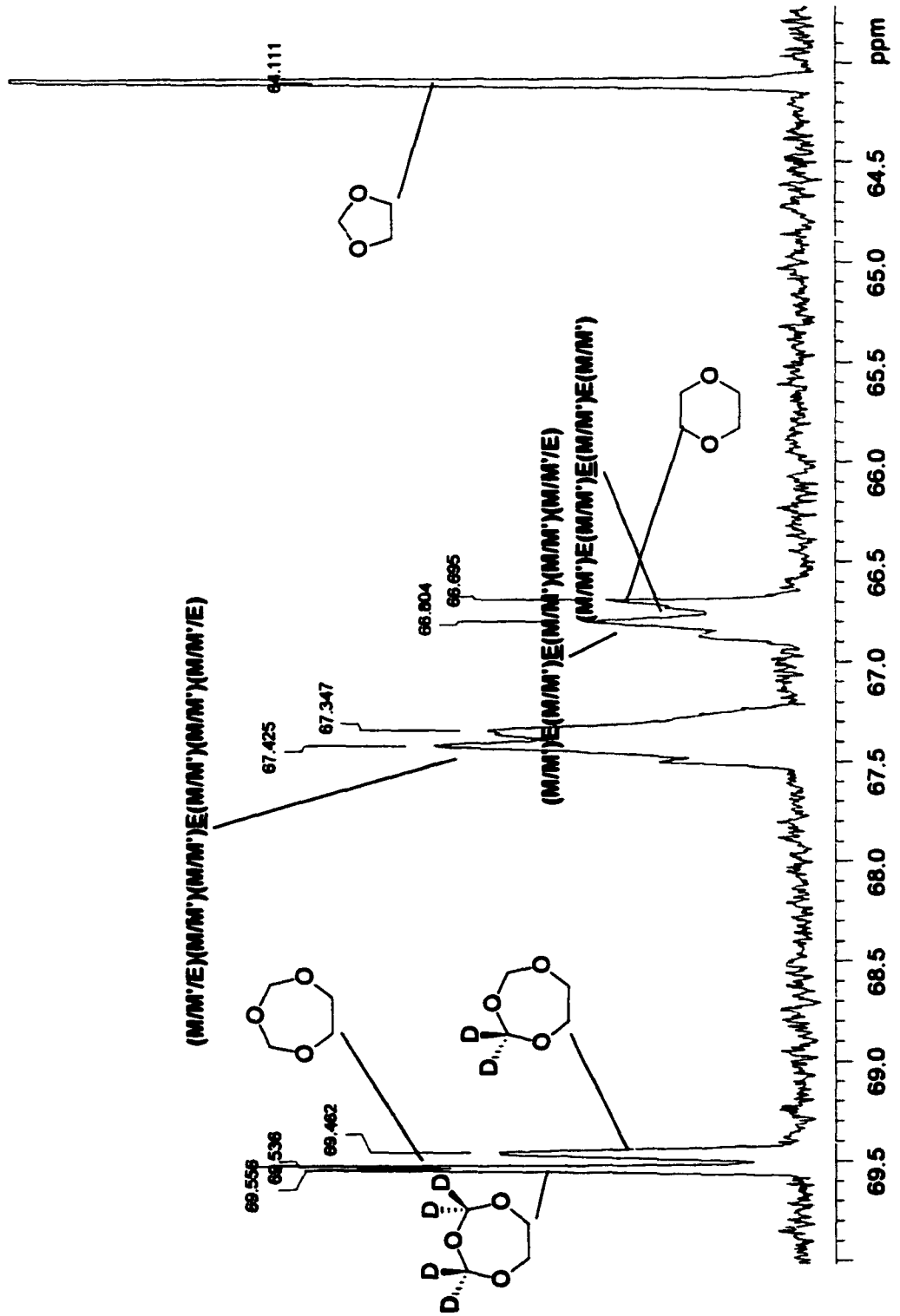

Figure (III.B.ii. 2) **DEPT** spectrum of **TOX/DOL-(2,2-d_2)** copolymerization-"E-Region. Monomers' mole ratio: (3,1), spectrometer: 600 **MHz** probe: **ID600-4**, **DOL(E)** conversion: 67 %.

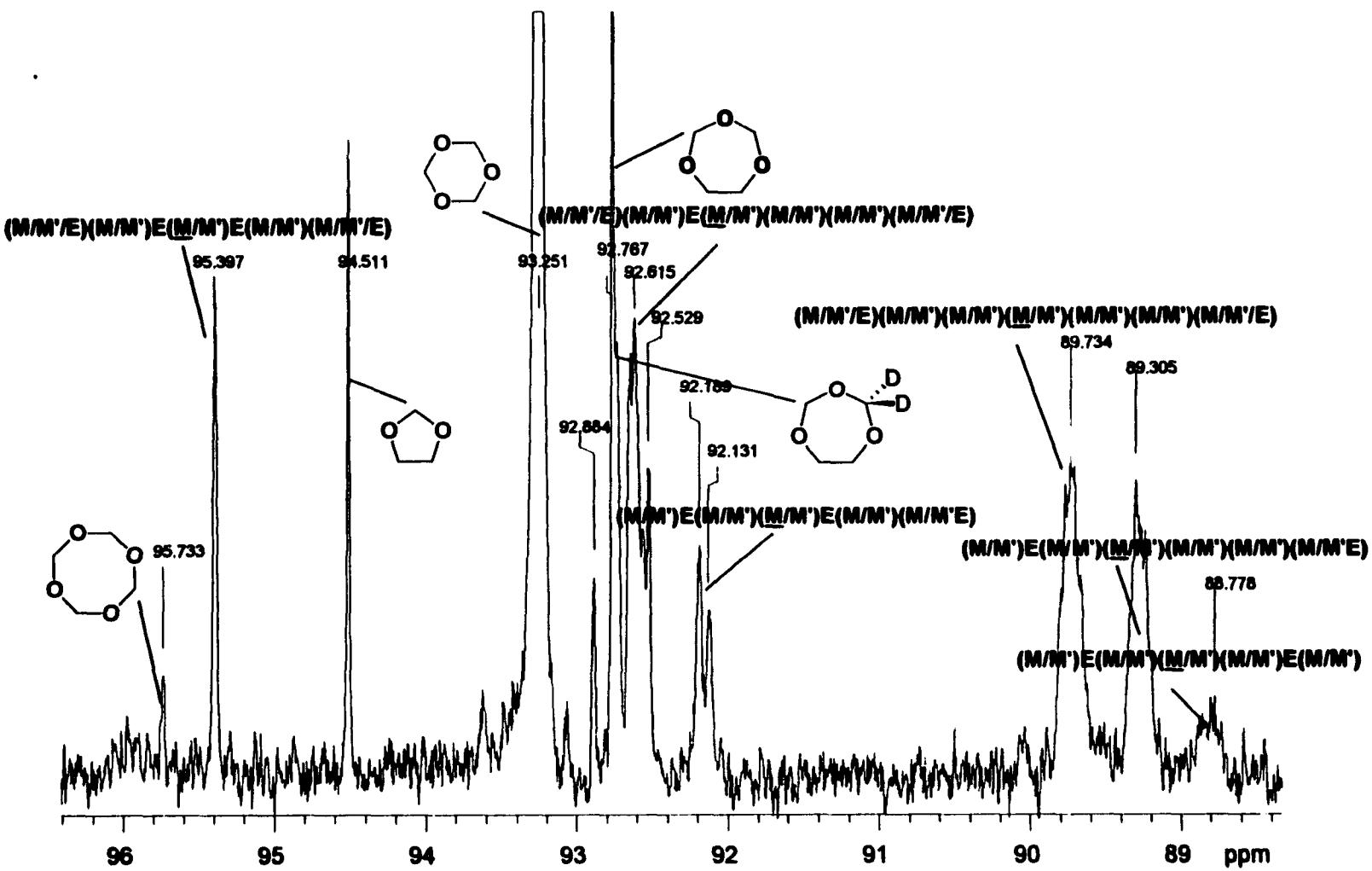

Figure (III.B.ii. 3) **DEPT** spectrum of **TOX/DOL-(2,2-d_2)** copolymerization- "Evidence for heptad resolution and α-deuterium effect". Monomers' mole ratio: (3,1), spectrometer: 600 **MHz**, probe: **ID600-z, DOL(E)** conversion: 67 %.

III.A.iv. TOX/DOL-(2,2-d_2) Copolymerization

III.A.iii. *In-Situ* ^{1}H NMR Analysis

Assignments and Discussion

In-situ ^{1}H NMR (600 MHz) spectra of the copolymerization of trioxane, **TOX**, with deuterium labeled dioxolane, **DOL-(2,2-d_2)**, showed significant reduction in overlap between **DOL(M)** peak and the following M-centered pentad sequences **(M/M')(M/M')(M'/M)(M/M')(M/M')**, **E(M/M')(M'/M)(M/M')(M/M')**, **E(M/M')(M'/M)(M/M')E**, **(M/M')E(M/M')(M/M')(M/M')** and **(M/M')E(M/M')(M/M')E**. This allows for the earlier detection of these pentad sequences. In addition, this deuterium labeled system allows us to focus on the kinetics involving all methylene oxide, 'M', species derived from **TOX**.

Before initiation, **DOL(M)** at 4.85 ppm was present in low concentration. This **DOL(M)** was carried over from the synthesis of **DOL-(2,2-d_2)** with 98.8% deuterium labeled paraformaldehyde and ethylene glycol as reactants. Comparing **DOL(M)** to **DOL(E)** peak area 0.19/2 to 23.73/4, the percent of unlabeled **DOL** in the comonomer melt before initiation was found to be 1.6. This agrees with the percentage purity of the deuterium labeled reactant, **-$(CD_2O)_n$-** used in the synthesis of **DOL-(2,2-d_2)**. At 2% **DOL(E)** conversion, the generation of unlabeled **DOL** and **TOP-(2,2-d_2)** were observed. The peak at 4.891 ppm is assigned to the acetal hydrogens of **TOP-(2,2-d_2)**, because this

TOP peak appeared shortly after initiation with **DOL-(2,2-d_2)** as one of the starting monomers. At this point, the corresponding **TOP(E)** peak located at 3.794 ppm is approximately twice as large as the **TOP(M)** peak. The pentads with **(M/M')(MM')(M/M')** at the center of the sequences **(M/M')(M/M')(M'/M)(M/M')(M/M')**, **E(M/M')(M'/M)(M/M')(M/M')**, and **E(M/M')(M'/M)(M/M')E** overlap with the **TOP(M)** peak were observed at 4% **DOL(E)** conversion. Their total peak areas were obtained by subtracting one half of **TOP(E)** peak area from the region containing these peaks. Of the six possible pentad sequences, only five were partially resolved **(Figure III.A.iii. 1)**. These are **(M/M')(M'/M)(M/M')(M/M')** at 4.91 ppm partially resolved from **E(M'/M)(M/M')(M/M')(M/M')** at 4.90 ppm, **(M/M')E(M/M')(M/M')E** at 4.82 ppm, partially resolved from **(M/M')E(M/M')(M/M')E** at 4.81 ppm, and **(M/M')E(M/M')E(M/M')** at 4.72 ppm. The **E(M'/M)(M/M')(M/M')E** peaks are possibly totally obscured by the **TOP(M)** peak at 4.89 ppm. The other sequence peaks observed at this time include **(M/M')(M/M')E(M/M')(M/M')**, **E(M/M')E(M/M')(M/M')** and **E(M/M')E(M/M')E**. These peaks gradually emerge from an initial overlap with the ^{13}**C** satellite peaks of **DOL(E)**, as their concentrations increase.

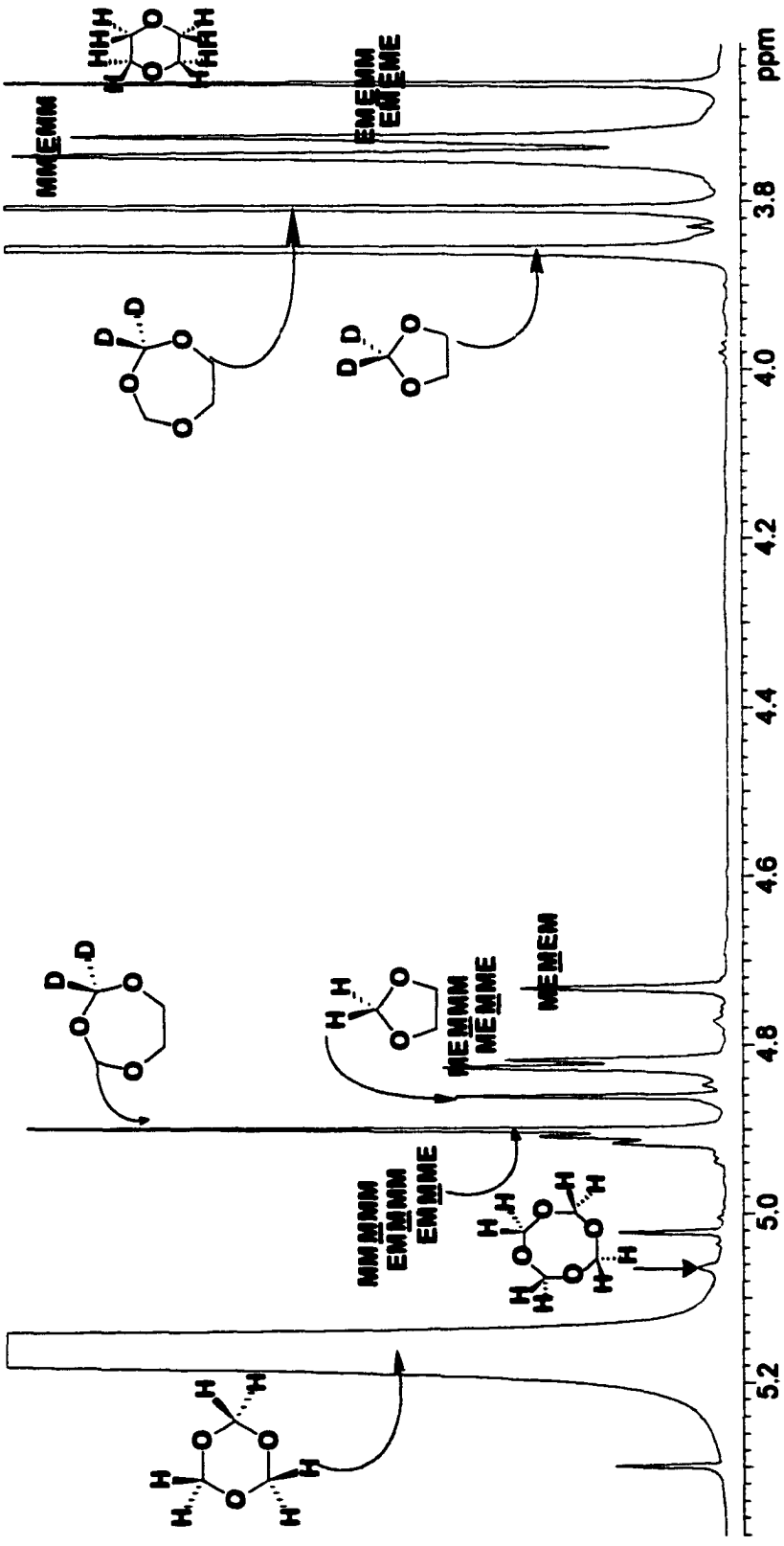

Figure (III.B.## 1) ^{1}H spectra of **TOX/DOL-(2,2-d $_2$)** copolymerization- "Assignment of Peaks in the ' M' and ' E' regions" Monomers' mole ratio: (3/1), **[BF$_3$OEt$_2$]**: 20 ppm, Spectrometer: 600 **MHz**, Probe: ID600-s **DOL(E)** Conversion:60%.

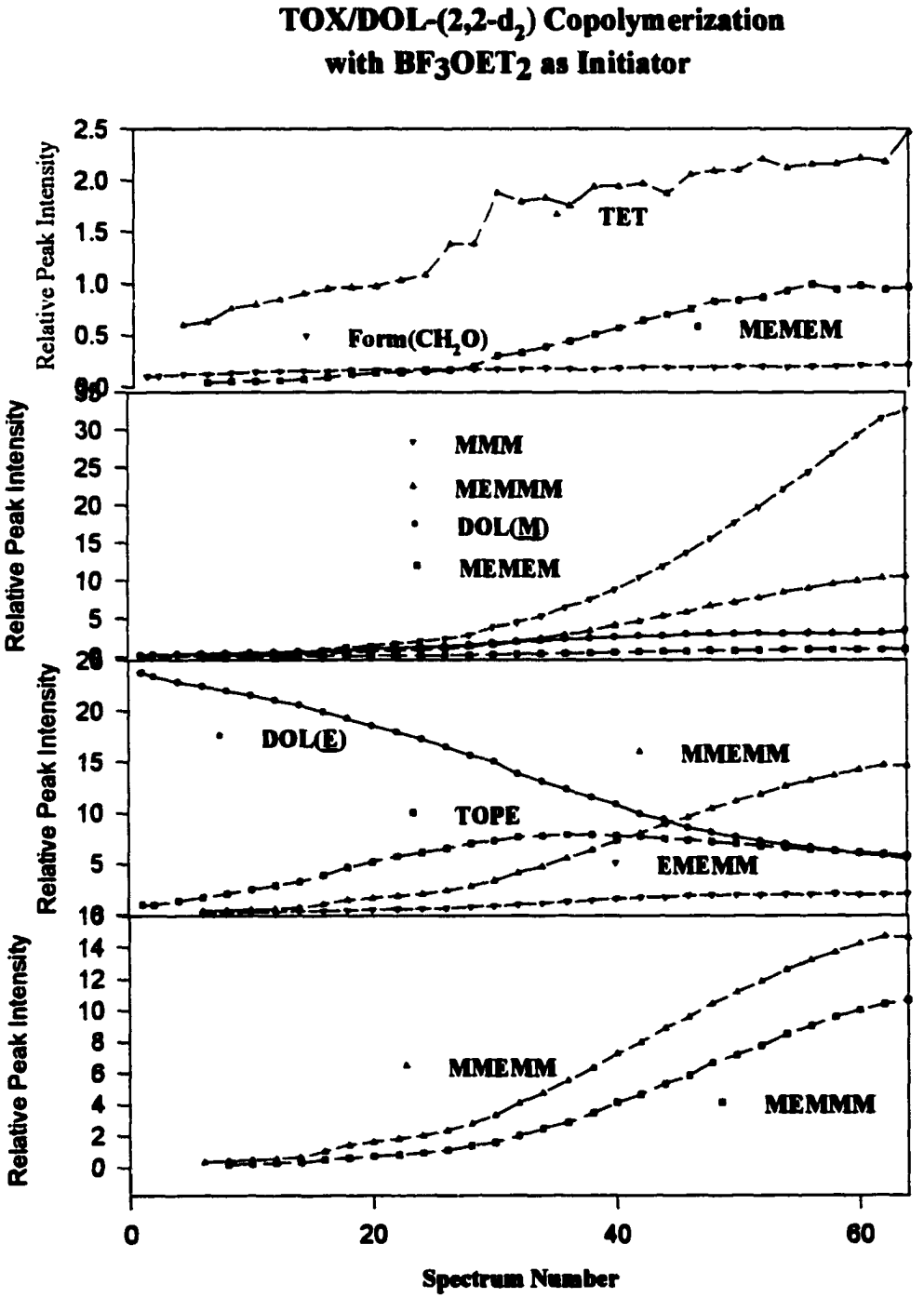

Figure (III.B.iii 2) Kinetic Curves of active components in TOX/DOL-(2,2-d_2) Copolymerization using BF_3OET_2 as initiator.

The kinetic profiles for the species involved in this copolymerization are represented in **Figure (III.B.iii. 2)**. From these kinetic curves, the average growth and consumption rates for each component at different stages were determined.

The rate curve of the active components are depicted in **Figure (III.B.iii 3)**:

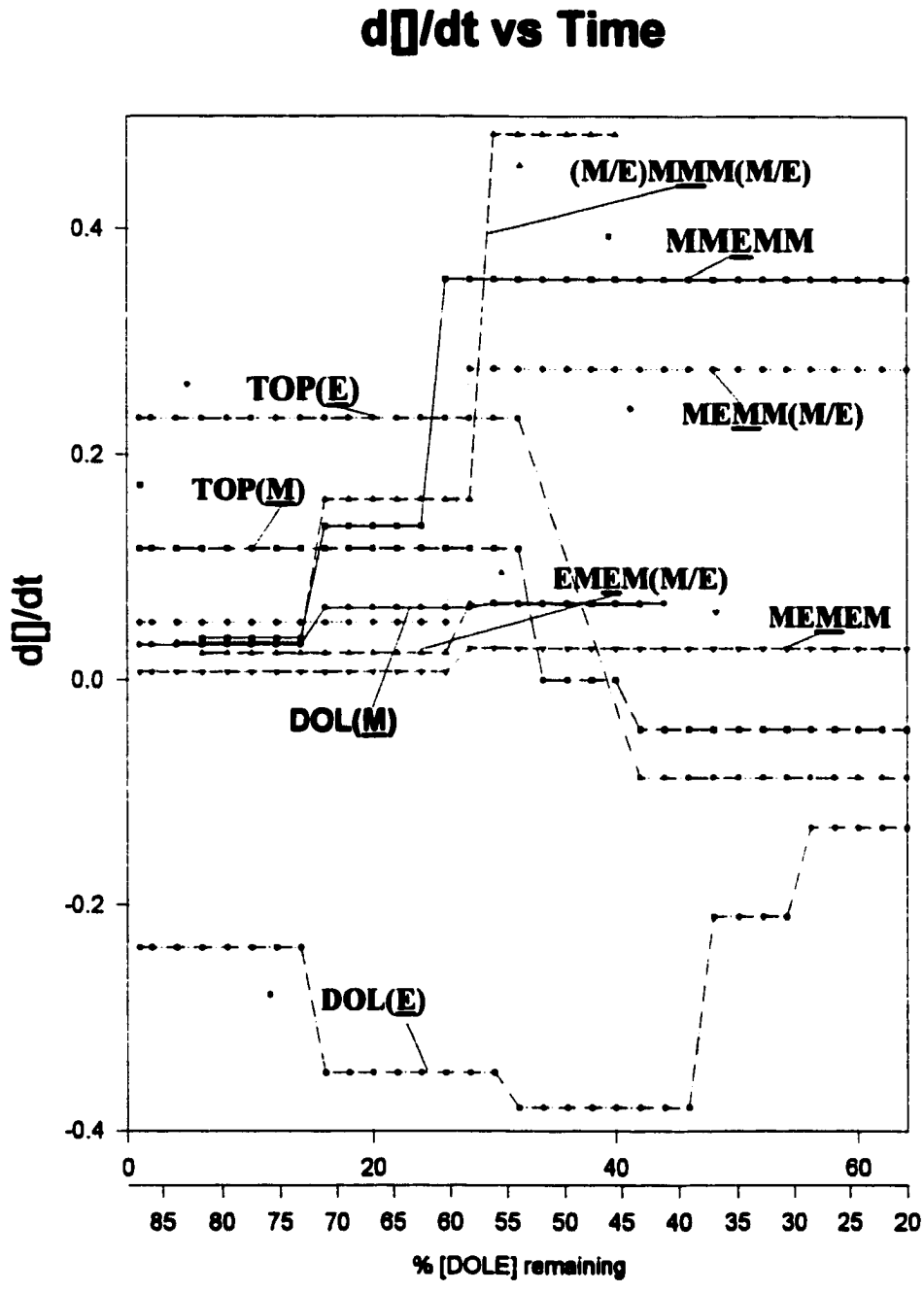

Figure (III.B.iii. 3) Magnified Rate Curves for active components in TOX/DOL -(2,2-d_2) copolymerization using BF_3OEt_2 as initiator.

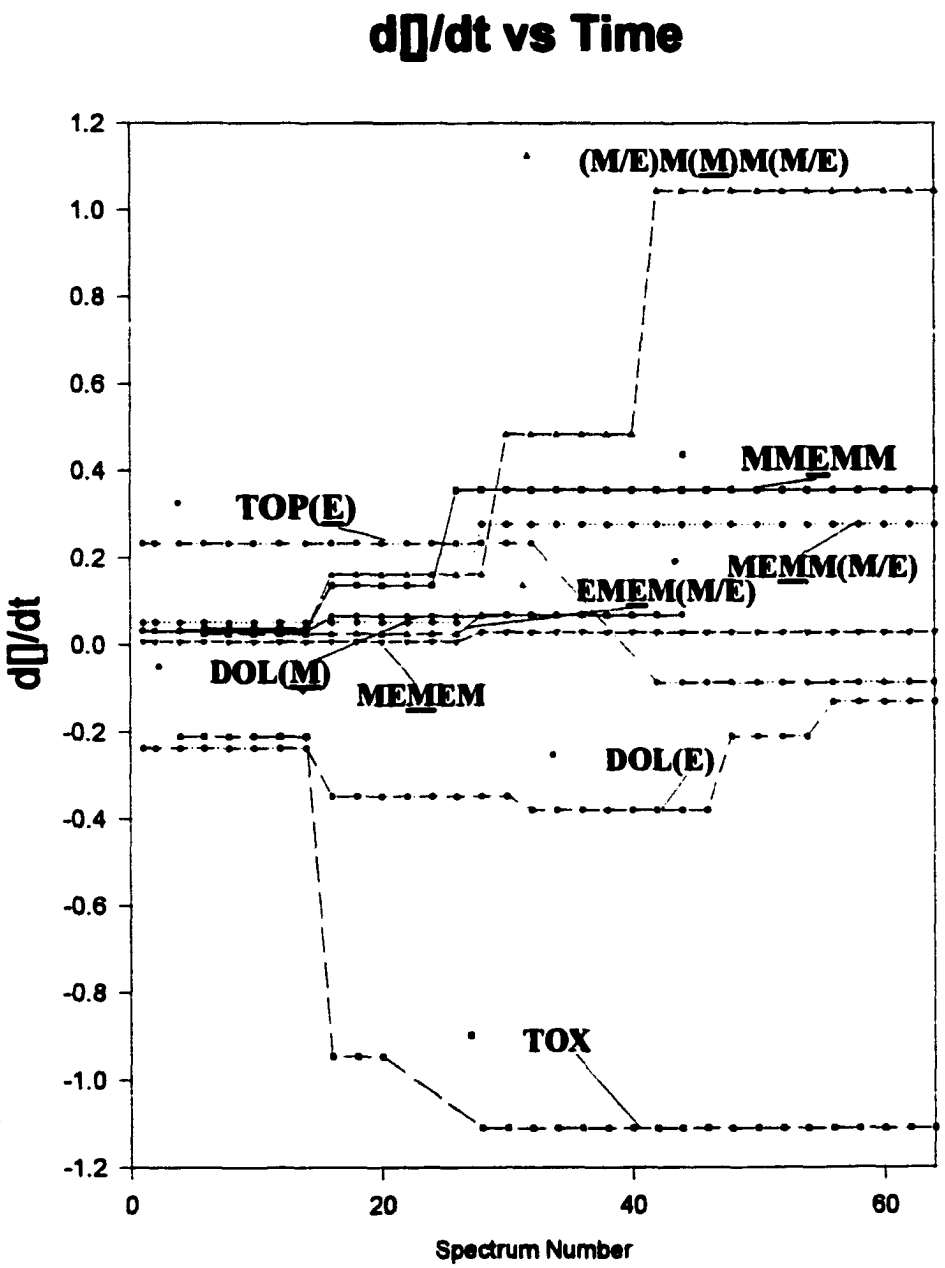

Figure (III.B.iii. 4) Rate Curves for active components in TOX/DOL -(2,2-d_2)- "Showing rate changes of TOX copolymerization using BF_3OEt_2 as initiator.

The symbol [] (**Figure III.B.iii. 3**) indicates concentration of different active components.

Stage 1

The initiation process remains the same as indicated in **Reactions (I.A.ii. 1-2)**. The higher concentration of **TOX** in comparison to **DOL-(2,2-d_2)** (10:1) results in both **DOL-(2,2-d_2)** and **TOX** initiation. After initiation, **TOX** dissociates to formaldehyde and protonated formaldehyde[5] (Reaction **III.B.iii 1**).

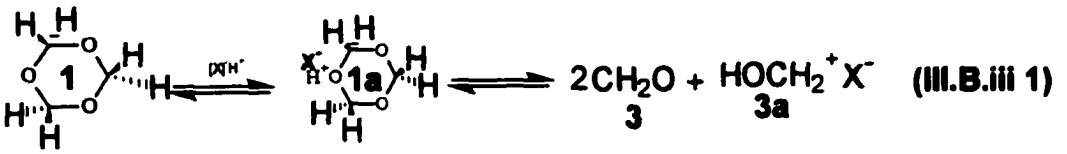

(III.B.iii 1)

The protonated formaldehyde generated can participate in the continued dissociation of **TOX** and the initiation of **DOL-(2,2-d_2)**.

Reaction (III.B.iii. 2) shows the initiation of **DOL-(2,2-d_2)** by boron trifluoride etherate/water complex to produce the protonated monomer.

(III.B.iii 2)

The protonated **DOL-(2,2-d_2)** is at equilibrium between the linear and cyclic structures (**Reaction III.B.iii. 2**). The cationic center on the linear structure is resonance

stabilized by the un-shared electron pairs of the adjacent oxygen[6]. Protonated **DOL-(2,2-d_2)** then reacts with formaldehyde to generate protonated **TOP-(2,2-d_2)**.

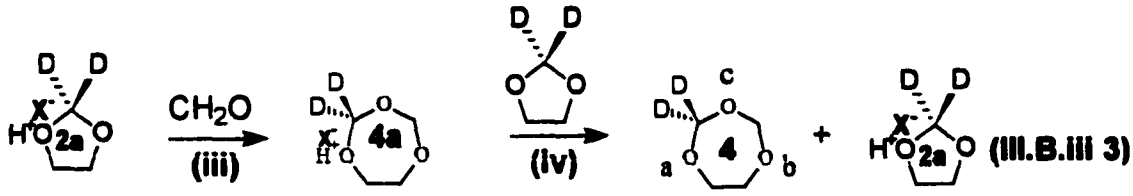

(III.B.iii 3)

Proton transfer from protonated **TOP-(2,2-d_2)** to the more basic **DOL-(2,2-d_2)** generates **TOP-(2,2-d_2)** **(Reaction III.B.iii 3)**.

Reaction (III.B.iii. 4) shows initiation with the carbenium ion of formaldehyde. This carbenium ion is generated by the dissociation of protonated **TOX**.

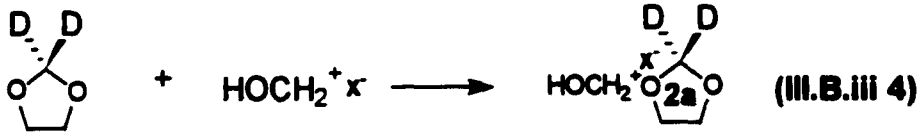

(III.B.iii 4)

Partially deuterated dioxolane **DOL-(2,2-d_2)** initiated with protonated formaldehyde can incorporate formaldehyde to generate activated trioxepane, **$HOCH_2^+$TOP-(2,2-d_2)**. This activated structure can generate sequences by copolymerizing with other monomers or charge transfer to **DOL-(2,2-d_2)** to produce **TOP-(2,2-d_2)**.

DOL synthesis

The generation of un-deuterated **DOL** peak in the initiated copolymer melt confirms the synthetic route that allows for the formation of **DOL** by inserting or expelling formaldehyde or deuterium labeled formaldehyde from activated **TOP**.

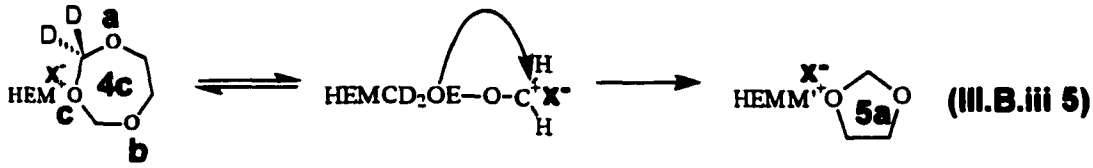

Charge transfer from '**c**' to the more basic oxygen '**a**' generates activated **DOL**. Equilibrium charge transfer to **DOL-(2,2-d_2)** then produces **DOL** (**Reaction III.B.iii 5**).

Generation of CD_2O

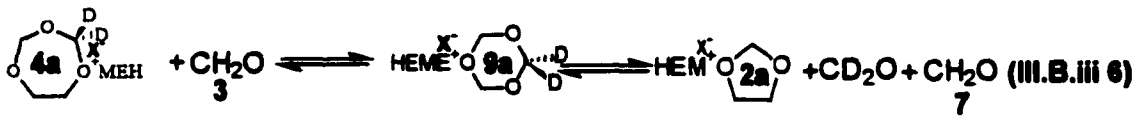

The insertion of CH_2O into structures (**4a**) result in the formation of (**9a**) (**Reaction III.B.iii 6**). The formation of (**9a**) early in the copolymerization reaction is followed by its rapid dissociation to give (**3**), (**7**), and (**2a**), as developed previously (**Section III A**).

Deuterium labeled formaldehyde generated from this mechanistic route inserts

into **4b** producing activated **TOX-(2,2-d_2)**. Further incorporation of deuterium labeled and or hydrogenated formaldehyde results in the possibility of generating activated **TET** with varying number of deuterium labeling.

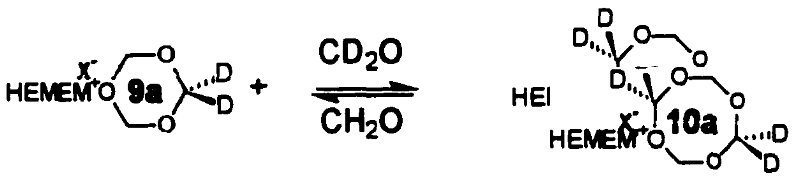

(III.B.iii 7)

Reaction (III.B.iii. 7) shows the generation of activated **TET-d_4**. Charge transfer to **DOL-(2,2-d_2)** produces **TET-d_4** and activated **DOL-(2,2-d_2)**, as shown in **Reaction (III.B.iii 8)**.

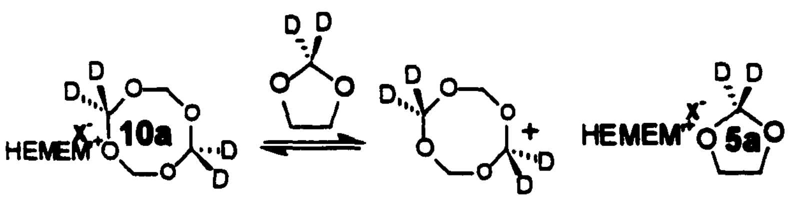

(III.B.iii 8)

Instead of forming **TET-d_4**, activated **TET-d_4** can also ring open to form the resonance stabilized carbenium ion followed by depolymerization to form formaldehyde, and deuterium labeled formaldehyde or copolymerize to form 'M' sequences.

The dissociation of activated **TET** to give formaldehyde or deuterium labeled formaldehyde leads to a synthetic route for the generation of partially deuterium labeled

TOX.

Sequences Formation

Although the generation of **TOP-(2,2-d_2)** is the most significant process in this stage of the reaction, rate data shows that **TOX** is being consumed faster than **DOL-(2,2-d_2)**, hence, formaldehyde from **TOX** is also reacting with **TOP-(2,2-d_2)** to generate several sequences (**Figure III.B.iii 9**).

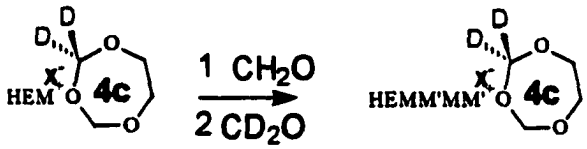

(III.B.iii 9)

These sequences and their experimentally determined rates include **(E/M/M')(M/M')(M'/M)(M/M')(E/M/M')** 8.4×10^{-4}M/min, **(M/M')E(M'/M)E(M/M')** 1.8×10^{-4}M/min, **(M/M')E(M'/M)(M/M')(E/M/M')** 1.3×10^{-3}M/min, **(M/M')(M'/M)E(M/M')(M'/M)** 4.7×10^{-4}M/min, and **E(M'/M)E(M/M')(M'/M)** 3.0×10^{-4}M/min. The rate of generation of '**E**' centered pentads in the **TOX-d_6/DOL** (**Section III A**) copolymerization system was found to be approximately twice the rate of generation of the '**E**' centered pentad in this experiment, due to factors including variation in water content. After adjusting for this overall rate difference for comparison, the '**M**' centered pentads with the exception of **(M/M')E(M'/M)E(M/M')** are being generated at a greater rate than in the **TOX-d_6/DOL** copolymerization system. This is to be expected, since in

the present system a much higher concentration of source of 'M', i.e. CH_2O, is available. The CH_2O molecule contributes to the formation of **TOP** and the pentad sequences. Whereas in the **TOX-d_6/DOL** copolymerization system the effect of deuterium labeled formaldehyde and deuterium labeled **TOX** could not be observed. In the case of the **(M/M')E(M)E(M/M')** pentad sequence, its relative low rate of generation is attributed to a restrictive route of generation involving the reactions of $4c/4_{a/b}$. The rates of generation for the **(E/M/M')(M/M')(M'/M)(M/M')(E/M/M')** and **(M/M')(M'/M)E(M/M')(M'/M)** sequences were maintained until 14% **DOLE** conversion.

Stage 11

At 14% **DOLE** conversion (**Figure III.B.iii. 4**), the increased consumption of **TOX** is followed by the increased generation of the **(E/M/M')(M/M')(M'/M)(M/M')(E/M/M')** $4.1x10^{-3}$M/min and **(M/M')(M'/M)E(M/M')(M'/M)** $1.7x10^{-3}$ M/min pentad sequences. The increased consumption of **TOX** at this point suggests its copolymerization with **TOP-(2,2-d_2)** to generate the aforementioned pentad sequences as opposed to its first dissociating to formaldehyde and then incorporating into polymer sequences (**Reaction III.B.iii 10**).

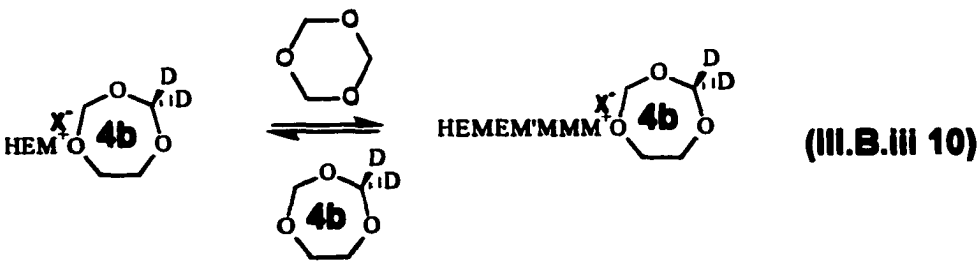

(III.B.iii 10)

This increased consumption of **TOP-(2,2-d_2)** results in the increased generation of **DOLM** from $7.9x10^{-4}$M/min to $1.6x10^{-3}$M/min. The rates of generation of the other pentad sequences were maintained until 34% **DOLE** conversion.

Stage III

At 34% **DOLE** conversion, the copolymerization of **DOL** with **TOP-(2,2-d_2)** results in the increased generation of all the pentad sequences. The net increase in rate of formation of these sequences are: **(M/M')(M/M')E(M/M')(M/M')** $4.5E^{-3}$ M/min, **(M'/M)E(M/M')(M/M')(M/M')** plus **(M'/M)E(M/M')(M/M')E** $7.0E^{-3}$ M/min, **(M/M'/E)(M/M')(M/M')(M/M')(M/M'/E)** $1.2E^{-2}$ M/min, **E(M'/M)E(M/M')(M/M')** plus **E(M'/M)E(M/M')E** $8.5E^{-4}$ M/min and **(M'/M)E(M/M')E(M/M')** $7.1E^{-4}$ M/min. The distribution of these rate data suggests that the transacetalization process is significant in this stage of the reaction. Although we see an increased net rate of formation for the two and three **'E'** pentad sequences, these rates are being dwarfed by the net rate of increase of the one **'E'** pentad sequences. These net rates of formation of the pentad sequences were maintained for the remainder of the reaction except for the net rate of formation for the **(M/M'/E)(M/M')(M/M')(M/M')(M/M'/E)** pentad sequences. The kinetic curve for these sequences revealed a net increased rate of formation at 61% **DOL(E)** conversion.

Stage IV

At approximately 60% **DOLE** conversion, the net rate of formation of the **(M/M'/E)(M/M')(M/M')(M/M')(M/M'/E)** pentad sequences make their final rate

increase to $2.7x10^{-2}$ M/min. This increase reflects the rapid reaction of formaldehyde to form polymethyleneoxide following their initial generation via the dissociation of **TOX**. The following scheme depicts the copolymerization reactions.

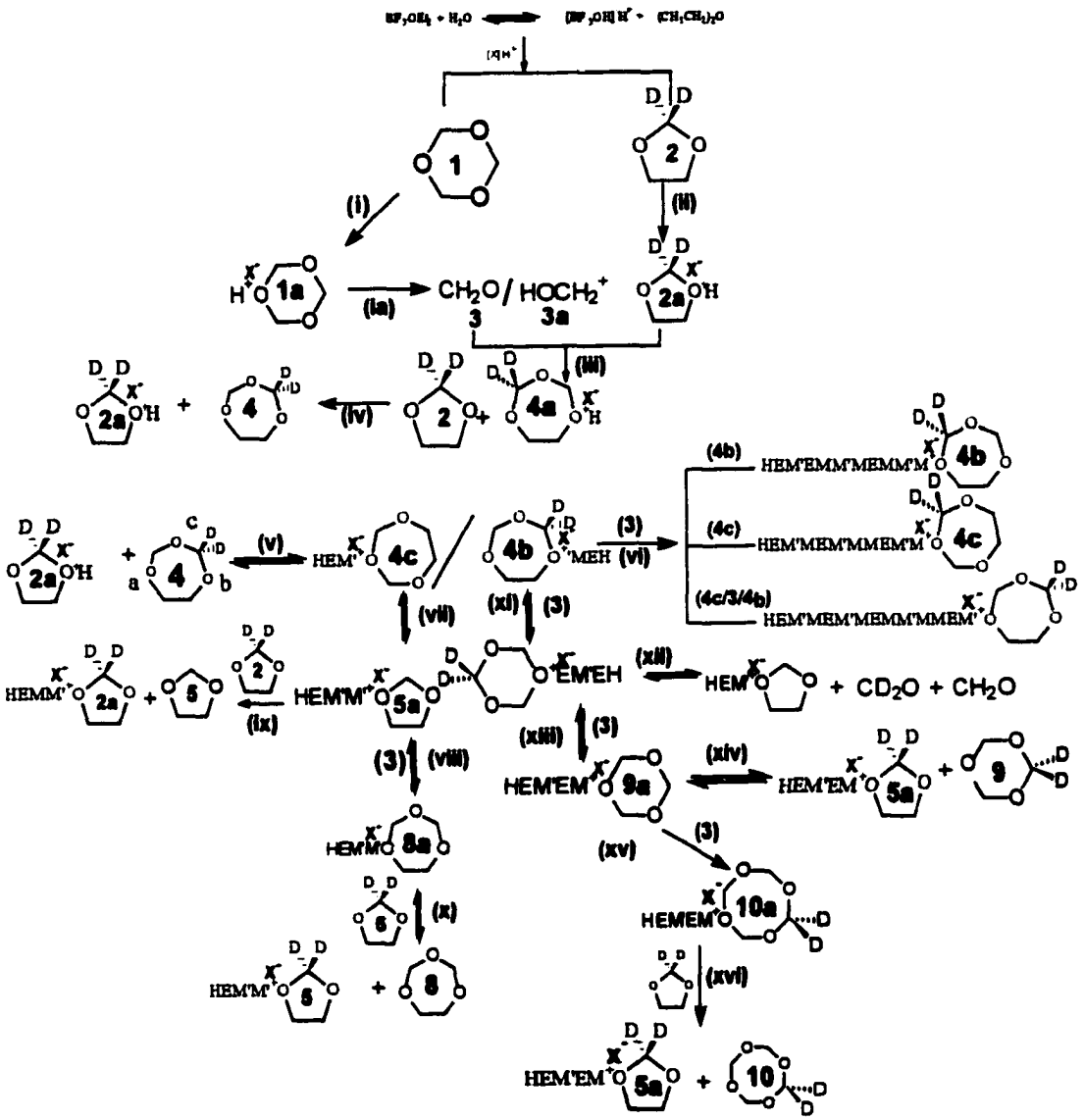

(Scheme 11)

III.C. DOL polymerization with ^{13}C labeled dimethoxymethane, $C^{13}H_3OCH_2OC^{13}H_3$ as Chain Transfer Agent.

In-situ ^{13}C NMR spectra of TOX, DOL homopolymerization and TOX/DOL copolymerizations in conjunction with $C^{13}H_3OCH_2OC^{13}H_3$ as ^{13}C labeled chain transfer agent were obtained to follow all aspects of $C^{13}H_3OCH_2OC^{13}H_3$ reactions. The assignment of resonance peaks and qualitative observation of active species support the mechanistic schemes derived in the previous sections.

The spectrum (**Figure III.C.i 1**) before initiation in the *in-situ* polymerization of DOL with ^{13}C labeled dimethoxymethane ($C^{13}H_3OCH_2OC^{13}H_3$) as chain transfer agent shows the following components: **DOL(M)** at 94.58 ppm, **DOL(E)** at 64.22 ppm, $C^{13}H_3OCH_2OC^{13}H_3$ at 54.05 ppm and ^{13}C labeled methanol at 49.06 ppm. The trace amount (3.8% of $C^{13}H_3OCH_2OC^{13}H_3$) of ^{13}C labeled methanol comes from the synthesis of dimethoxymethane with 99% ^{13}C labeled methanol and formaldehyde as reactants and purification with sodium beads.

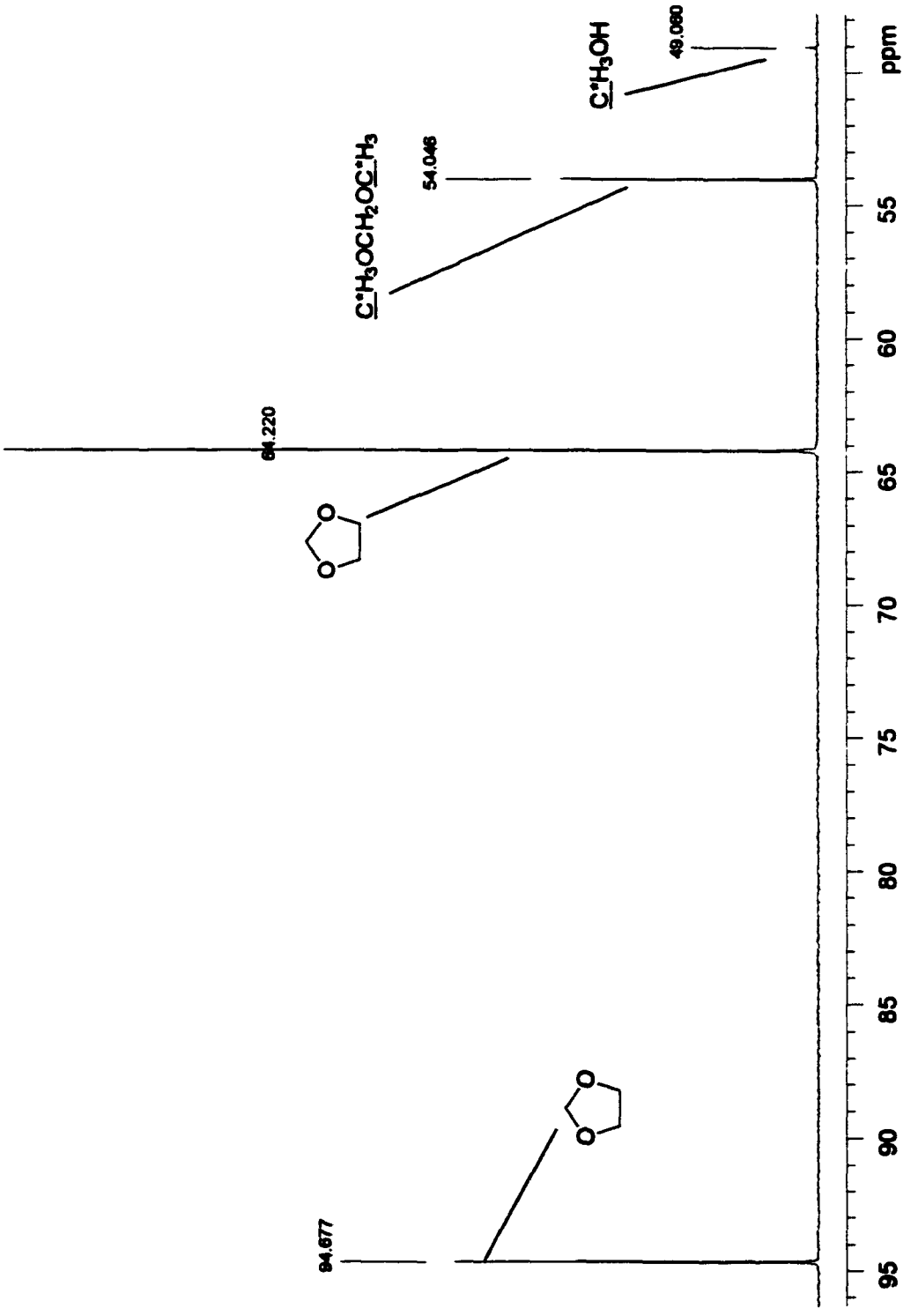

Figure (III.C.1.1) ^{13}C spectrum before initiation of **DOL** polymerization with ^{13}C labeled dimethoxymethane as chain transfer agent. Monomers' mole ratio: (3,1), spectrometer: 600 **MHz**, probe: **ID600-a**.

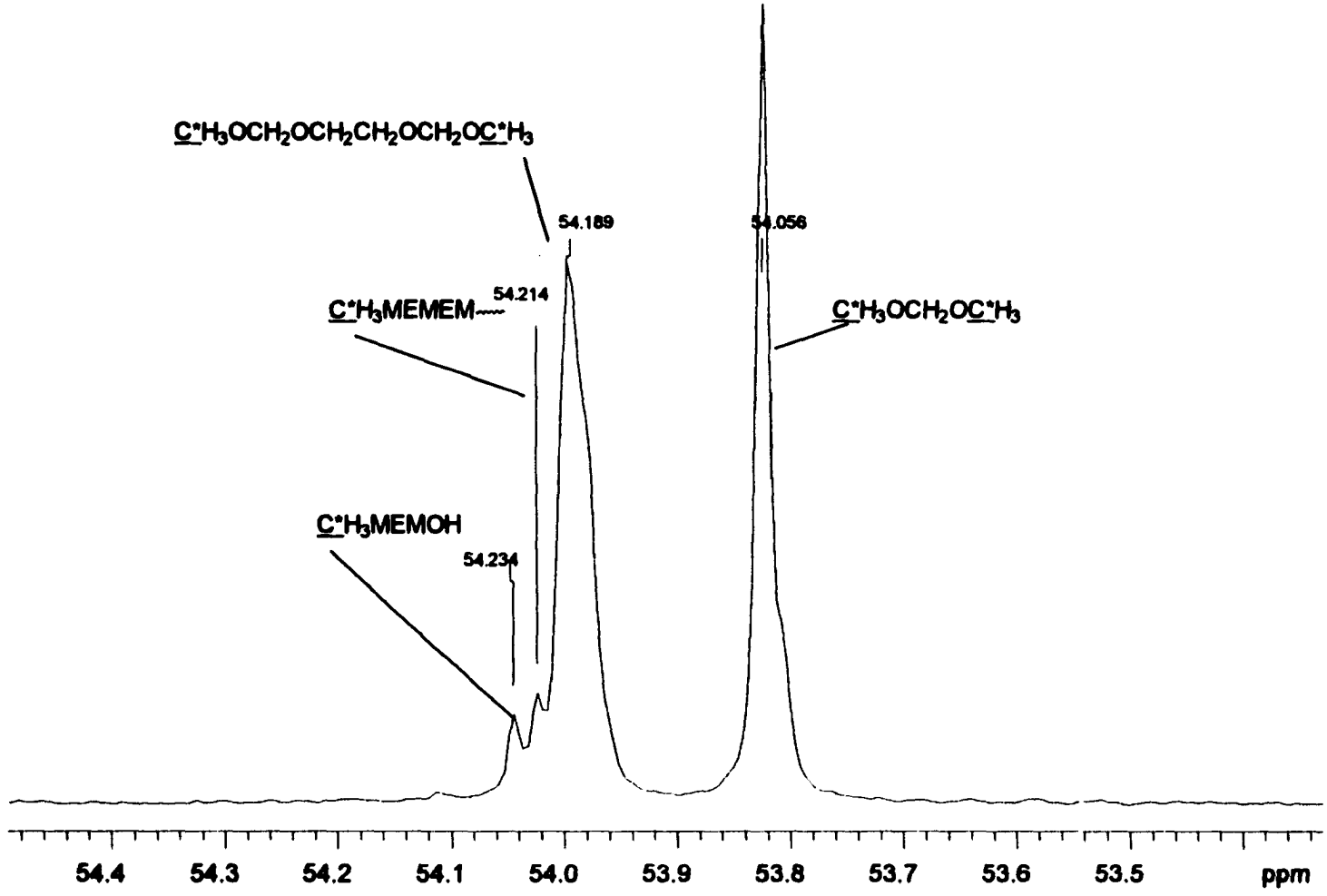

Figure (III.C.i 2) ^{13}C spectrum of **DOL** polymerization with ^{13}C labeled dimethoxymethane as chain transfer agent- "Intermediate Assignment". Monomers' mole ratio: (3,1), spectrometer: 600 **MHz**, probe: ID600-s, **DOL(E)** conversion: 12 %.

Assignments and Discussion.

At 12 % **DOL(E)** conversion, endgroups including $\underline{C}^{13}H_3OMEMOH$ at 54.23 ppm, $\underline{C}^{13}H_3OMEM\sim$ at 54.21 ppm and intermediate $\underline{C}^{13}H_3OMECH_2O\underline{C}^{13}H_3$ at 54.19 ppm were observed (**Figure III.C.i 2**). The generation of $\underline{C}^{13}H_3OMECH_2O\underline{C}^{13}H_3$ points to the processes in **Reaction (III.C.i 1)**. In this reaction, the initiator and chain transfer agent first associates allowing the developing carbenium ion to transfer to **DOL**, forming the initiated structure shown and labeled methanol.

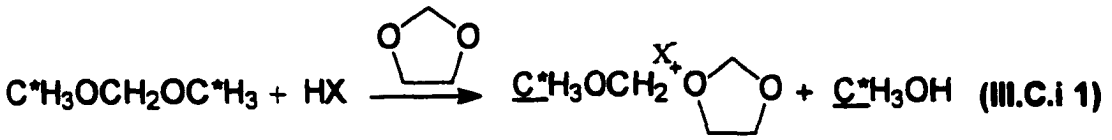

(III.C.i 1)

The labeled methanol produced in this reaction and $C^{13}H_3OCH_2OC^{13}H_3$ then reacts with the propagating oxonium ion to produce the intermediate $\underline{C}^{13}H_3OMECH_2O\underline{C}^{13}H_3$. The recorded growth for the intermediate $\underline{C}^{13}H_3OMECH_2O\underline{C}^{13}H_3$ at the expense of the chain transfer agent supports termination of initiated **DOL** by labeled dimethoxymethane (**Reaction III.C.i 2**).

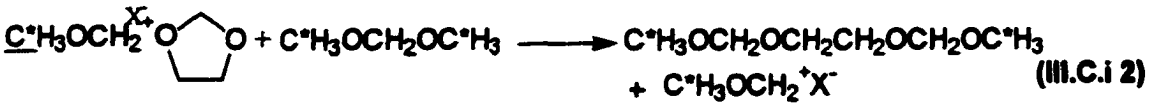

(III.C.i 2)

The reaction also regenerates the initiating species $C^{13}H_3OCH_2^+X^-$. The

termination of the propagating oxonium ion by labeled methanol also produces the intermediate and the initiator **HX** as shown in **Reaction (III.C.i 3)**.

The initiator then attacks the chain transfer agent, repeating the process of generating the intermediate. This mechanism is supported by the observation that the representative peak for ^{13}C labeled methanol, one of the initial product in chain transfer did not significantly change due to its consumption in **Reaction (III.C.i 3)**. The gradual growth of '$\underline{C}^{13}H_3OMEM\sim$' at the expense of this intermediate and the other methoxyl endgroups are also observed **Figure (III.C.i 3)**.

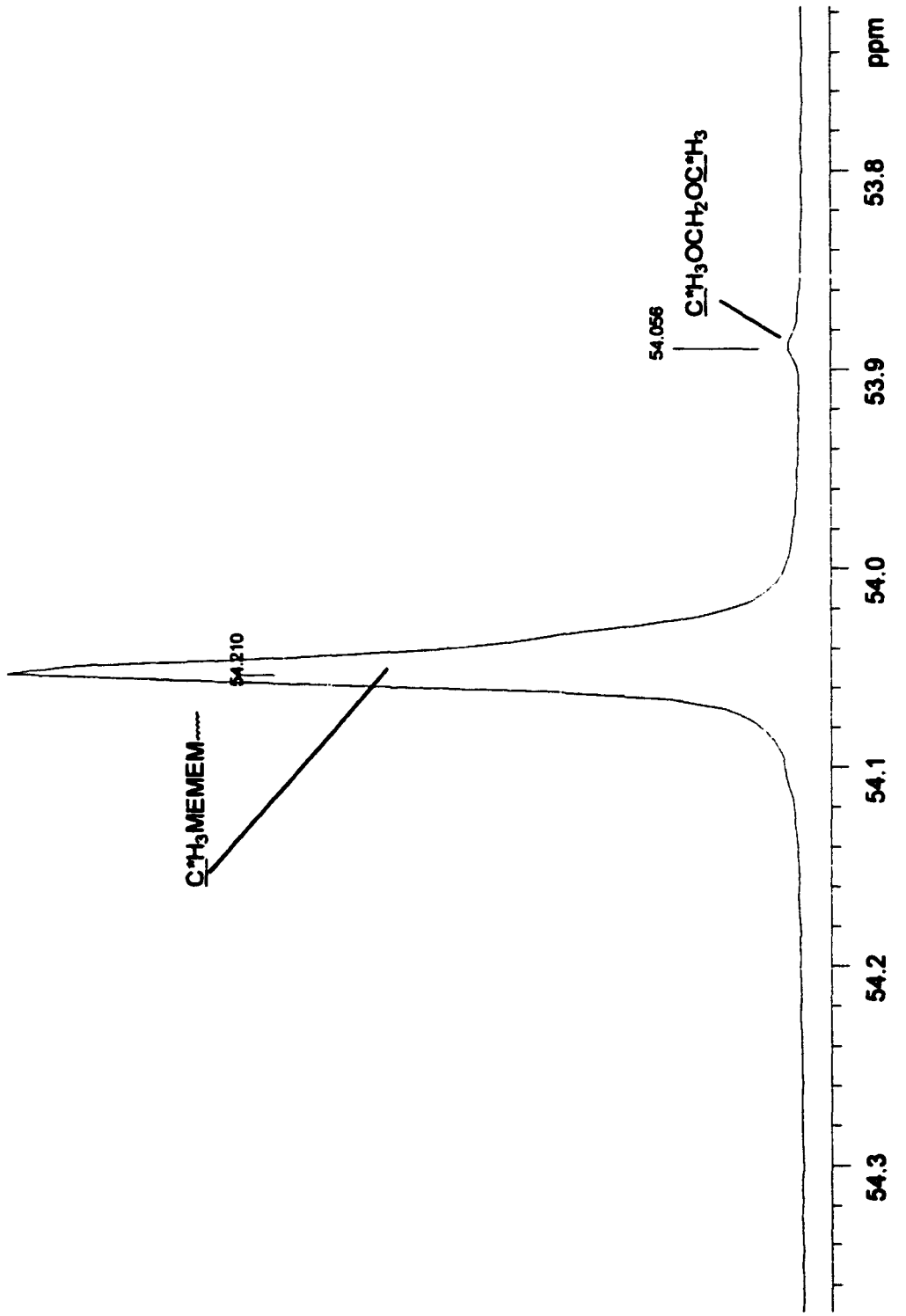

Figure (III.C.i 3) ^{13}C spectrum of **DOL** polymerization with ^{13}C labeled dimethoxymethane as chain transfer agnt- "$\underline{C}^{*}H_3MEM$-' Assignment". Monomers' mole ratio: (3,1), spectrometer: 600 MHz, probe: ID600-s, **DOL**(E) conversion: 76 %.

TOX polymerization with ^{13}C labeled dimethoxymethane as Chain Transfer Agent.

The spectrum before initiation **Figure (III.C.ii i)** in the ***in-situ*** polymerization of **TOX** with ^{13}C labeled dimethoxymethane ($C^{13}H_3OCH_2OC^{13}H_3$) as chain transfer agent shows **TOX** at 93.23 ppm, $C^{13}H_3OCH_2OC^{13}H_3$ at 54.05 ppm and ^{13}C labeled methanol at 49.02 ppm. As expected, ^{13}C labeled methanol is also observed here **(Section III.C.i)**.

Assignments and Discussion.

At 5% **TOX** conversion, the development of different endgroup peaks were observed **(Figure III.C.ii 2)**. These groups include $\underline{C}^{13}H_3$ **OMMM~** at 54.84 ppm, $\underline{C}^{13}H_3OMMCH_2O\underline{C}^{13}H_3$ at 54.78 ppm and $\underline{C}^{13}H_3OMMMOH$ at 54.73 ppm. The growth for the intermediate $\underline{C}^{13}H_3OMMCH_2O\underline{C}^{13}H_3$ at the expense of the chain transfer agent shows that reactions involving termination are taking place. The initiation of **TOX** at the initial stage of polymerization results in dissociation to produce formaldehyde and resonance stabilized carbenium ions. This carbenium ion can react with water, ethanol, or dimethoxymethane **(Reaction III.C.ii 1)**.

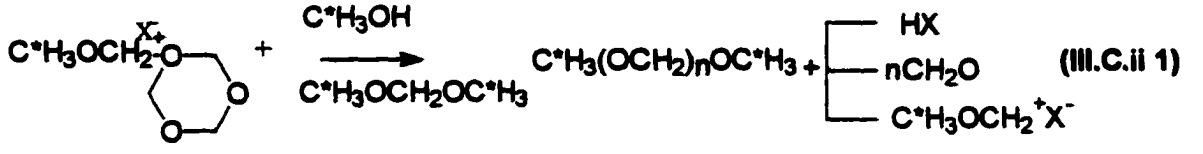

(III.C.ii 1)

The gradual growth of '$\underline{C}^{13}H_3$**OMMM~**' at the expense of $\underline{C}^{13}H_3OCH_2O\underline{C}^{13}H_3$, $C^{13}H_3OH$ and $\underline{C}^{13}H_3OMMCH_2O\underline{C}^{13}H_3$ as polymerization progressed is observed. The

peaks intensities at 54.78 and 54.73 ppm do not increase after initial growth and then gradually decrease later in the reaction. Their gradual decrease towards the end of the reactions illustrates their involvement in chain transfer reactions.

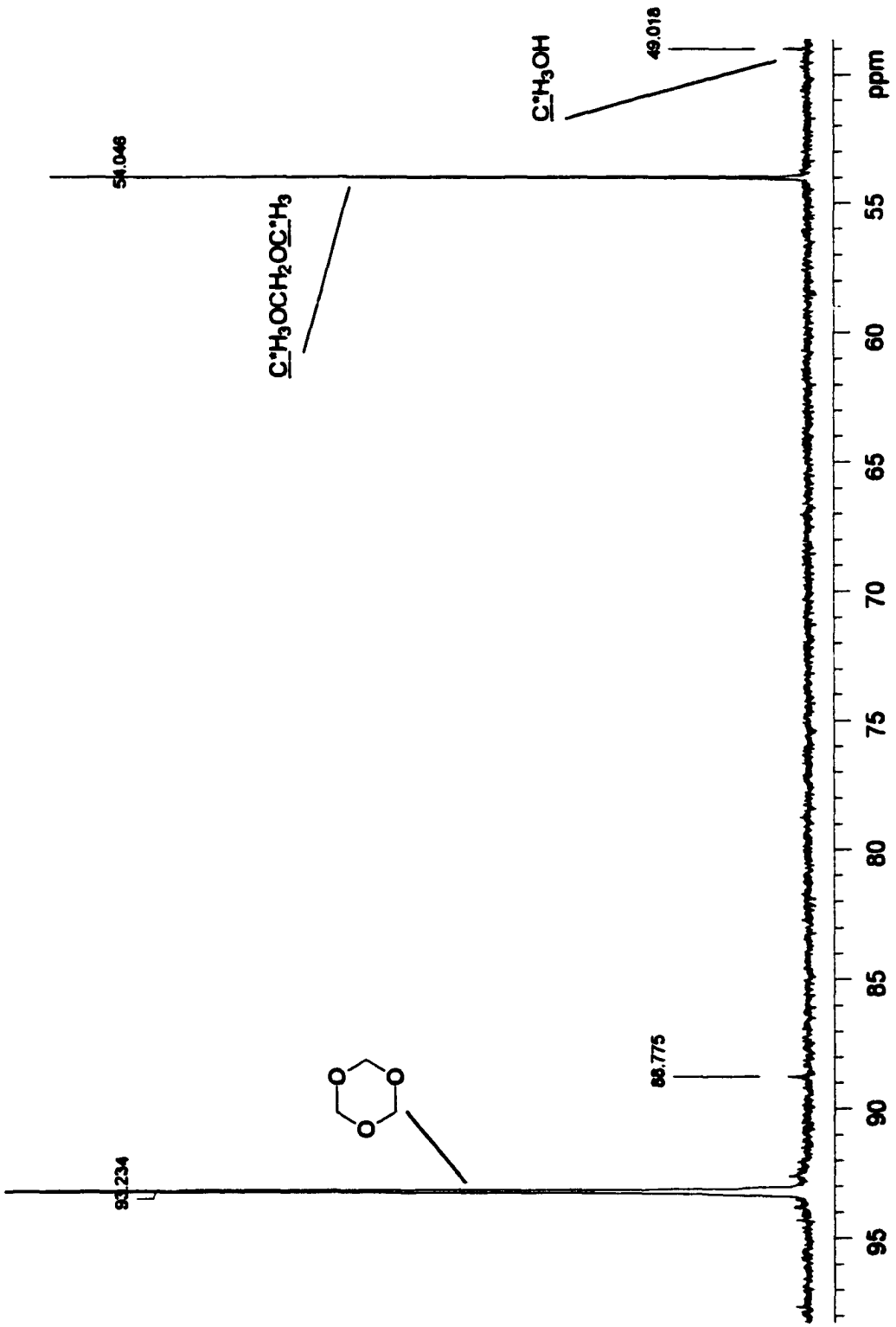

Figure (III.C.ii 1) ^{13}C spectrum before initiation of **TOX** polymerization with ^{13}C labeled dimethoxymethane as chain transfer agent. Monomers' mole ratio: (3,1), spectrometer: 600 **MHz** probe: **ID600-4** .

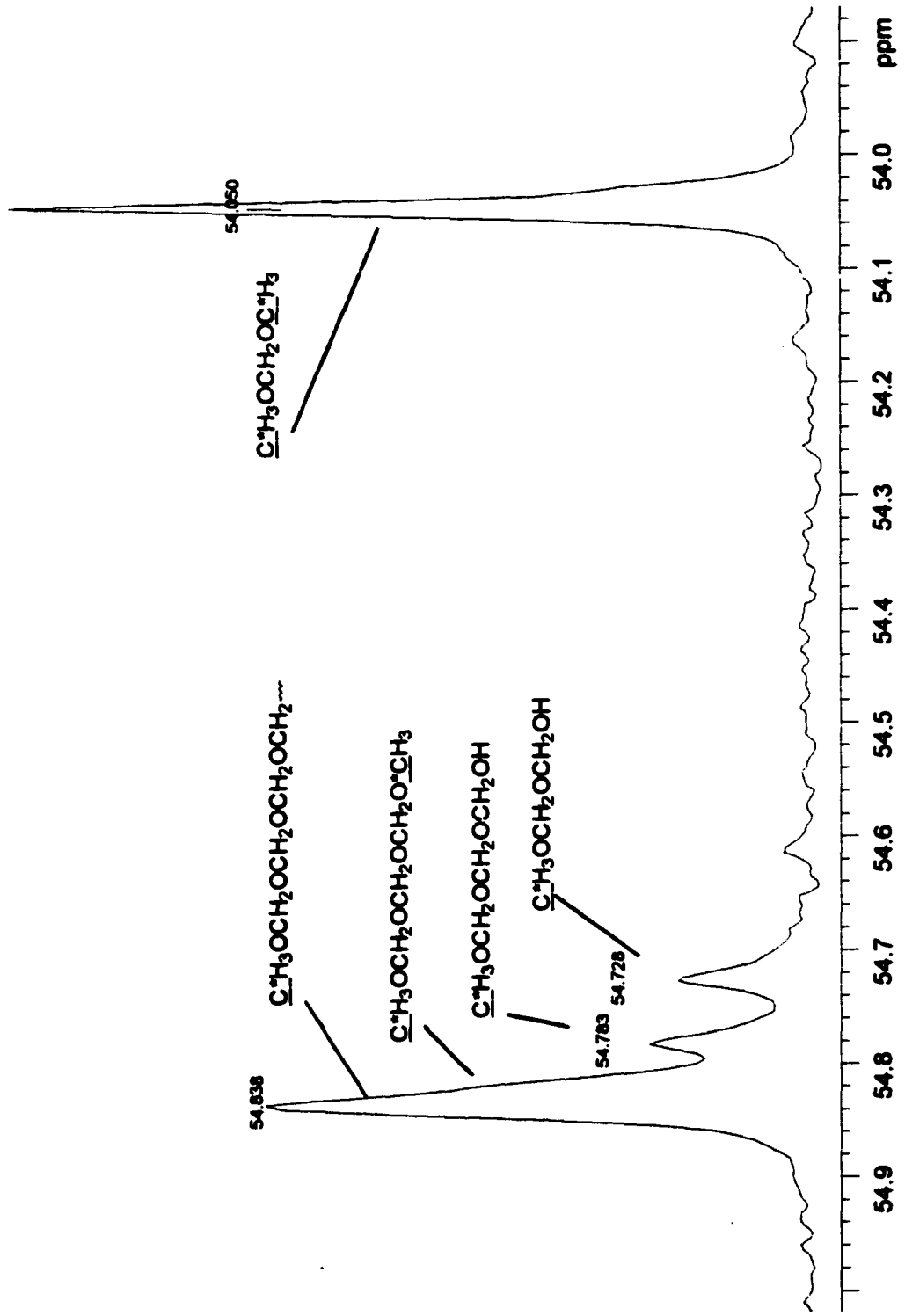

Figure (III.C.ii 2) ^{13}C spectrum of **TOX** polymerization with ^{13}C labeled dimethoxymethane as chain transfer agent'Evidence for $C^{13}H_3MMM$~ dominance'. Monomers' mole ratio: (3,1), spectrometer: 600 **MHz** probe: **ID600-s, TOX** conversion: 5%.

III.C. TOX, DOL Copolymerization with $C^{13}H_3OCH_2OC^{13}H_3$ as Chain Transfer Agent

III.C.iii. *In-Situ* ^{13}C NMR Analysis

Assignments and Discussion.

The fourth spectrum after initiation (**Figure III.C.iii. 1**) for this system with 3-to-1 **TOX/DOL** ratio show the following resonances: $\underline{C}^{13}H_3OCH_2O\underline{C}^{13}H_3$ at 54.03 ppm, $\underline{C}^{13}H_3OMMM\sim$ at 54.82 ppm, $\underline{C}^{13}H_3OMMCH_2O\underline{C}^{13}H_3$ at 54.77 ppm, $\underline{C}^{13}H_3OMMEM\sim$ at 54.75 ppm, $\underline{C}^{13}H_3OMMCH_2OH$ at 54.72 ppm, and $\underline{C}^{13}H_3OMEM$ at 54.18 ppm. The rapid initial growth of the $\underline{C}^{13}H_3OMMEM\sim$ supports early **TOP** initiation. The $\underline{C}^{13}H_3OMEM\sim$ sequence dominates early in the copolymerization. This reflects the reactions of the two symmetrical reactive sites on **TOP** generating '$\underline{C}^{13}H_3OCH_2(EMM)\sim$' with twice the concentration of '$\underline{C}^{13}H_3OCH_2(MEM)\sim$' which is formed from the single acetal reactive site of **TOP**. The $\underline{C}^{13}H_3OCH_2O\underline{C}^{13}H_3$ and $\underline{C}^{13}H_3OH$ peaks vanishes early in the copolymerization.

The peak assigned to $\underline{C}^{13}H_3OMMM\sim$ dominates at the end of the pre-cloud period (**Figure (III.C.iii. 2)**, reflecting the higher total concentration of **M** units (**M/E** = 10/1) in the comonomer melt. The $\underline{C}^{13}H_3OMECH_2O\underline{C}^{13}H_3$ intermediate grows rapidly at the start of the copolymerization and maintains its concentration followed by gradually conversion to $\underline{C}^{13}H_3OMEM\sim$ towards the end of the pre-cloud period. At this point, the $\underline{C}^{13}H_3OMEM\sim$ concentration begins to decrease due to transacetalization reactions

resulting in the increasing concentration of the $\underline{C^{13}}H_3OMMM\sim$ sequence.

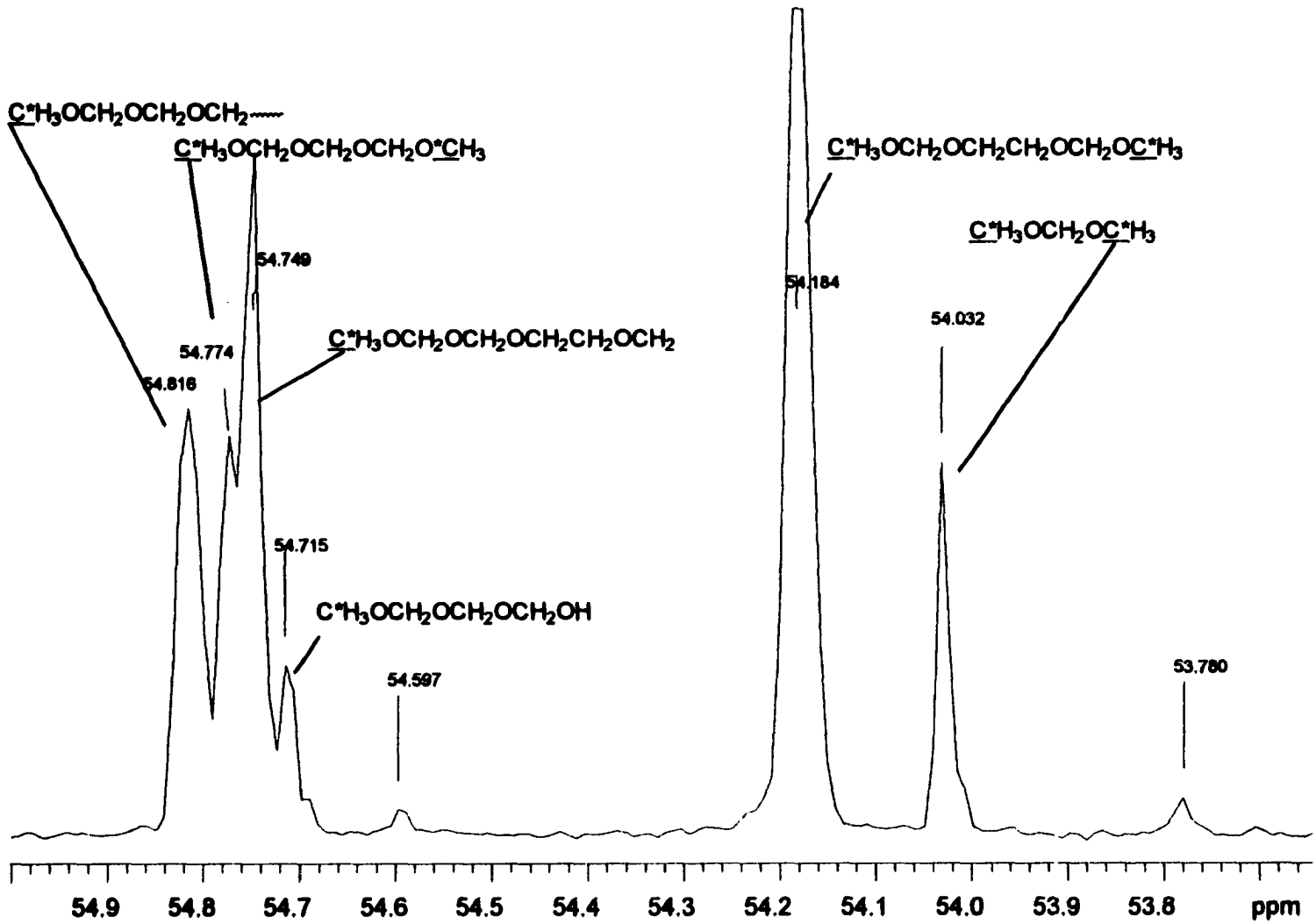

Figure (III.C.iii 1) **^{13}C spectrum of TOX/DOL copolymerization with ^{13}C labeled dimethoxymethane as chain transfer agent"Methoxy end-group Assignment". Monomers' mole ratio: (3,1), spectrometer: 600 MHz, probe: ID600-s, DOL(E) conversion: 30 %.**

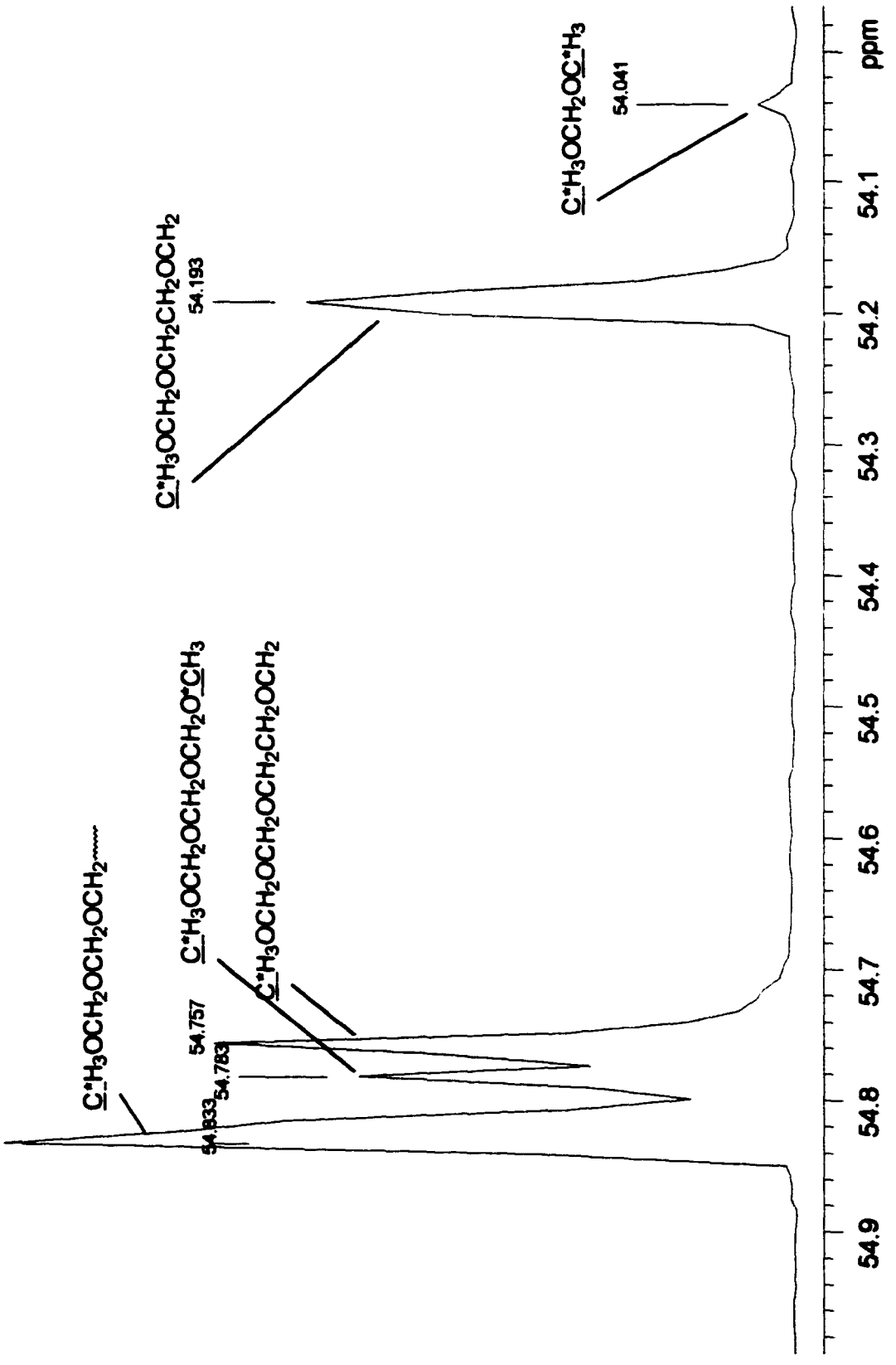

Figure (III.C.iii 2) ^{13}C spectrum of **TOX/DOL** copolymerization with ^{13}C labeled *dimethoxymethane* as chain transfer agent - "Dominant Methoxy end-group Peaks". Monomers' mole ratio: (3,1), spectrometer: 600 **MHz**, probe: **ID600-s**, **DOL(E)** conversion: 76 %.

In the "M region" of TOX/DOL/$C^{13}H_3OCH_2OC^{13}H_3$ copolymerization Figure (III.C.iii. 3), the following resonances are observed: $C^{13}H_3OCH_2OC^{13}H_3$ at 96.62 ppm, (M/E)MEMEM(M/E) at 95.30 ppm, DOL(M) at 94.49 ppm TOX at 93.23 ppm, TOP(M) at 92.68 ppm, (M/E)MEMMM(M/E) at 92.55 ppm and 92.52 ppm, (M/E)MEMME(M/E) at 92.10 ppm, (M/E)MMMMM(M/E) at 89.66 ppm and 89.64 ppm, (M/E)MMMME(M/E) at 89.19 ppm and 89.14 ppm and (M/E)EMMME(M/E) at 88.74 ppm. These sequence peaks show heptad resolutions for those with less than two 'E' units within the sequence. As an example, the (M/E)MMMME(M/E) heptad shows two peaks resulting from the possibility of 'M' or 'E' placement on the edges of the pentad without an 'E' unit. For heptads with intervening "E" between the center "M" and the "M/E' edge, their resolution is not possible due to the higher shielding effect of the larger 'E' (~CH_2CH_2O~) in comparison to 'M' (~CH_2O~). The heptad resolution in this experiment was instrumental in assigning the methoxy end-group sequence peaks.

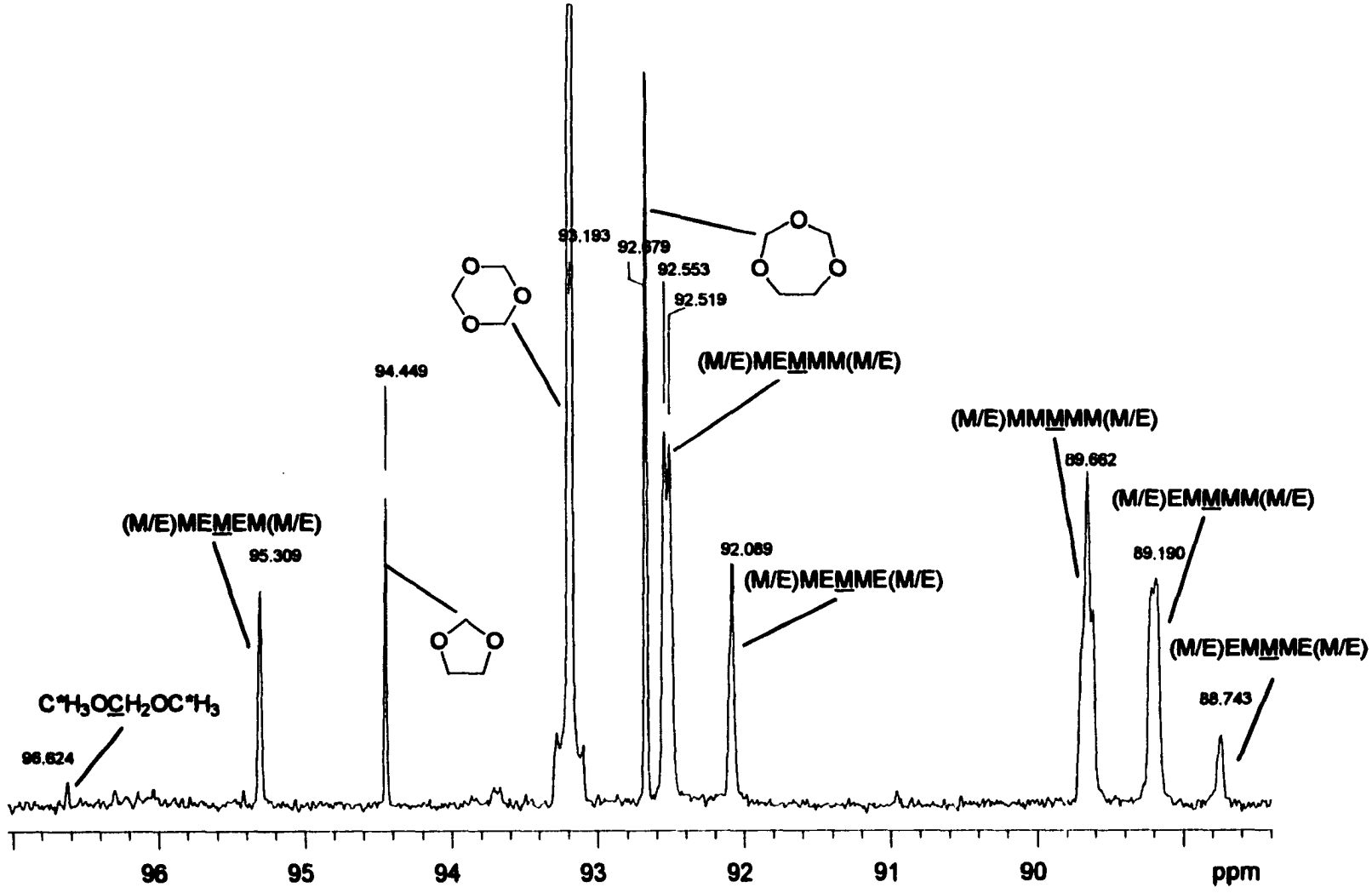

Figure (III.C.iii 3) **^{13}C spectrum of TOX/DOL copolymerization with ^{13}C labeled dimethoxymethane as chain transfer agent"M-region Heptad resolution". Monomers' mole ratio: (3,1), spectrometer: 600 MHz, probe: ID600-s, DOL(E) conversion: 76 %.**

III.C.iv. TOX, DOL, $C^{13}H_3OCH_2OC^{13}H_3$ reactions

The initiation of $C^{13}H_3OCH_2OC^{13}H_3$ leads to the generation of the resonance stabilized carbenium ion shown (**Reaction III.C.iv 1**).

The resonance stabilized carbenium ion then initiates **DOL** producing the structure containing the tert-oxonium ion shown (**Reaction (III.C.iv 2)**).

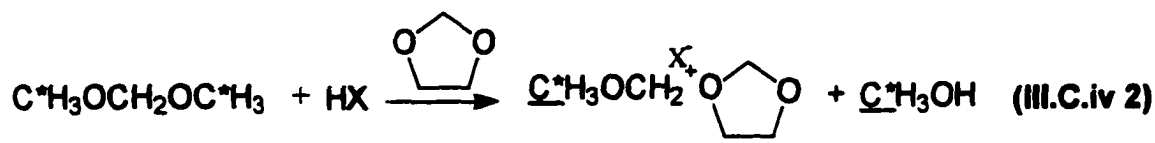

Initiated **DOL** then incorporates formaldehyde to produce initiated **TOP**. The incorporation of formaldehyde followed by an inter-molecular cationic shift to **DOL** result in the formation of **TOP** (**Reaction III.C.iv 3**).

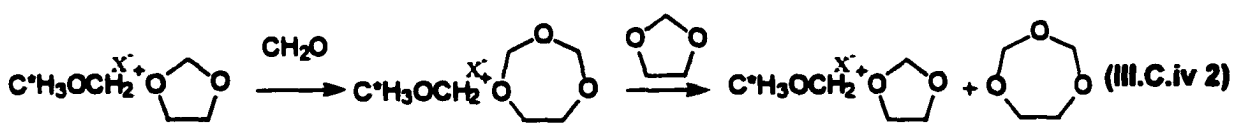

The reaction of initiated **TOX** or **DOL** with $C^{13}H_3OCH_2OC^{13}H_3$ forms stable intermediates such as $\underline{C}^{13}H_3OMECH_2O\underline{C}^{13}H_3$ and $\underline{C}^{13}H_3OMMCH_2O\underline{C}^{13}H_3$ respectively.

These intermediates gradually converts to methoxy capped sequences via transacetalization as the copolymerization reactions progresses.

References

[1] Rahman, A., *Nuclear Magnetic Resonance Basic Principles*, Springer - Verlag, New York, Berlin, Heidelberg, Tokyo, (1986) P.227

[2] David A. Forsyth, James H. Botkin, and Virginia M. Osterman, "*Long-Range Intrinsic NMR Isotope Shifts as a probe of Hyperconjugation," Demonstration of the Angular Dependence in Bicyclic Carbocation*, Journal of the American Chemical Society, V.106 (Dec. 12, 84) p. 7663-6.

[3] Werner, M. CUNY Thesis, 1996.

[4] Walker, J., *Formaldehyde*, 3rd ed., Robert E. Krieger Publishing Co., New York, (1975) pp. 191-199.

[5] Lu, N., Collins, G.L., Yang, N. L. *Macromol. Chem., Macromol. Symp.*, **42/43**, 425-439 (1991).

[6] Jaacks, Volker. Adv. Chem. Ser. **91**, 371 (1969).

[7] Weissermel, K., Fisher, E., Gutweiler, K., Hermann, H. D. Cherdron, H., Angew. Chem. Int. Ed., 1967, **6**, 526

[8] Collins, G. L., Greene, R. K., Benardinelli, F. M., Ray, W. H. J. Polym. Sci. Polym. Chem. Ed., 1981, **17**, P. 667

[9] Odian, G., *Principles of Polymerization*, 3rd ed., John Wiley and sons, inc. (1991) p. 456.

[10] Odian, G., *Principles of Polymerization*, 3rd ed., John Wiley and sons, inc. (1991) p. 552.

V. Conclusion and Proposed Experiments

A. Conclusion

A comprehensive analysis of data from proton, C-13 and DEPT NMR for the TOXd_6/DOL and TOX/DOL-(2,2-d_2) systems yields for the first time a detailed mechanistic description of the pre-cloud period of TOX/DOL copolymerization. Several aspects of these sequences of event corroborate with C-13 experiments using C-13 labeled dimethoxymethane as chain transfer agent in TOX/DOL copolymerization. Based on kinetic evidence from proton NMR and qualitative observation of C-13 and DEPT NMR, the following series of events were deduced.

After the protonation of TOX and DOL, TOX dissociates to form formaldehyde and protonated formaldehyde. The resonance stabilized carbenium ion of protonated formaldehyde participates efficiently in the continued dissociation of TOX, while formaldehyde inserts into protonated DOL forming protonated TOP. Proton transfer from protonated TOP to the more basic DOL or formaldehyde results in the formation of TOP and the regeneration of protonated DOL or protonated formaldehyde. The regenerated protonated DOL along with formaldehyde continues the process of generating TOP. The protonated DOL is also the cationic species that initiates copolymerization by reacting with TOP at its two different reactive sites. The polymerization of TOP through its two different reactive sites along with copolymerization *via* insertion of formaldehyde generates all observed sequences. The MMMMM and EMMMM pentads dominate later via transacetalization processes and the copolymerization of TOX and TOP. Following these sequences of events, the copolymerization of TOP and DOL results in a slight increase in generation of the "two and three E sequences", EMEME, EMEMM and

MEMEM. At this point, transacetalization takes on a major role resulting in the gradual depletion of the **EMEME, EMEMM** and **MEMEM** pentads. Towards the end of these reactions, **TOX** and formaldehyde copolymerization marks the end of the pre-cloud period and the onset of formation of copolymer crystal. Although **DOL** is a *co*monomer initially added, its contribution *via* direct copolymerization to sequence formation is not significant throughout the entire copolymerization reactions.

The kinetics of methoxy end-group sequences supports the early initiation of **TOP** at its two different reactive sites to form the end-group sequences $C^{13}H_3OCH_2OCH_2CH_2OCH_2\sim$. and $C^{13}H_3OCH_2OCH_2OCH_2CH_2OCH_2\sim$. These reactions occur simultaneously with the reaction of **DOL** and chain transfer agent to produce the intermediate, $C^{13}H_3OCH_2OCH_2CH_2OCH_2OC^{13}H_3$. The concentration of this intermediate increased steadily initially followed by its chain transfer reactions to form the methoxy end-group sequence $C^{13}H_3OCH_2OCH_2CH_2OCH_2\sim$. This occurs simultaneously with the transacetalization processes involving the "**E** containing end-group" sequences forming the $C^{13}H_3OCH_2OCH_2OCH_2\sim$ end-group sequence.

B. Proposed Experiments

i. TOX-d_6, DOL, $C^{13}H_3OCH_2OC^{13}H_3$ Copolymerization

The experiment of **TOX-d_6, DOL, $C^{13}H_3OCH_2OC^{13}H_3$** copolymerization affords an increased dynamic range resolution suited for the study of end-groups. The ^{13}C labeling of the chain transfer agent $C^{13}H_3OCH_2OC^{13}H_3$ will also result in additional information in both ^{13}C and ^1H NMR experiments.

The partially or fully deuterated methoxy and formate endgroups can be formed from deuteride or hydride abstraction (**Reaction IV.B.i-1**). Again, because deuteration cause changes in chemical shift, the endgroups formed in their reactions will be distinct from each other. **TOX-d_6/DOL** and $C^{13}H_3OCH_2OC^{13}H_3$ copolymerization will also produce methoxy, ethanol and hemiacetal endgroups.

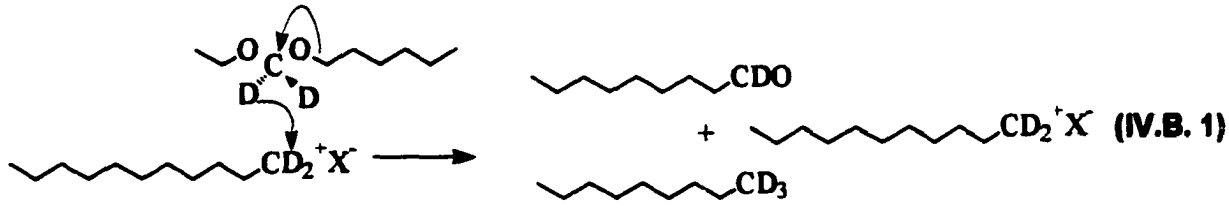

(IV.B. 1)

The termination of the chain by the chain transfer agent produces methoxy endgroups that are resolved according to triad sequences connected to the endgroups and various degrees of deuteration within these triads.

The termination of the copolymer via reaction with the labeled chain transfer agent gives

the ^{13}C labeled methoxy ended chains and initiator (**Reaction IV.B.i-2**).

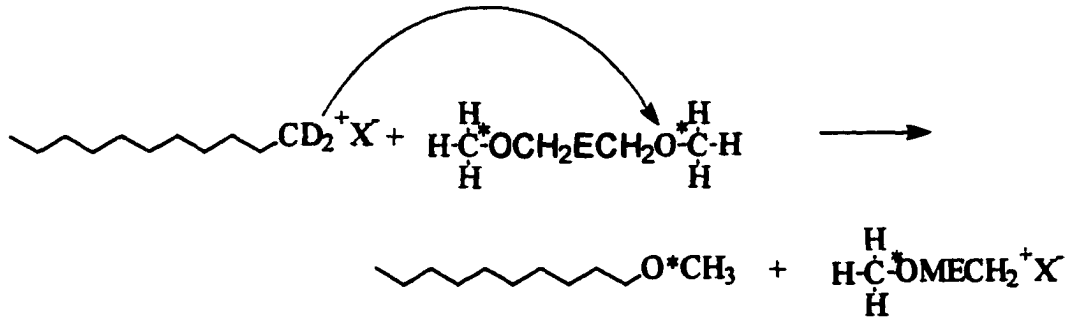

(IV.B.i- 2)

ii. TOX, DOL-(2,2-d_2) $C^{13}H_3OCH_2OC^{13}H_3$ Copolymerization

The labeled initiator reacts with **DOL-(2,2-d_2)** to give the structure shown in **Reaction (IV.B.ii-1)**. The ^{13}C **NMR** peak of this structure will be shifted down field because of the electron withdrawing effect of the cationic center.

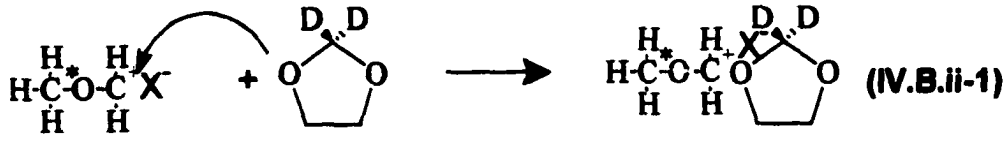

(IV.B.ii-1)

Reaction (IV.B.ii-2) shows one of the three possible resonance stabilized structures associated with the initiation of **DOL-(2,2-d_2)**. The other two resonance stabilized structures are associated with initiated **TOP-(2,2-d_2)**. All these structures have different chemical environments, hence different chemical shifts, which will allow the quantitation of the equilibrium constant for their structures with the ^{13}C labeled groups showing high intensity. The

structure for initiated **DOL** is shown in **Reaction (IV.B.ii-2)**.

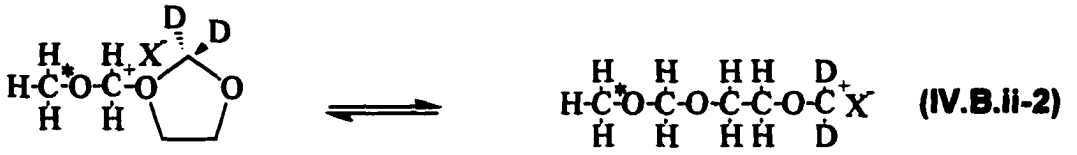

(IV.B.ii-2)

The termination of the copolymerization can produce different structures (**Reaction IV.B.ii-3**). The differences are varying degree of deuteration associated with the chain transfer agents and the labeled methoxy endgroup.

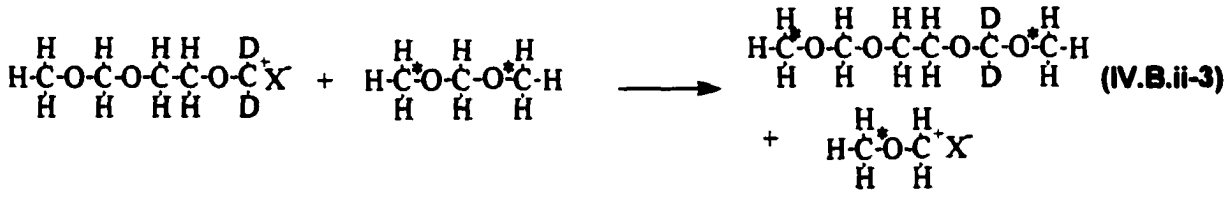

(IV.B.ii-3)

In situ Distortionless Enhancement Polarization Transfer, **DEPT**, **^{1}H, HMQC, HMBC** and **^{13}C NMR** experiments using 600 **MHz** spectrometer will be conducted to follow the copolymerization of **TOX/DOL-(2,2-d_2)** with **$C^{13}H_3OCH_2OC^{13}H_3$** as chain transfer agent. The aforementioned pulse sequences will also be used for the analysis of **TOX-d_6/DOL** copolymerization with **$C^{13}H_3OCH_2OC^{13}H_3$** as chain transfer agent. These experiments will give direct evidence to kinetics and mechanism involving each component. In the **DOL-(2,2-d_2)**, **TOX**, **$C^{13}H_3OCH_2OC^{13}H_3$ NMR** experiments, the sequence peaks observed for the endgroups will be different due to the interaction of **DOL-(2,2-d_2)**. As an example, **^{1}H NMR** experiments used to monitor this copolymerization will show an increased number of endgroup peaks

resulting from interaction with deuterated nuclei. In addition, the peaks' integrals of all the observable components will be used to generate kinetic curves. An analysis of these curves will give rates of resolved components at selected concentrations and polymerization intervals. The mechanistic, kinetic and distribution behavior of the deuterated components can be investigated by considering long range deuterium effect associated with adjacent placement to the detected nuclei. **DEPT** experiments also lowers the lattice relaxation time, T_1, in comparison to ^{13}C experiments, leading to a highly efficient procedure to obtain better signal to noise ratio in a shorter spectrometer time.

Bibliography

[1] Staudinger, H. *Die Hochmolecularen Organischen Verbindungen*, Springer: Berlin, (1932)

[2] Jaacks, Volker. Adv. Chem. Ser. **91**, 371 (1969).

[3] Weisermel, K., Fisher, E., Gutweiler, K., Hermann, H. D., Cherdron, H., Angew. Chem. Int. Ed. **6**, 526 (1967).

[4] Lu, N., Collins, G. L., Yang, N. L. *Makromolek. Chem., Macromolec. Symp.*, **42/43**, 425 (1991)

[5] Collins, G.L., Greene, R.K., Benardinelli, F. M., Ray, W.H. J. Polym. Sci. Polym. Chem. Ed. **19**, 1597 (1971).

[6] Werner, M. CUNY Ph.D. Thesis, 1996.

[1] Werner, M. CUNY Ph.D. Thesis, 1996.

[1] Rahman, A., *Nuclear Magnetic Resonance Basic Principles*, Springer - Verlag, New York, Berlin, Heidelberg, Tokyo, (1986) P.227

[2] David A. Forsyth, James H. Botkin, and Virginia M. Osterman, "*Long-Range Intrinsic NMR Isotope Shifts as a probe of Hyperconjugation," Demonstration of the Angular Dependence in Bicyclic Carbocation*, Journal of the American Chemical Society, V.106 (Dec. 12, 84) p. 7663-6.

[3] Werner, M. CUNY Thesis, 1996.

[4] Walker, J., *Formaldehyde*, 3rd ed., Robert E. Krieger Publishing Co., New York, (1975) pp. 191-199.

[5] Lu, N., Collins, G.L., Yang, N. L. *Macromol. Chem., Macromol. Symp.*, **42/43**, 425-439 (1991).

[6] Jaacks, Volker. Adv. Chem. Ser. **91**, 371 (1969).

[7] Weissermel, K., Fisher, E., Gutweiler, K., Hermann, H. D. Cherdron, H., Angew. Chem. Int. Ed., 1967, **6**, 526

[8] Collins, G. L., Greene, R. K., Benardinelli, F. M., Ray, W. H. J. Polym. Sci. Polym. Chem. Ed., 1981, **17**, P. 667

[9] Odian, G., *Principles of Polymerization*, 3rd ed., John Wiley and sons, inc. (1991) p. 456.

[10] Odian, G., *Principles of Polymerization*, 3rd ed., John Wiley and sons, inc. (1991) p. 552.